

Human Research Program
Human Health Countermeasures Element

Evidence Report

Risk of Spaceflight-Induced Intracranial Hypertension and Vision Alterations

Approved for Public Release: July 12, 2012

Version 1.0

National Aeronautics and Space Administration
Lyndon B. Johnson Space Center
Houston, Texas

Risk of Microgravity-Induced Visual Impairment/Intracranial Pressure (ICP)

AUTHORS:

David J. Alexander, MD¹

C. Robert Gibson, OD²

Douglas R. Hamilton MD, PhD¹

Stuart M. C. Lee, MS¹

Thomas H. Mader, MD³

Christian Otto, MD⁴

Cherie M. Oubre, PhD¹

Anastas F. Pass, OD, MS, JD⁵

Steven H. Platts, PhD⁶

Jessica M. Scott, PhD⁴

Scott M. Smith, PhD⁶

Michael B. Stenger, PhD¹

Christian M. Westby, PhD⁴

Susana B. Zanello, PhD⁴

*¹Wyle Science, Technology & Engineering Group
Houston, TX, USA*

*²Coastal Eye Associates
Webster, TX, USA*

*³Alaska Native Medical Center
Anchorage, Alaska, USA*

*⁴Universities Space Research Association
Houston, TX, USA*

*⁵University of Houston
Houston, TX, USA*

*⁶NASA Johnson Space Center
Houston, TX, USA*

Table of Contents

I. PRD RISK TITLE: RISK OF SPACEFLIGHT-INDUCED INTRACRANIAL HYPERTENSION/VISION ALTERATIONS.....	1
II. EXECUTIVE SUMMARY	1
III. INTRODUCTION	2
IV. SPACEFLIGHT EVIDENCE.....	7
A. Summary of Existing Long-Duration Flight Data.....	7
B. Summary of Human System Spaceflight Physiology.....	19
1. Ocular Evidence.....	19
2. Spaceflight-Induced Cardiovascular Adaptations.....	48
3. Spaceflight-Induced Central Nervous System Adaptations.....	66
V. CONTRIBUTING FACTORS	78
A. Potential In-flight Factors.....	78
1. Alterations in Carbon Dioxide (CO ₂) Metabolism	78
2. Alterations in Sodium	82
3. Exercise.....	82
B. Genetic Factors/Markers.....	84
1. One-Carbon Metabolism (Homocysteine).....	84
2. Biomarkers.....	84
VI. CASE DEFINITION/CLINICAL PRACTICE GUIDELINES	85
VII. GAPS	86
VIII. CONCLUSIONS	87
IX. REFERENCES	88
X. APPENDICES	103
Appendix A: Previous and Expanded In-flight Medical Requirements Testing for Crewmembers (MEDB 1.10).....	103
Appendix B: Additional Central Nervous System Work/Topic Areas that will be Incorporated into the Evidence Base	104
Appendix C: Acronyms	105

I. PRD RISK TITLE: Risk of Spaceflight-Induced Intracranial Hypertension/Vision Alterations

Given that all astronauts are exposed to microgravity and cephalad-fluid shift, and given that both symptomatic and asymptomatic astronauts have exhibited optic nerve sheath edema on magnetic resonance imaging, there is a high probability that all astronauts have idiopathic intracranial hypertension to some degree, and that those susceptible (via eye architecture, anatomy, narrow disc) have a high likelihood of developing either choroidal folds or optic-disc edema, and that the degree of that edema will determine long-term or permanent vision loss, sequelae, or impairment.

II. EXECUTIVE SUMMARY

Over the last 40 years there have been reports of visual acuity impairments associated with spaceflight through testing and anecdotal reports. Until recently, these changes were thought to be transient, but a comparison of pre and postflight ocular measures have identified a potential risk of permanent visual changes as a result of microgravity exposure. There are limited pre and postflight measures to define the risk and even less in-flight data is available. These data show that there is a subset of crewmembers that experience visual performance decrements, cotton-wool spot formation, choroidal fold development, optic-disc edema, optic nerve sheath distention, and/or posterior globe flattening with varying degrees of severity and permanence. These changes define the visual impairment/intracranial pressure (VIIP) syndrome. It is thought that the ocular structural and optic nerve changes are caused by events precipitated by the cephalad-fluid shift crewmembers experience during long-duration spaceflight. It is believed that some crewmembers are more susceptible to these changes due to genetic/anatomical predisposition or lifestyle (fitness) related factors. Three important systems – ocular, cardiovascular, and central nervous – will be evaluated to understand the risk of developing the VIIP syndrome. Several hypotheses have been proposed to explain the identified visual acuity and structural changes including increased intracranial pressure, localized ocular changes such as ocular hypotony, decreased venous compliance, and alterations in cerebrospinal fluid dynamics. As there are little data to determine the extent or cause of the VIIP syndrome, there is a knowledge gap related to etiology of the changes and the postflight resolution. This lack of knowledge gives the basis for increased pre, in-, and postflight monitoring to characterize the risk. It will be very important to determine the risk of developing the VIIP syndrome and if there is an increase in severity corresponding to mission duration for exploration class missions. Although the leading hypothesis is that increased intracranial pressure underlies the observed changes in affected crewmembers, due to the paucity of intracranial pressure measurements in these crewmembers the term optic-disc edema will be used in this report, rather than the term papilledema.

III. INTRODUCTION

To date, fifteen long-duration crewmembers have experienced in-flight and postflight visual and anatomical changes including optic-disc edema, globe flattening, choroidal folds, and hyperopic shifts as well as documented postflight elevated intracranial pressure (ICP). In the postflight time period, some individuals have experienced transient changes while others have experienced changes that are persisting with varying degrees of severity. While the underlying etiology of these changes is unknown at this time, the NASA medical community suspects that the microgravity-induced cephalad-fluid shift and commensurate changes in physiology play a significant role. The Human Health and Performance Directorate (formerly the Space Life Sciences Directorate [SLSD]) has assembled a VIIP project team to address this issue using a comprehensive project plan with regard to operations and research.

NASA has determined that the first documented case of a U.S. astronaut affected by the VIIP syndrome occurred in an astronaut during a long-duration International Space Station (ISS) mission. The astronaut noticed a marked decrease in near-visual acuity throughout the mission. This individual's postflight fundoscopic examination and fluorescence angiography revealed choroidal folds inferior to the optic disc and a cotton-wool spot in the right eye, with no evidence of optic-disc edema in either eye. The left eye examination was normal. The acquired choroidal folds gradually improved but were still present 3 years postflight. Brain MRI, lumbar puncture, and OCT were not performed preflight or postflight on this astronaut.

Additional cases of altered visual acuity have been reported since, and one case has included the report of a scotoma (visual field defect), which resulted in the astronaut having to tilt his head 15 degrees to view instruments and procedures. These visual symptoms persisted for over 12 months after flight. This type of functional deficit is not only of concern to the individual, but is of concern to the mission and the ISS program managers.

An alteration in visual acuity associated with spaceflight is not a new finding. Reports documented through medical testing, research, and anecdotal reports have circulated over the last 40 years. Mader et al. [1] recently provided case studies of seven long-duration astronauts who underwent extensive postflight medical examinations in response to reports of changes in visual acuity. Though these clinical findings were important unto themselves, the retrospective analysis of questionnaires posed to 300 short and long-duration crewmembers furthered our understanding of the phenomenon with the indication that these spaceflight-induced vision changes are not unique. Changes in visual acuity are not uncommon in astronauts, although there appears to be a higher prevalence among long-duration crewmembers. Specifically, 29% of short-duration and 60% of long-duration crewmembers reported degradation of long distance or near-visual acuity, which in some long-duration cases did not resolve in the years after the mission. In the seven ISS astronaut case studies, preflight eye examinations were normal, but most reported diminished visual acuity in flight that persisted after the mission. There is a constellation of symptoms and physiologic changes referred to as the VIIP syndrome, and a great deal of individual astronaut variability, where some astronauts are asymptomatic while others exhibit structural changes and large changes in visual acuity. Unfortunately, there is a general lack of data to more definitively link the cause(s) of the vision changes. Mader et al.[1] propose that cephalad-fluid shifts associated with microgravity may be a primary contributor

with downstream effects, with specific reference to the changes in the ocular structures, the optic nerve, and ICPs.

As a result of the Mader et al. [1] findings, further examination of medical data on the affected long-duration ISS crewmembers was performed to better characterize the constellation of symptoms and anatomical and physiologic changes. After exposure to spaceflight of 5 to 6 months duration, seven astronauts were discovered to have neuro-ophthalmic findings. The findings consist of disc edema in 5 astronauts, globe flattening in five astronauts, nerve fiber layer (NFL) thickening by OCT in six of the astronauts, complaints of a decrement in near vision in seven astronauts, choroidal folds in five astronauts, and cotton-wool spots in three astronauts. Five of the seven astronauts with complaints of altered near vision were documented to have a pre to post-mission hyperopic shift of equal to or greater than + 0.50 diopters (D) spherical equivalent refraction in one or both eyes (range +0.50 D to +1.50 D). Five of these seven were noted to have globe flattening by MRI. Lumbar punctures performed in four astronauts with disc edema showed opening pressures of 22, 21, 28, and 28.5 cm H₂O performed at 60, 19, 12 and 57 days post-mission, respectively. One astronaut has a sustained opening pressure of 22 cm H₂O 1700 days after flight. Disc edema was graded with the Modified Frisén Scale. Table 1 provides key points of clinical information for each astronaut obtained preflight, during the ISS mission and postflight, in no particular order. Data is available and approved for release for seven cases at this time. The evidence report will be updated as additional data is collected, analyzed, and or released. Disc edema was graded with the Modified Frisén Scale.

Risk of Microgravity-Induced Visual Impairment/Intracranial Pressure (ICP)

Table 1: Summary of VIIP Case Data Available at Time of Publication

ISS/Crew Member	Mission Duration	Refractive Change	Intraocular Pressure (mmHg)	Fundoscopic Exam Postflight	Disc Edema (Frisén)	OCT Postflight	Eye MRI Postflight	CSF Pressure Postflight (cmH2O)
							Globe Flattening	
CASE 1	6 months	Preflight: OD: -1.50 sph OS: -2.25-0.25x135 Postflight: OD: -1.25 -0.25x005 OS: -2.50-0.25x160	Preflight: 15 OU Postflight: 10 OU	<ul style="list-style-type: none"> Choroidal folds OD Cotton wool spot OD 	Edema: No disc edema	<ul style="list-style-type: none"> Choroidal folds still visible inferior to the OD disc (R+ >5yrs) 	MRI not performed Globe Flattening: Not assessed	Not measured
CASE 2	6 months	Preflight: OD: +0.75 OS:+0.75-0.25x165 Postflight: OD: +2.00 sph OS: +2.00-0.50x140	Preflight: 14 OU Postflight: 14 OU	<ul style="list-style-type: none"> Bilateral disc edema OD>OS Choroidal folds OD > OS Cotton wool spot OS 	Edema: Grade 1 OD and OS	<ul style="list-style-type: none"> NFL thickening c/w disc edema 	Optic nerve sheath distension OD and OS Globe Flattening: OD and OS	Elevated <ul style="list-style-type: none"> 22 at R+66 days; 26 at R+17 months; 22 at R+19 months)
CASE 3	6 months	Preflight: OD: -0.50 sph OS: -0.25 sph Postflight: Plano Plano	Preflight: 10 OU Postflight: 10 OU	<ul style="list-style-type: none"> Bilateral disc edema OD>OS Small hemorrhage OD 	Edema: Grade 3 OD Grade 1 OS	<ul style="list-style-type: none"> Severe NFL thickening OD>OS c/w Disc edema 	Optic nerve sheath distension OD Globe Flattening: None observed	Elevated <ul style="list-style-type: none"> 21 at R+19 days
CASE 4	6 months	Preflight: OD: -0.75-0.50x100 OS: plano-0.50x090 Postflight: OD: +0.75-0.50x105 OS: +0.75-0.75x090	Preflight: 15/13 Postflight: 11/10	<ul style="list-style-type: none"> Disc edema OD Choroidal folds OD 	Edema: Grade 1 OD	<ul style="list-style-type: none"> Mild NFL thickening OD>OS c/w disc edema Choroidal folds OD 	Optic nerve sheath distension and tortuous optic nerves OD>OS Globe Flattening: OD > OS	Elevated <ul style="list-style-type: none"> 28.5 at R+57 days
CASE 5	6 months	Preflight: OD: -5.75-1.25x010 OS: -5.00-1.50x180 Postflight: OD: -5.00-1.50x015 OS: -4.75-1.75x170	Preflight: 14/12 Postflight: 14/12	<ul style="list-style-type: none"> Normal 	Edema: No disc edema	<ul style="list-style-type: none"> Subclinical disc edema Mild/moderate NFL thickening OD 	Optic nerve sheath distension and tortuous optic nerves Globe Flattening: OD and OS	Not measured

Risk of Microgravity-Induced Visual Impairment/Intracranial Pressure (ICP)

CASE 6	6 months	Preflight: OD: +0.25 OS: +0.25-0.50x152	Preflight: 14 OU Postflight: 14 OU	<ul style="list-style-type: none"> • Disc edema OD • Cotton wool spot OS 	Edema: Grade 1 OD	<ul style="list-style-type: none"> • Mild NFL thickening c/w disc edema • Choroidal folds OD 	Optic nerve sheath distension OD>OS	Not Measured
		Postflight: OD: +2.00-0.50x028 OS: +1.00 sph					Globe Flattening: OD > OS	
CASE 7	6 months	Preflight: OD: +1.25 sph OS: +1.25 sph	Preflight: 16 OU Postflight: 12/14	<ul style="list-style-type: none"> • Disc edema OU • Choroidal folds OD>OS 	Edema: Grade 1 OD and OS	<ul style="list-style-type: none"> • Moderate NFL thickening c/w disc edema OD and OS • Choroidal folds OD and OS 	Optic nerve sheath distension OD and OS	Elevated • 28 at R+12 days
		Postflight: OD: +2.75 sph OS: +2.50 sph					Globe flattening: OD and OS	

(OD=right, OS=left, OU=both eyes, sph=sphere, OCT=optical coherence tomography, MRI=magnetic resonance imaging, CSF=cerebral spinal fluid, NFL=retinal nerve fiber layer, R+=return to Earth; [presented by number of days, for example, R+19 is 19 days after return to Earth])

It is important to recognize that visual symptoms reported by astronauts in the past were often minor, transient, not accompanied by other symptoms or significant clinical findings, and are a common finding in the general population of 40 to 50-year-old individuals. Increased ICP was not suspected and no testing was performed to evaluate changes. Due to potential functional visual deficits from induced hyperopic shifts, persistent symptoms, and the acquisition of detailed anatomical images suggesting architectural alterations, NASA is taking a much more aggressive approach to addressing this problem through the VIIP project.

A VIIP Summit was held in February 2011 to solicit input and recommendations from a diverse group of experts from the fields of medicine and research, and to function as the forum in which the scope of the problem was defined. A subset of these experts will serve on a Research and Clinical Advisory Panel (RCAP) to provide guidance for the future research project. A summary of the meeting and recommendations can be found in The Visual Impairment Intracranial Pressure Summit Report [2].

NASA's Space and Clinical Operations Division, in collaboration with the VIIP project, has implemented an expanded set of medically required preflight, in-flight, and postflight testing (Appendix A: MedB 1.10) to determine the existence and degree of the ophthalmic and ICP alterations. To facilitate the in-flight collection of data, the Space Medicine Division and the VIIP project have increased the on-orbit imaging capability by recently flying a video fundoscope and state-of-the-art hand-held tonometer, and developing procedures for eye ultrasound to characterize globe flattening and increases in optic nerve sheath diameter (ONSD). The Space Medicine Division and the VIIP project are also developing a study to evaluate a noninvasive ICP monitoring device for the clinical evaluation of ICP preflight, in flight, and postflight. This increased capability and expanded set of tests are used to inform the medical treatment of the individual astronauts as well as characterize the manifestation of the pathology to inform the astronaut corps and the spaceflight community in general. The results of these tests and images can function on an individual level to inform medical care and occupational health decisions. On a population level, these results can inform risk management decisions. Additionally, all of these data are used in conjunction with human research data acquired over the life of the space program to determine the potential scope of the forward research plan.

Note: A wide variety of pressure types are mentioned throughout the document, including ICP/cerebrospinal fluid (CSF) opening pressure, intraocular pressure (IOP), central venous pressure (CVP), capillary fluid pressure, interstitial pressure, mean arterial pressure, arterial pulse pressure, and partial pressure of CO₂ (ppCO₂). While different publications may report these pressures in either mm Hg or cm H₂O, to maintain consistency of units in this report, this document will report ICP/CSF opening pressures in cm H₂O (and in cases where a quoted reference used mm Hg the value in cm H₂O will be given in parentheses). All other types of pressures mentioned previously (IOP, CVP, etc.) will be reported in mm Hg (and in cases where a quoted reference used cm H₂O the value in mm Hg will be given in parentheses).

IV. SPACEFLIGHT EVIDENCE

A. Summary of Existing Long-Duration Flight Data

The first U.S. case of visual changes observed on orbit was reported by a long-duration astronaut that noticed a marked decrease in near-visual acuity throughout his mission onboard the ISS, but at no time reported headaches, transient visual obscurations, pulsatile tinnitus, or diplopia. His postflight fundus examination (Figure 1) revealed choroidal folds inferior to the optic disc and a single cotton-wool spot in the inferior arcade of the right eye. The acquired choroidal folds gradually improved but were still present 3 years postflight. The left eye examination was normal. There was no documented evidence of optic-disc edema in either eye. Brain MRI, lumbar puncture, and OCT were not performed preflight or postflight on this astronaut.

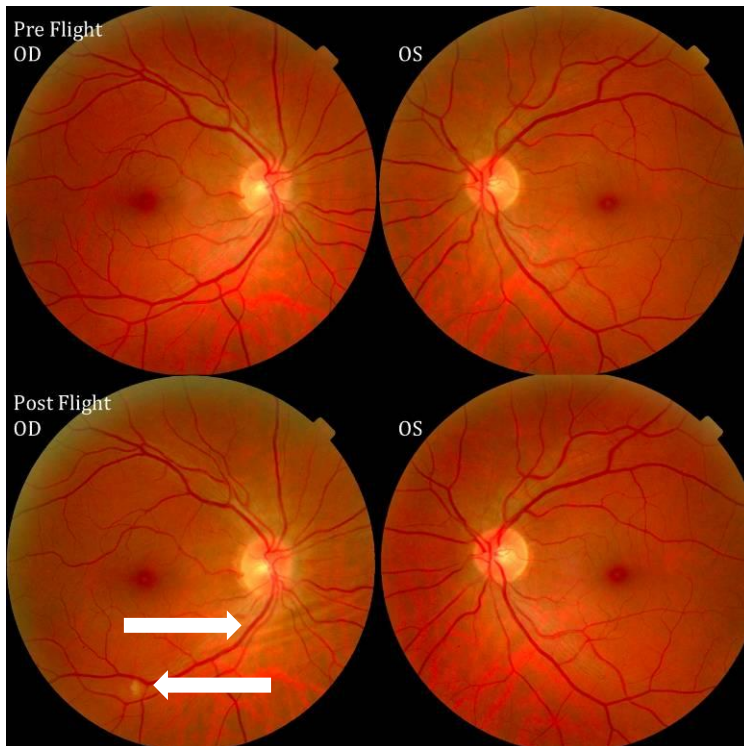


Figure 1: Fundus examination of first case of visual changes from long-duration spaceflight. Fundus examination revealed choroidal folds inferior to the optic disc and a single cotton-wool spot in the inferior arcade of the right eye (white arrows).

The second case of visual changes secondary to long-duration spaceflight onboard the ISS was reported approximately 3 months after launch when the astronaut noticed that he could now only see the Earth clearly while looking through his reading glasses. This change continued for the remainder of the mission without noticeable improvement or progression. He did not complain of transient visual obscurations, headaches, diplopia, pulsatile tinnitus, or visual changes during eye movement. In the months since landing he has noted a gradual but incomplete improvement in vision.

Fluorescein angiography confirmed the choroidal folds (Figure 2). A magnetic resonance angiography (MRA) and magnetic resonance venogram (MRV) were normal. An OCT confirmed the increased retinal nerve fiber layer (NFL) thickening consistent with optic-disc edema nasally and demonstrated a normal macular retinal NFL thickness. A lumbar puncture, 2

months after return to Earth, documented a borderline opening pressure of 22 cm H₂O (normal range 6.8-20.4 cm H₂O) with normal CSF composition. The astronaut had additional postflight lumbar punctures with documented opening pressures of 26 and 22 cm H₂O at 17 and 19 months, respectively, with no improvement in visual acuity.

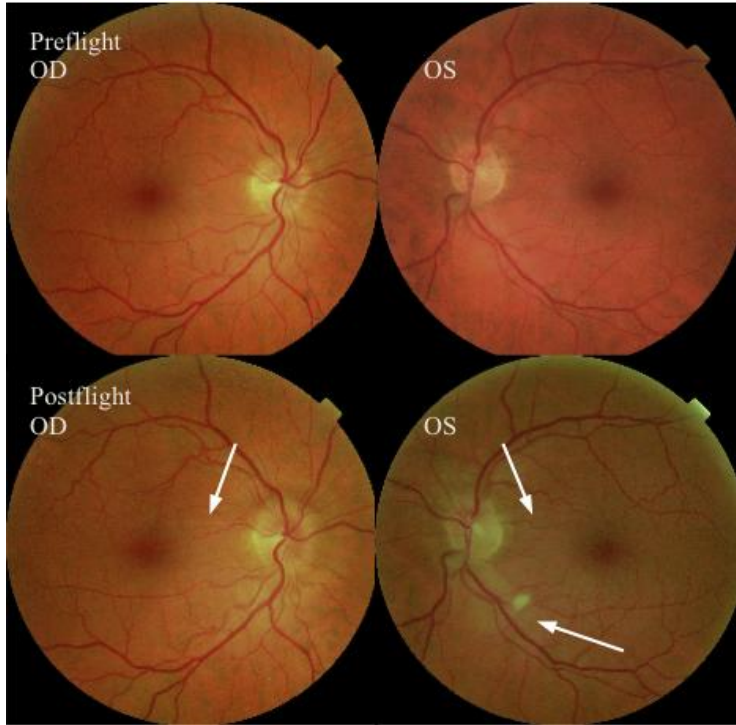


Figure 2: Fundus examination of second case of visual changes from long-duration spaceflight. Fundoscopic images showing, choroidal folds (white arrows) in the papillomacular bundle area in the right eye and left eye and a cotton-wool spot (bottom arrow) at the inferior arcade in the left eye. Both optic discs show grade 1 disc edema.

The third case of visual changes secondary to spaceflight onboard the ISS presented asymptotically with no changes in visual acuity during the mission and no complaints of headaches, transient visual obscurations, diplopia, or pulsatile tinnitus. Upon return to Earth, no eye issues were reported by the astronaut at landing. Fundus examination revealed bilateral, asymmetrical disc edema (OD: grade 3 on the Frisén scale; OS: grade 1) (Figure 3). There was no evidence of choroidal folds or cotton-wool spots. A small hemorrhage was observed inferior to the optic disc in the right eye. This astronaut had the most pronounced optic-disc edema of all the astronauts reported to date, but had no choroidal folds, globe flattening, or hyperopic shift. At 10 days post-landing an MRI of the brain and orbits was normal. However, there appeared to be a mild increase in CSF signal around the right optic nerve. A MRV showed no evidence for cerebral venous sinus thrombosis. An OCT showed marked NFL thickening (OD>OS) consistent with optic-disc edema (Figure 4). A lumbar puncture, 19 days after return to Earth, documented a mildly elevated opening pressure of 21 cm H₂O (normal range 6.8-20.4 cm H₂O) with normal CSF composition.

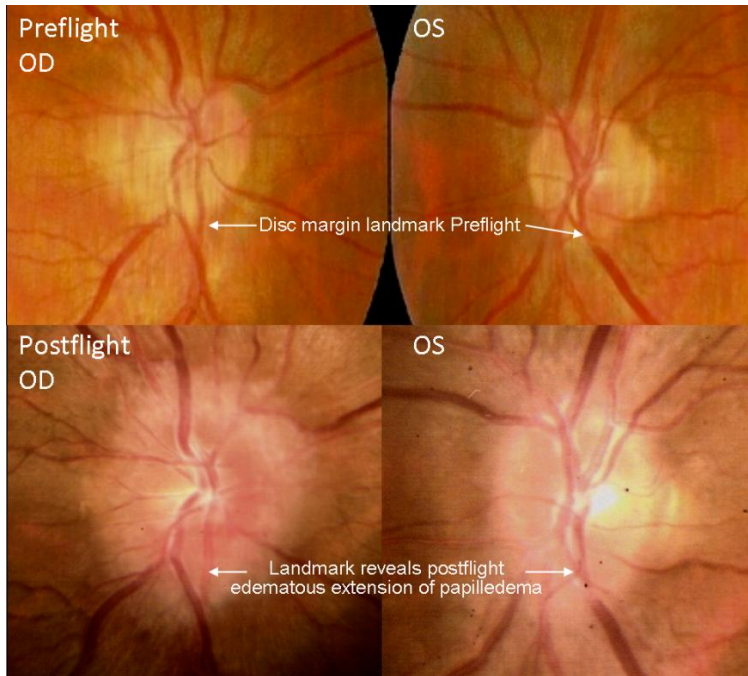


Figure 3: Fundus examination of third case of visual changes from long-duration spaceflight. Fundoscopic images of the right and left optic disc showing profound grade 3 edema at the right optic disc and grade 1 edema at the left optic disc. Adapted from Mader TH et al. [1] with permission from Elsevier, obtained via Copyright Clearance Center, Inc.

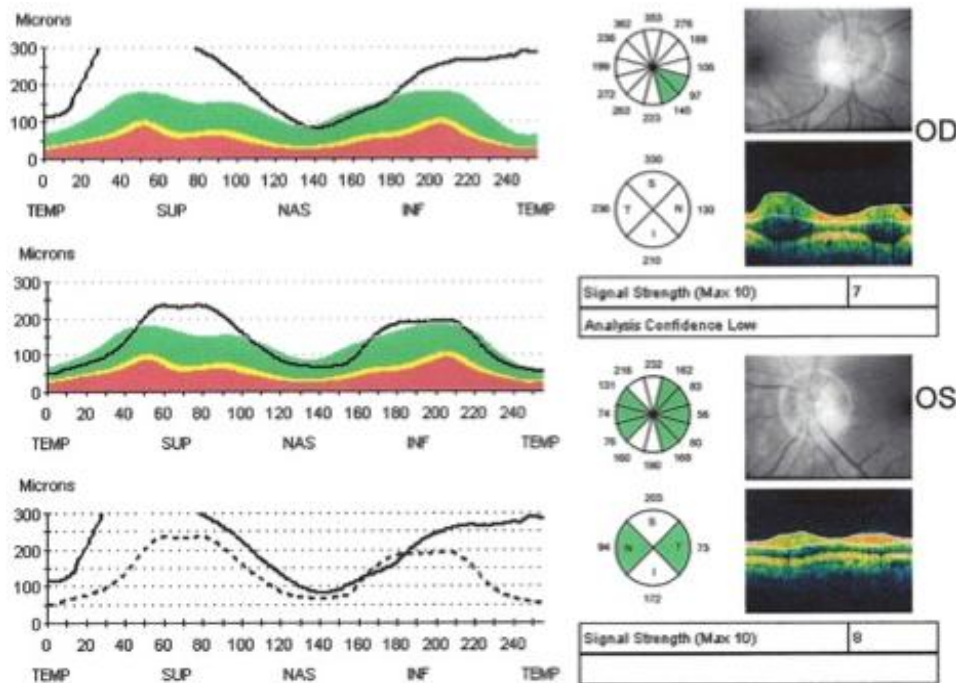


Figure 4: OCT examination of third case of visual changes from long-duration spaceflight. Postflight Zeiss Stratus OCT scans show significant NFL thickening (black line upper panel) consistent with the observed bilateral optic-disc edema (OD>OS). Retinal Nerve Fiber Layer (RNFL) Thickness Profile – The black line indicates the thickness values of the patient’s scan around the optic disc from temporal, superior, nasal, inferior to temporal (TSNIT). Colors indicate comparison versus normative database. Green: Within normal limits, with values inside the 95% normal range. Yellow: Borderline, with values outside 95% but within 99% confidence interval of the normal distribution ($.01 < P < .05$). Red: Outside normal limits, with values outside 99% confidence interval of the normal distribution.

The fourth case of visual changes on orbit was significant for a past medical history of transsphenoidal hypophysectomy for macroadenoma, but postoperative imaging showed no residual or recurrent disease. Approximately 2 months into the ISS mission the astronaut noticed a progressive decrease in near-visual acuity in his right eye and a scotoma in his right temporal field of vision. He described the scotoma to be fixed and translucent such that he could not read normal 12-point font through it and it was the ‘shape’ of a football held upright at arm’s length’. The astronaut denied transient visual obscurations, headaches, diplopia, pulsatile tinnitus, or vision changes during eye movement and environmental parameters including carbon dioxide (CO₂) were within the normal operating levels of the ISS for the duration of the mission (CO₂ levels on the ISS are nominally between 2.3 to 5.3 mm Hg). During the mission the astronaut used a topical corticosteroid and oral ketoconazole for a facial rash, occasional vitamin D supplements, and promethazine to treat symptoms of space adaptation syndrome. He had never used tetracycline or nalidixic acid. He participated in two EVAs during the mission and was not exposed to any toxic fumes.

Preflight eye examination of the fourth astronaut with the scotoma revealed a cycloplegic refraction of $-0.75-0.50 \times 100$ on the right and plano -0.50×090 on the left, correctable in each eye to 20/15. He had a reading add of +2.00 OU. Ten days postflight, the astronaut with the scotoma had a visual acuity that was correctable to 20/15 with a cycloplegic refraction of $+0.75-0.50 \times 105$ on the right and to $+0.75-0.75 \times 090$ on the left. He never experienced losses in subjective best-corrected acuity, color vision, or stereopsis. Fundus examination revealed mild, nasal disc edema (grade 1 Frisén scale) of the right eye with choroidal folds extending from the disc into the macula.

During this mission, another ISS long-duration astronaut reported the fifth case of decreased near-visual acuity after 3 weeks of spaceflight requiring additional 1 to 2 diopters (D) in his glasses to read procedures and handle equipment. CO₂, cabin pressure, and oxygen (O₂) were reported to be within the allowable levels during all missions and none of the astronauts were exposed to any toxic fumes.

External expert consultants to NASA [3] concluded that “the data seem to point to an eye/orbit-centered problem, and intracranial hypertension as the mechanism seems less likely, although it cannot be completely ruled out at this point in time”. In-flight ocular ultrasound exams were performed on the astronauts who represented the fourth and fifth cases of visual changes during a space mission to rule out increased ONSD, posterior globe flattening, detached retina, chorioretinopathy, raised optic disc, and confirm normal anterior eye anatomy. The ocular ultrasound was used because previous studies had validated the procedure [4-8] and NASA had successfully performed ultrasound examination of the eye on board the ISS with a nonexpert operator using remote guidance.[9] The remotely guided ultrasound examinations of the eye in these astronauts demonstrated posterior flattening of the globe, dilated optic nerve sheaths, bilaterally distended jugular veins, and a raised right optic disc in the astronaut with the scotoma (Figures 5 and 6). Image files of a near and far acuity chart and an Amsler grid were uploaded and printed on orbit. Both astronauts reported near-visual acuity decrements.

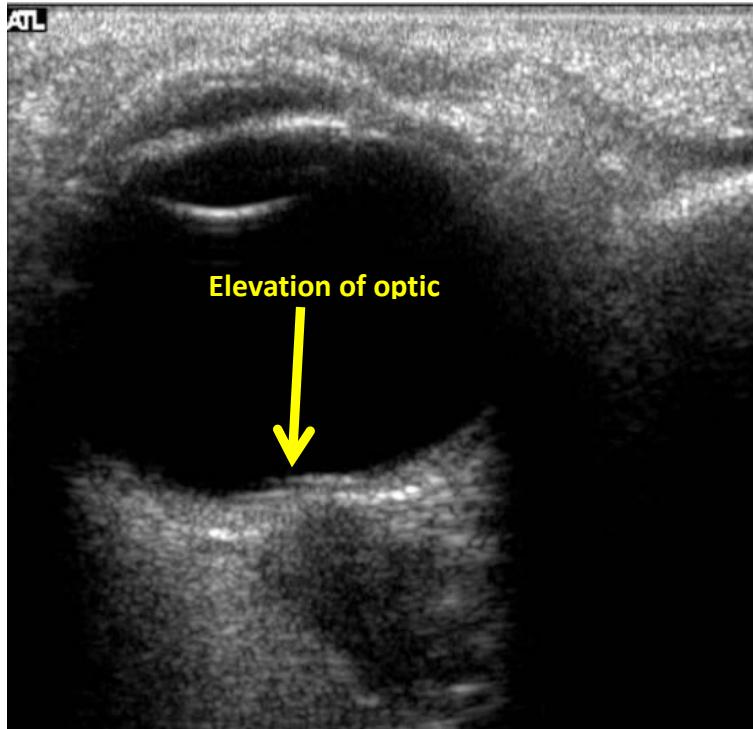


Figure 5: On-orbit ultrasound of posterior orbit of the fourth case of visual changes from long-duration spaceflight. In-flight ultrasound image of the right eye showing posterior globe flattening and a raised optic disc consistent with optic-disc edema and raised ICP.

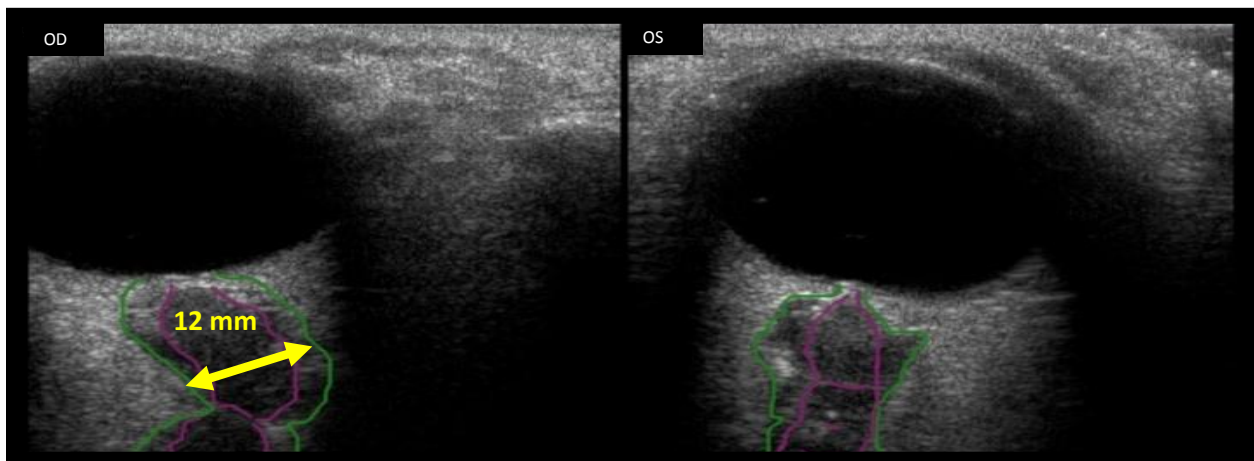


Figure 6: On-orbit ultrasound of optic nerves of the fourth case of visual changes from long-duration spaceflight. In-flight ultrasound shows proximal kinking and increased ONSD of approximately 12 mm that is consistent with raised ICPs. Optic nerve shown in purple and the ONSD in green.

Three weeks after the ultrasound examination and Amsler grid testing, reading glasses (2.5 D and 3.25 D) were delivered to the ISS via a Shuttle mission and one astronaut reported that the 3.25 D glasses worked best. A video-ophthalmoscope system was also delivered to the ISS from the Shuttle and remotely guided dilated fundoscopic exams (Figure 7) were performed on both astronauts during the presleep period (so other activities would not be impacted by the visual acuity loss from Tropicamide drops). The astronauts took turns being the operator and subject during these examinations and were given preflight fundoscopic images to use as references. The fundoscopic video and captured images were downloaded from the ISS and sent to neuro-ophthalmological consultants who determined that the temporal location and shape of the

reported scotoma was thought to be consistent with disc edema (that is, enlarged blind spot). The other astronaut had a normal fundoscopic exam. Consultants agreed that no treatment was indicated at this time and that these images would serve as a baseline to follow throughout the rest of the mission. The inability to measure IOP on the ISS was also a factor in deferring any pharmacological interventions. Monthly remotely guided ocular ultrasound, dilated video fundoscopic, and visual acuity exams were performed for the duration of the mission. These images allowed experts on the ground to make a diagnosis of mild optic-disc edema in the right eye. Postflight fundus examination revealed mild, nasal optic-disc edema (grade 1 Frisén Scale) of the right eye with choroidal folds extending from the disc into the macula. Postflight OCT confirmed optic-disc edema and choroidal folds (Figure 8).

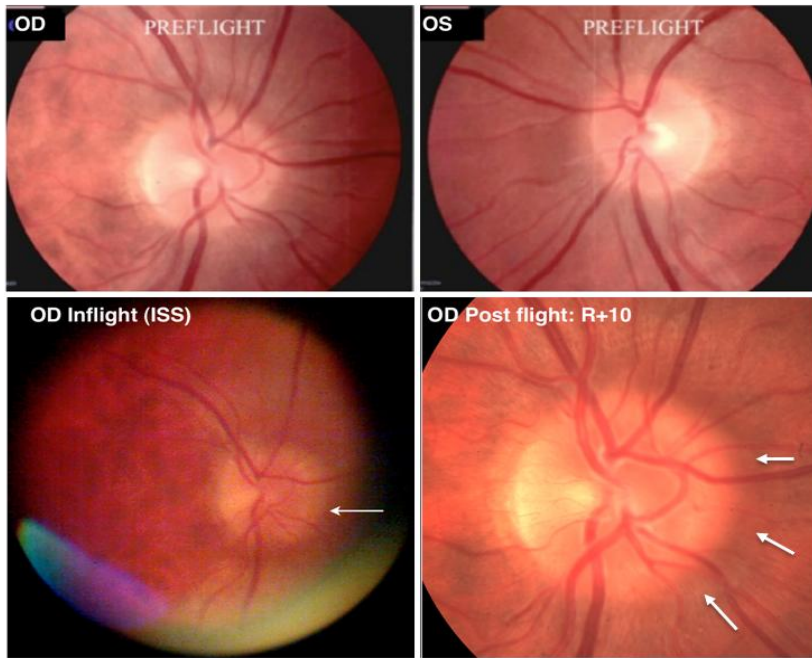


Figure 7: Fundus images from the ISS of the fourth case of visual changes from long-duration spaceflight. (Top) Preflight optic nerve head photography. (Bottom left) In-flight (ISS) photography of the right optic disc obtained by remote guidance showing “C” halo associated with Grade 1 edema. (Bottom right) Postflight (R+10) shows the “C” halo edema effect in greater detail with subtle nerve fiber glutting beyond the border of the edematous disc (arrows). Adapted from Mader TH et al. [1] with permission from Elsevier, obtained via Copyright Clearance Center, Inc.

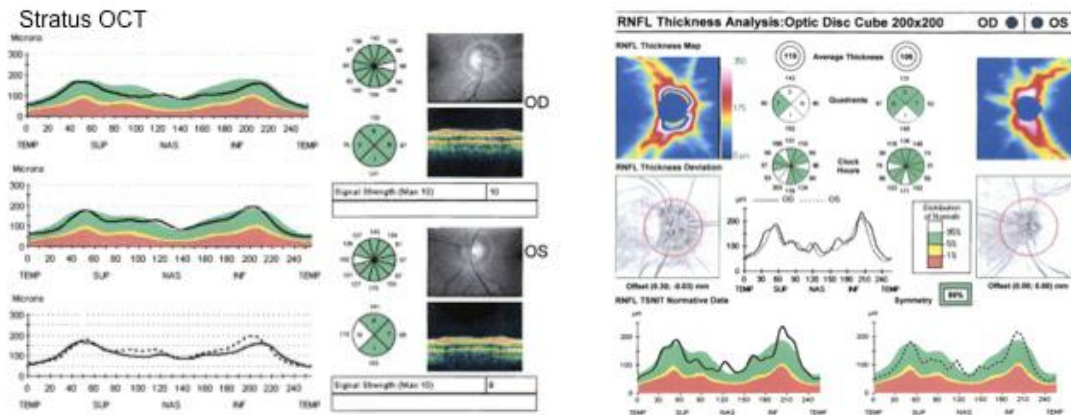


Figure 8: OCT of the fourth case of visual changes from long-duration spaceflight (right). Preflight Zeiss Stratus OCT showing the right and left NFL ‘TSNIT’ curve (left). Postflight Zeiss Cirrus OCT showing increased thickness of nerve fiber layer ‘TSNIT’ due to disc edema. Greater increase is noted in the right eye inferior consistent with postflight optic-disc photography.

During the fourth and fifth astronauts' mission, immediate postflight astronaut return was implemented allowing for 3-Tesla MRI images of the eye to be obtained within 3 days of landing. Previously, astronauts were scheduled to recover for 21 days after landing in Star City, Russia and 3-Tesla MRI facilities were not available. As these crews did not have preflight 3-Tesla head and orbit MRI's, the standard 1.5-Tesla head MRI, MRA, and MRV obtained upon selection into the ISS training flow, several years before mission assignment, were used to confirm the absence of increased ONSD or posterior globe flattening preflight.

The MRI of the brain and orbits performed on the fourth astronaut 30 days after return documented bilateral severely dilated optic nerve sheaths, right greater than left, bilateral flattening of the posterior globe, right greater than left, and thickened tortuous optic nerves (Figures 9–11). An intracranial MRV and MRA subsequently obtained showed no abnormalities. A lumbar puncture, 57 days after return to Earth, documented an elevated opening pressure of 28.5 cm H₂O with normal CSF composition.

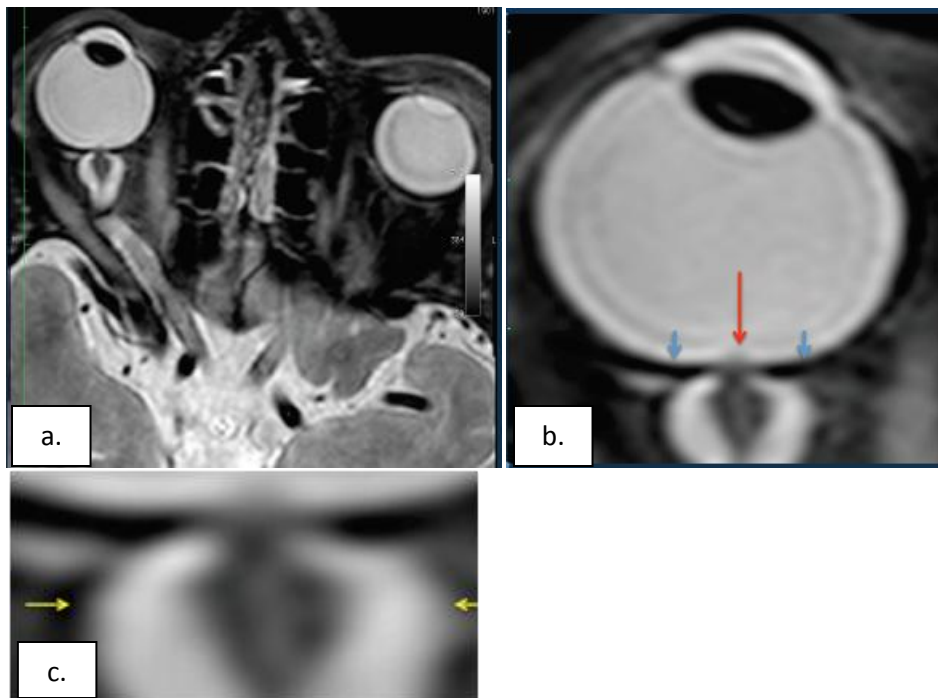


Figure 9: MRI (R+30 days) of the fourth case of visual changes from long-duration spaceflight (a). There remains bilateral severe optic sheath dilatation. The right optic sheath diameter measures 10 to 11 mm (b and c); and the left optic sheath diameter measures 8 mm. These numbers are similar to the R+3 examination. There is evidence of papilledema on the right eye only. There is residual flattening of the posterior globes. The optic nerve remains thickened bilaterally measuring up to 5 mm on the right and 4 mm on the left. There also remains bilateral tortuosity of the optic nerve sheaths with the kink at the optic nerve sheath approximately 1.1 cm behind the posterior margin of the globe. Red arrow depicts the optic-disc edema, blue arrows show the flattened globe and the yellow arrows illustrate the distended optic nerve sheath. Figure 9b reproduced from Mader TH et al. [1] with permission from Elsevier, obtained via Copyright Clearance Center, Inc.

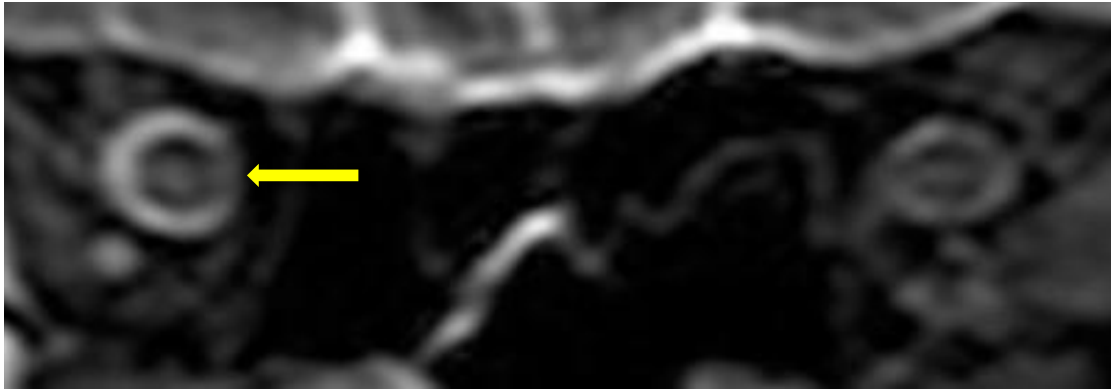


Figure 10: MRI (R+30 days) of the fourth case of visual changes from long-duration spaceflight. There is prominence of central T2-hyperintensity of the optic nerves bilaterally, right greater than left approximately 10 to 12 mm posterior to the globe (arrow) that represents an element of optic nerve congestion.

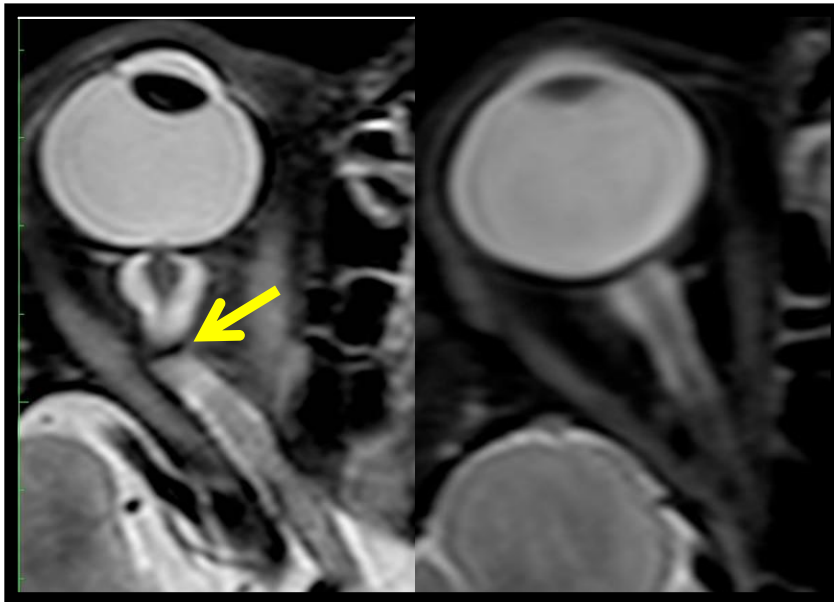


Figure 11: MRI (R+30 days) of the fourth case of visual changes from long-duration spaceflight. Tortuous optic nerve and kink on left (arrow). Control orbit on right.

The fifth case of visual changes observed on the ISS was noticed only 3 weeks into his mission. This change continued for the remainder of the mission without noticeable improvement or progression. He never complained of headaches, transient visual obscurations, diplopia, pulsatile tinnitus, or other visual changes.

The preflight eye examination revealed a cycloplegic refraction of $-5.75-1.25 \times 010$ on the right, and $-5.00-1.50 \times 180$ on the left, correctable in each eye to 20/20 with a reading add of +1.75 OU. Dilated eye examination and fundus photos were normal. Upon return to Earth he noted persistence of the vision changes he observed in space. Postflight visual acuity was correctable to 20/20 OU with a manifest and cycloplegic refraction of $-5.00-1.50 \times 015$ on the right and $-4.75-1.75 \times 170$ on the left and a reading add of +2.25 OU. He never experienced losses in subjective best-corrected acuity, color vision, or stereopsis. His fundus examination

was normal with no evidence of disc edema or choroidal folds. However, an MRI of the brain and orbits, and ultrasound of the globes performed 8 days after landing, revealed bilateral posterior globe flattening, distended optic nerve sheaths, and tortuous optic nerves. OCT showed significant NFL thickening relative to preflight values and a normal macula (Figure 12). A lumbar puncture was not performed. This case is interesting because the astronaut did not have disc edema or choroidal folds but was documented to have NFL thickening, globe flattening, a hyperopic shift, and subjective complaints of loss of near vision.

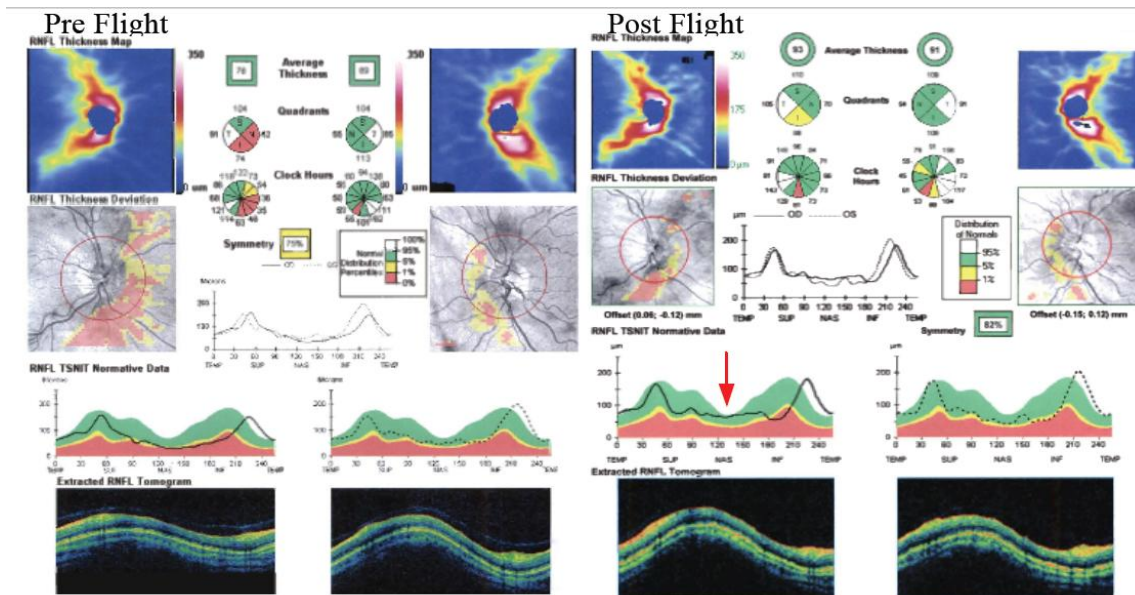


Figure 12: OCT (R+13 days) of the fifth case of visual changes from long-duration spaceflight (left). Preflight Zeiss Cirrus OCT showing right and left NFL ‘TSNIT’ (right). Postflight Zeiss Cirrus OCT shows increased thickness of the nasal (red arrow) NFL. Greater increase is noted in the right eye in the nasal quadrant NFL thickness; 42 μm preflight to 70 μm postflight. Fundus and optic-disc imaging did not show presence of observable disc edema.

The sixth case of visual changes of an ISS astronaut was reported after return to Earth from a 6-month mission, when he noticed that his far vision was clearer through his reading glasses. A fundus examination was performed 3 weeks postflight that documented mild (grade 1) nasal optic-disc edema in the right eye only. There was no evidence of disc edema in the left eye or choroidal folds in either eye (Figure 13). MRI of the brain and orbits, performed 46 days after return, revealed bilateral flattening of the posterior globe, right greater than left, and a mildly distended right optic nerve sheath. There was also evidence of optic-disc edema in the right eye.

Fundus examination and OCT, performed 60 days postflight, documented mild disc edema and a ‘new onset’ cotton-wool spot in the left eye 2-disc diameters superior temporal to the disc, just inside the superior arcade. This was not observed in the fundus photographs taken 3 weeks postflight (Figure 14).

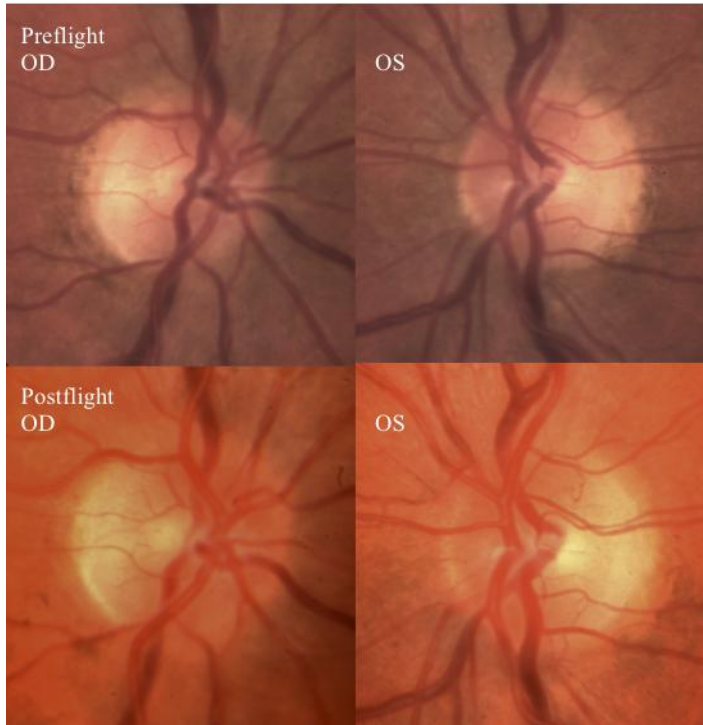
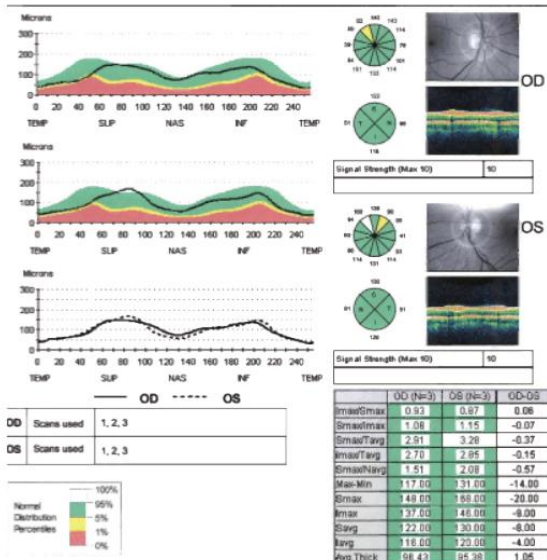


Figure 13: Fundus examination of the sixth case of visual changes from long-duration spaceflight. Preflight images of normal optic disc. Postflight right and left optic disc showing grade 1 (superior and nasal) edema at the right optic disc.

Optical Coherence Tomography
Pre Flight (Zeiss Stratus)



Post Flight (Zeiss Cirrus)

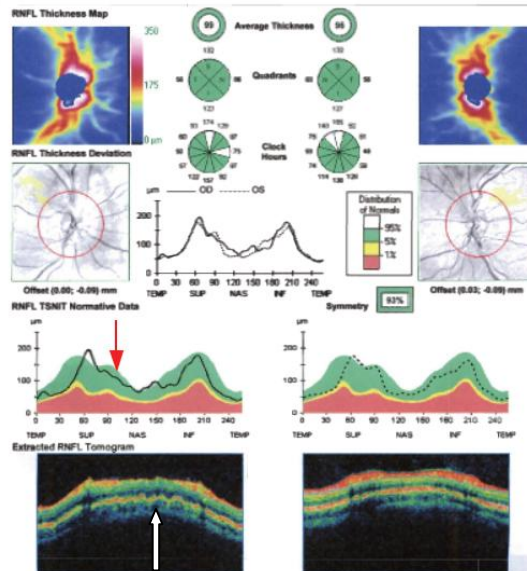


Figure 14: OCT of sixth case of visual changes from long-duration spaceflight. Preflight Zeiss Stratus OCT showing the NFL 'TSNIT' curve. Postflight Zeiss Cirrus OCT showing a 50 μ increase in thickness (50% increase) of the nerve fiber layer at the superior and inferior poles (red arrow) consistent with changes seen in postflight optic nerve head photography. Choroidal folds are also visible (white arrow).

The seventh case of visual changes associated with spaceflight is significant in that it was eventually treated postflight. His preflight cycloplegic refraction was +1.25 sphere in both eyes with a normal fundus exam. Approximately 2 months into the ISS mission the astronaut reported a progressive decrease in his near and far acuity in both eyes that persisted for the remainder of the mission. At approximately 3 to 4 months into the 6-month mission he noticed that his normal 'Earth' prescription progressive glasses were no longer strong enough for near tasks at which time he began using his stronger 'Space Anticipation Glasses' (+1.25 D more plus). He never complained of transient visual obscurations, headaches, diplopia, pulsatile tinnitus, or vision changes during eye movement. The ISS cabin pressure, CO₂, and O₂ levels were reported to be at normal operating levels during the mission (of note, the CO₂ levels on the ISS are nominally between 2.3 to 5.3 mm Hg, equal to 10-20 times the normal terrestrial atmospheric level, which is 0.23 mmHg). He was not exposed to any toxic substances. Three days after his return to Earth his visual acuity was correctable to 20/20 OU with a cycloplegic refraction of +2.75 sphere on the right, and +2.50 sphere on the left. He never experienced losses in subjective best-corrected acuity, color vision, or stereopsis. A fundus examination revealed mild bilateral optic-disc edema (grade 1), and choroidal folds (Figures 15 and 16).

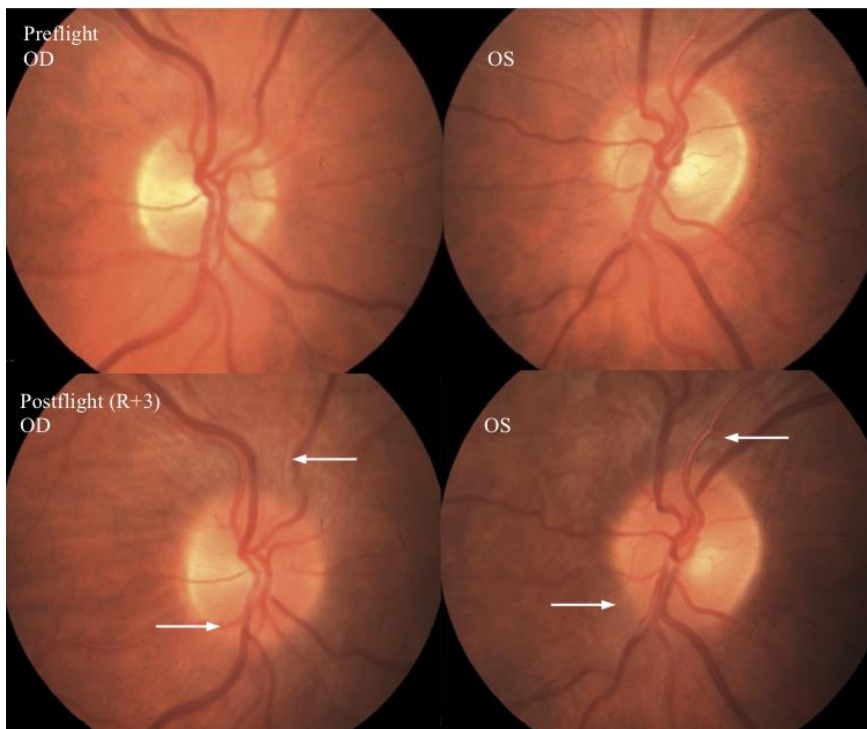


Figure 15: Preflight images of the right and left optic discs (upper). Postflight images of the ONH showing in more detail the extent of the edematous optic-disc margins and glutting of the superior and inferior nerve fiber layer axons OD and OS (arrows) (lower).

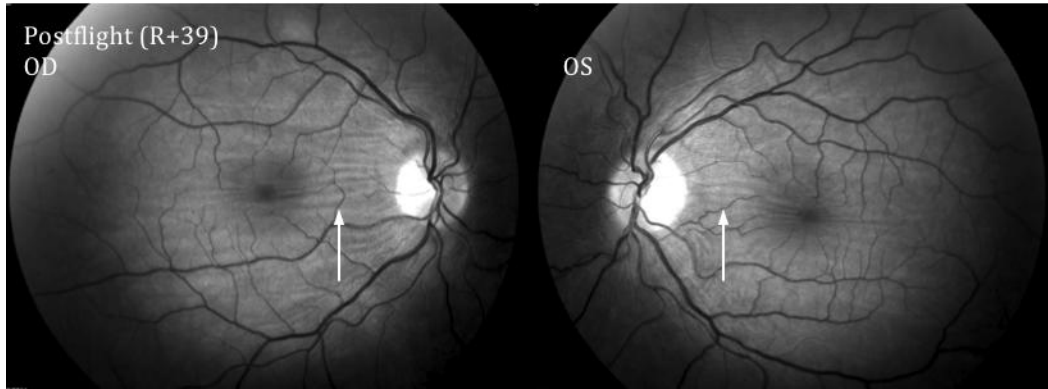


Figure 16: Postflight at 'return to Earth +39 days' (R+39) red-free fundus photography highlighting the extent of the horizontal choroidal and retinal folds in the posterior fundus (OD>OS). Adapted from Mader TH et al. [1] with permission from Elsevier, obtained via Copyright Clearance Center, Inc.

An OCT confirmed optic-disc edema and choroidal folds. An MRI of the brain and orbits performed 6 days postflight documented bilateral flattening of the posterior globes, distended optic nerve sheaths and optic-disc edema. A lumbar puncture, 12 days after return to Earth, documented an elevated opening pressure of 28 cm H₂O with normal CSF composition.

The astronaut was treated with 500 mg Diamox twice daily and his opening pressure decreased to 19 cm H₂O. This astronaut's creatinine increased to 1.8 after 2 weeks and therefore his dose was decreased to 250 mg twice daily for 3 months.

The disc edema, posterior globe flattening, choroidal folds, and hyperopic shift seen in cases 2, 4, 6, and 7 appear consistent with findings of increased intracranial hypertension. Cases 2, 4, 6, and 7 presented with optic nerve sheath distention and posterior globe flattening as documented by MRI 23, 30, 46, 6, and 7 days post-mission, respectively. Additionally, cases 4 and 7 had elevated lumbar puncture opening pressures of 28.5 and 28 cm H₂O at 57 days and 12 days, respectively after returning to Earth. The CSF opening pressures of cases 2 and 3 were measured 66 days and 19 days, respectively after return to Earth and were not dramatically elevated but were above the normal range of approximately 10 to 20 cm H₂O for a healthy adult [10].

In summary, although a definitive etiology for these findings is unknown, it has been hypothesized that venous congestion in the brain and/or eye, brought about by cephalad-fluid shifts and which may have exacerbated choroidal volume changes, may be a unifying pathologic mechanism. In light of the observations of vision change, optic-disc edema, choroidal folds, and changes in the ocular ultrasound, head and orbit MRI, increased ICP, and fundoscopic image changes, NASA has initiated an enhanced occupational monitoring program for all mission astronauts with special attention to signs and symptoms related to ICP.

Interestingly, similar findings have previously been reported among Russian cosmonauts who flew long-duration missions on the MIR Orbital Space Station (the station was operational until 2001). The findings, published by Myasnikov and Stepanova in 2008 [11], were part of a study evaluating the retina by ophthalmoscopy, linear velocity of blood flow in the straight venous sinus of the brain by transcranial Doppler, and structural changes in the brain by MRI, under the

premise that psychological difficulties reported in long-duration crewmembers could be caused by impaired in-flight cerebral hemodynamics. The study included 16 cosmonauts, of which 8 were found to have mild to moderate optic-disc edema on landing day, corresponding to NASA's CPG class 3 and 4. In addition to optic-disc edema, transcranial Doppler confirmed elevation of linear velocity of blood flow in the straight venous sinus of the brain in 9 of 13 crewmembers who underwent Doppler testing, with flow velocities ranging from 30-47 cm/sec (normal range 14-28 cm/sec). MRI of the brain was obtained in 10 of the crewmembers, with one exhibiting "signs of moderate intracranial hypertension" although the signs themselves are not described. This crewmember was noted to have congenital low-lying cerebellar tonsils, which were thought to have impeded CSF outflow from the cranium into the spinal canal. A second MRI obtained three months postflight reported resolution of the signs of intracranial hypertension. Of note, the spaceflight environment of the MIR was very similar to that of the ISS, including exposure to both microgravity and high levels of CO₂.

B. Summary of Human System Spaceflight Physiology

1. Ocular Evidence

This section is a compendium of how evidence gathered from the literature and astronaut data pertaining to anatomical and physiologic changes observed in relation to extended stay in spaceflight relates to pathophysiologic conditions on Earth that share common signs and symptoms with the former. It is intended to assist with the initial characterization of the risk of visual impairment and ICP.

a) Visual Acuity Disturbance and Elevated ICP in Spaceflight

Mader et al. provided a review of seven of the fifteen documented cases reported of male astronauts, 50.2 +/- 4.2 years, who have experienced in-flight visual changes [1]. Since Mader's publication, a review of data has identified eight additional cases, although some are identified with less precise detection methods. The seven cases described by Mader correspond to astronauts who spent 6 months on board the ISS. The ophthalmic findings consisted of disc edema in five cases, globe flattening in five (all of which demonstrated optic sheath distention), choroidal folds in five, 'cotton-wool spots' in three, nerve fiber layer thickening detected by OCT in six, and decreased near vision in seven astronauts. Five out of seven cases with near vision complaints had a hyperopic shift of 0.50 D cycloplegic refractive change or more between pre and post-mission. Some of these refractive changes remain unresolved years after flight. Lumbar punctures performed in four cases with disc edema (out of 7) revealed opening pressures of 22, 21, 28, and 28.5 cm H₂O, performed at 60, 19, 12, and 57 days post-mission, respectively. While the etiology remains unknown, it is proposed that these findings may represent manifestations of a pathologic process related to (but not limited to) the eye and the optic nerve, the brain, and the vascular system (venous congestion in the brain and the eye orbit), in concert with intracranial effects caused by cephalad-fluid shifts experienced during microgravity exposure.

b) *Intraocular Pressure (IOP)*

Intraocular pressure (IOP) is determined by the production, circulation and drainage of ocular aqueous humor and is described by the equation:

$$IOP = F/C + PV$$

where F=aqueous fluid formation rate, C = aqueous outflow rate, and PV = episcleral venous pressure.

In the general population, IOP ranges between 10 and 20 mm Hg with an average of 15.5 mm Hg. Diurnal variation for normal eyes is between 3 and 6 mm Hg, with a nocturnal peak independent of body position change (Figure 17) [12-14]. Besides circadian variation, IOP has been shown to increase by 3 to 4 mm Hg in both normal and glaucomatous patients lying supine, regardless of the time of the day [15].

Aqueous flow averages 2.9 $\mu\text{L}/\text{min}$ in young healthy adults and 2.2 $\mu\text{L}/\text{min}$ in octogenarians, and has a circadian pattern [16]. Twenty-four-hour assessment in glaucoma and sleep studies [14] evidenced that IOP peaks roughly around 5:00 to 5:30 in the morning (during sleep period), and aging has a shifting effect delaying the peak post-awakening [17]. Aqueous humor is produced in the ciliary body. There are two drainage routes for aqueous humor. The majority (up to 80%) is through the trabecular meshwork consisting of the uveal and corneoscleral meshwork, the endothelial lining of Schlemm's canal, the collecting channels and aqueous veins. After having passed through the trabecular outflow pathways, aqueous humor drains into the episcleral venous system. The second drainage route is via the uveoscleral outflow pathway that is less well defined and understood. Fluid in this pathway ultimately drains into the lymphatic system. Calculated uveoscleral outflow is 25% to 57% of total aqueous flow in healthy 20 to 30-year olds and decreases with age [16].

Episcleral venous pressure in healthy humans is in the range of 7 to 14 mm Hg with values between 9 to 10 mm Hg typically [18]. This is the only component of aqueous humor dynamics that is affected by body position. Episcleral venous pressure increases by 3.6 mm Hg by changing body position from seated to supine. Any increase in episcleral venous pressure results in decreased trabecular meshwork aqueous outflow and a corresponding increase in IOP. In fact, a change in episcleral venous pressure of 0.8 mm Hg corresponds to a change in IOP of 1 mm Hg. Moreover, trabecular and uveoscleral outflow is reduced in ocular hypertension.

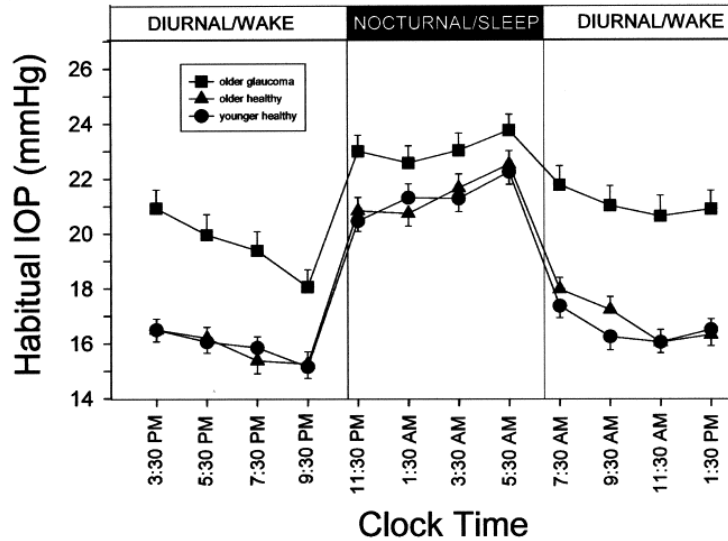


Figure 17: Correlation between office and peak nocturnal IOP in healthy subjects and glaucoma patients. Reproduced from Mosaed S, Liu JHK, Weinreb RN [14], with permission from Elsevier, obtained via Copyright Clearance Center, Inc.

Ocular hypertension, generally considered as an IOP greater than 21 mm Hg, is the most important risk for glaucoma. The Ocular Hypertension Treatment Study showed that the incidence of glaucomatous damage in subjects with ocular hypertension was up to 3% for IOPs of 21 to 25 mm Hg, up to 26% for IOPs of 26 to 30 mm Hg, and approximately 42% for subjects with an IOP higher than 30 mm Hg [19]. In approximately 3% of people with ocular hypertension, retinal vein occlusion may occur that could lead to vision loss. Age greater than 40 years is a risk factor for the development of both ocular hypertension and primary open-angle glaucoma. An epidemiological study has also shown a relationship between glaucoma and myopic refractive error, age, and IOP [20]. Therefore, monitoring of IOP is currently performed in NASA astronauts during spaceflight missions on board the ISS.

c) Optic-Disc Edema, Increased ICP, and Mechanical Deformation of the Globe

The unique anatomy of the subarachnoid space allows the intracranial CSF to reach the orbital subarachnoid space (SAS), which presents a ‘cul-de-sac’ anatomy at the ONH. The SAS contains a complex system of arachnoid trabeculae and septa that divide the subarachnoid space and that may play a role in the hydrodynamics of the CSF inside the optic nerve. The dural sheath surrounds the SAS, which in turn surrounds the optic nerve. Consequently, the optic nerve and disc can be affected by disorders of elevated ICP; as pressure increases in the intracranial space this could be transmitted to the ONH. This represents a third, and nonvascular means by which the IOP may be adversely impacted through mechanical deformation of the posterior globe.

Jenkins [21] examined 20 subjects with increased ICP and papilledema, and found bulging of the terminal optic sheath subarachnoid space into the posterior aspect of the globe at the ONH in 18 patients, regardless of the cause of ICP. It was determined that dilatation of the sheath surrounding the optic nerve resulted in a ‘ballooning’ of the ONH, causing it to protrude into the globe. This resulted in an increased pressure gradient between the SAS and the vitreous with resultant transarachnoid transudation of fluid secondary to the pressure gradient, possibly into the optic disc and the vitreous of the globe. Thus, a significant factor in early disc swelling or

papilledema is papillary protrusion. Of note, Jinkins reported that protrusion precedes any obvious arterial abnormality in the optic disc and that such changes in the pressure gradient manifest rapidly, appearing within the first 24 hours of increased ICP. Thus, data collection close to the 24-hour mark of entry into microgravity may be an important benchmark. When severe dilatation of the distal optic subarachnoid space occurs, all of the regional neural as well as vascular structures are involved and are compressed and distorted. This mechanical action compromises flow emanating from all vascular sources as well as the venous drainage, leading to stasis, congestion, and decreased axonal perfusion [22, 23]. This has important implications in patients with abnormal pressure gradients at the ONH of variable duration, but with ‘normal’ visual testing [24], as may be the case in long-duration spaceflight of up to 6 months. It indicates that injury to the optic nerve may already be significant by the time visual acuity begins to suffer. Conversely, three ISS astronauts have manifested a refractive change and no evidence of optic-disc edema.

d) *Correlation of ICP to IOP – The Hydrodynamic and Vascular Relationship*

Currently, the gold standard for monitoring ICP is the ventriculostomy tube, which is not feasible in spaceflight. However, several authors have reported that ICP is related to IOP, which can serve as a surrogate measure [25-27]. This is based on the anatomical relationships between the intracranial contents and the eye. During cephalad-fluid shift, as occurs in microgravity or horizontal bed rest, venous pressure in the vessels above the heart increases. In addition, intracranial CSF volume increases [28]. Both of these phenomena increase total volume of the brain in the rigid cranium that increases ICP. Prolonged elevations in intracranial venous pressures, also known as venous insufficiency, may exacerbate ICP by precipitating cerebral interstitial edema due to an increased pressure gradient between the parenchymal interstitial space and the intracranial venous space. Normally, a certain amount of capillary fluid volume will diffuse into the interstitial space, carrying nutrients to cells and metabolic byproducts away from them. This diffusion process follows a favorable pressure gradient. However, if the post-capillary venule pressure is elevated, there may be an accumulation of interstitial fluid, even in the face of elevated driving pressure, that contributes to intracranial volume and hence further raising ICP.

Elevated ICPs are transmitted to the eye via the vascular connections. The ophthalmic vein is the primary venous conduit between the intracranial cavernous sinus, a thin-walled cavity that is easily compressible and receives venous blood draining from the eyes, brain, and face before draining out to the internal jugular veins, via the inferior petrosal sinuses. The cavernous sinus, a paired venous structure, lies in the base of the skull on either side of the sella turcica (which contains the pituitary gland) and slightly lateral and posterior to the optic chiasm. The lack of gravity-assisted drainage from the brain, under microgravity conditions, could result in a rise in cephalad venous pressure. The end result might be a relative decrease in the normal pressure gradient between the CSF and the venous blood. Presumably, this could lead to a chronic but uniform elevation in CSF pressure. As Kramer et al. suggest, one manifestation of this chronic elevation in ICP may be compression of the pituitary gland. In fact, pituitary dome concavity, suggestive of chronic pituitary gland compression by increased ICP, was recently documented by MRI after spaceflight [29]. Resting directly upon the cavernous sinus is the subarachnoid space and the third ventricle that both circulate CSF, in addition to the mass of the cerebral

hemispheres. Thus, increases in ICP due to elevated CSF pressure, cerebral edema, and or venous congestion will be transmitted directly to the cavernous sinus and the ophthalmic vein. This relationship has been documented in previous studies. Khanna et al. [30] identified 11 patients with elevated ICP (> 20 mm Hg, equivalent to >27 cm H₂O) (range 25 to 40 mm Hg, equivalent to 34 to 54 cm H₂O), due to cerebral edema, that demonstrated bilateral superior ophthalmic vein (SOV) enlargement equal to or greater than 3 mm. Lirng et al. [31] and Chen et al. [32] reported SOV diameters in patients with normal ICP to be 1.6 mm and 1.83 mm respectively. Khanna et al. [30] found that the SOV enlargements followed ICP elevations either immediately or several hours later. More importantly, the SOV enlargement resolved after treatment for the cerebral edema and normalization of ICP. Lirng et al. [31] compared the SOV diameters of 18 patients with elevated ICP (>20 cm H₂O, up to 40 cm H₂O, SOV = 3.0 mm), and 48 patients with normal ICP (6 to 20 cm H₂O) SOV = 1.6 mm, and found a significant difference between the measurements ($P < .001$). Note that 20 and 40 cm H₂O equal to 14.7 and 29.4 mm Hg, respectively. In a subsequent study, Chen et al. [32] compared SOV diameters in 13 patients with normal ICP (mean = 12.63 cm H₂O) and 13 with intracranial hypotension (mean = 3.5 cm H₂O) and found a significantly reduced SOV diameter in the hypotensive ICP group (0.90 mm) compared to the normal ICP group (1.85 mm), further evidence of the relationship of intracranial hydrodynamics between the intracranial contents and the SOV.

As the ophthalmic vein and its tributaries that drain venous blood from the eye have no valves, impaired venous outflow or even retrograde flow may occur in the face of elevated pressures transmitted from the cavernous sinus. The ophthalmic vein supports all venous drainage from the eye. Its two branches; the superior ophthalmic vein and the much smaller inferior ophthalmic vein, merge to drain into the cavernous sinus. Elevated ICP and venous pressures are ultimately transmitted to the eye, via the ophthalmic vein, along three pathways. The most significant is via the choroidal veins that drain blood from the choroid, a rich vascular network that lies between the outer sclera of the eye and the inner retina. The choroidal veins drain into the vortex veins that subsequently drain into the superior and inferior ophthalmic vein. Almost the entire blood supply of the eye comes from the choroidal vessels. Thus, relatively large shifts in volume can occur, in comparison to other ocular vasculature, thereby contributing significantly to IOP. According to Smith and Lewis [33], 20 μ L of additional blood volume in the choroid can an IOP increase up to 20 mm Hg.

The second pathway is via the episcleral veins, which lie within the sclera and drain the percolated aqueous humor from the anterior chamber after it passes through the trabecular meshwork. The episcleral veins drain both indirectly into the vortex veins via the anterior ciliary veins, and directly into the vortex veins, which drain into the superior and inferior ophthalmic vein. It is well known from the study of glaucoma, that elevations in episcleral venous pressure cause a direct rise in IOP due to the decreased facility (outflow) of aqueous humor via the trabecular meshwork, thereby increasing the pressure within the anterior chamber of the eye [16]. In contrast, choroidal engorgement elevated IOP due to increases in episcleral venous pressure can take 20 minutes or more to occur. In summary, episcleral venous pressure is influenced by venous drainage pressure in the superior/inferior ophthalmic veins, cavernous sinus, and even internal and external jugular veins, a contributing mechanism for rising IOP in the supine position [13]. Thus, any abnormality leading to increased venous pressure in the venous drainage system downstream from the eye can lead to elevated IOP if the episcleral

venous pressure is increased as occurs in jugular vein obstruction, superior vena cava obstruction and cavernous sinus thrombosis [16].

The third and most minimal route of transmission of elevated venous pressure and ICP is via the central retinal vein (CRV). The effect of CRV engorgement on IOP is likely minimal; however, rising retinal vein pressures can cause retinal hemorrhages. The CRV drains venous blood from the retina. It exits the eye alongside the retinal artery through the optic nerve before exiting the subarachnoid space and the optic nerve sheath. Beyond that point, it has several anatomical variations and may join the superior or sometimes the inferior ophthalmic vein, or less often the cavernous sinus directly [34]. The CRV is also directly influenced by ICP during its course through the subarachnoid space within the optic nerve sheath.

e) ICP and IOP Correlation Studies

Given the vascular and hydrodynamic relationships between the intracranial compartment and the eye, several researchers have suggested detecting increases in ICP noninvasively by measuring IOP. Lashuka et al. [25] compared measurements of ICP to IOP in 27 patients with a mean age of 59.6 years, 56% male, all with ventriculostomy tubes. The IOP readings were taken with a handheld tonometer. All patients with an abnormal ICP value (> 20 cm H₂O) had an elevated IOP (> 20 cm H₂O, or 14.7 mm Hg), and all patients with a normal ICP (< 20 cm H₂O) had a normal IOP (< 20 cm H₂O, or 14.7 mm Hg). A high correlation was found between ICP and IOP, with $r = 0.83$. In another prospective study, [26] measured IOP in 50 patients with a mean age of 33.6 years, 58% women, all undergoing a clinically indicated lumbar puncture. Elevated ICP was defined as > 14.76 mm Hg (20 cm H₂O), and elevated IOP as > 20.5 mm Hg. Of the 27 patients with an increased ICP, 23 had an elevated IOP. There was a significant correlation between ICP and IOP, $r = 0.955$ ($P < .001$). In contrast, [35] Czarnik et al. [36] found no correlation between ICP and IOP ($r = 0.227$) after serial measurements in 40 coma patients with ventriculostomy.

However, other observations pose doubt as to the correlation between IOP and ICP and therefore the value of IOP as a predictive measure of ICP [36, 37].

Recently, Spentzas [27] offered an eloquent explanation for why IOP may not always correlate well with ICP in a prospective study of 36 children with severe head injuries. They found that the correlation of ICP with IOP disappeared below the normal cutoff for raised ICP (< 20 cm H₂O) ($r = 0.274$). However, when ICP was > 20 cm H₂O the correlation became significant ($r = 0.705$). Consequently, Spentzas et al. reported that handheld tonometry had a good ability to rule in elevated ICP (> 20 cm H₂O) with a specificity of 97.4% [27]. Thus, IOP measurements had a high positive predictive value, making it a good screening test to rule in elevated ICP, but only at elevated ICP values.

f) IOP in Spaceflight

Preliminary data has shown that IOP is elevated above ground-based values upon initial exposure to microgravity. As there are no valves in the veins in the eye and the brain, there is no venous pump as in the legs, to facilitate blood return to the heart. Thus, in microgravity, where

no venous pump or gravity exist, blood stagnates and accumulates in the veins, which results in the distended facial and neck veins noted in astronauts, a reflection of the elevated venous pressure. This has also been recorded as changes in leg girth, facial edema, and verbal reports of head fullness and nasal stuffiness. The venous engorgement elevates the cerebral post-capillary venous pressure. Congestion in the venous system will cause a concomitant rise in pressure in the episcleral vessels of the eye and will increase the resistance to aqueous-humor outflow, leading to a rise in IOP (Mader et al. [16, 38]).

Two experiments have examined IOP in parabolic flight. Draeger and colleagues documented a mean 5-mm increase in IOP during the free-fall phase of parabolic flight with a hand-held applanation tonometer, which has been superseded by more accurate instruments [39]. Mader et al. [38] also measured IOP during parabolic flight using a TonoPen. They found that IOP increased 7 mm Hg on average, from a mean baseline value of 12 mm Hg, to an in-flight mean of 19 mm Hg (N = 11). A number of investigators have recorded IOP values during the initial phases of spaceflight. Draeger [39] reported an initial 20% to 25% increase in IOP 44 minutes into a Shuttle flight using a hand-held applanation tonometer. In a subsequent experiment, Draeger et al. [40] documented a 92% increase in IOP in two cosmonauts on board a Soyuz vehicle, bound for the Mir Space Station, 16 minutes after reaching microgravity [40]. In a follow-up 6-day experiment on board STS-55, the German D2 mission, diurnal IOP was recorded and a 114% increase in IOP was noted 16 minutes after reaching microgravity [41]. However, subsequent values were not significantly higher than preflight values. Astronauts with higher baseline IOP may be particularly vulnerable to a rise in IOP associated with microgravity exposure [20].

However, previous bed rest and KC-135 parabolic flight studies have documented that this rise in IOP is almost instantaneous [42]. As aqueous humor is produced by the ciliary body at a rate of only 3 $\mu\text{L}/\text{min}$, it would take several minutes at least for this mechanism to cause a measureable rise in IOP. Thus the quick rise in IOP after assuming the recumbent position or upon entering microgravity cannot be explained on the basis of increased episcleral venous pressure alone. This sudden rise in IOP is more likely caused by engorgement of intraocular uveal tissue, principally the choroid. The choroid is drained by the vortex veins and lacks auto regulation. With the head in the dependent position, or with the cephalad-fluid shifts associated with microgravity, the pressure in the vortex venous system rises. This rise in venous pressure is thought to inhibit venous drainage from the choroid thus causing a relatively stagnant expansion of blood in the choroidal vasculature. As ocular fluids within the eye are incompressible this sudden bolus of blood within the choroid would lead to an abrupt increase in IOP. This theory is further supported by the fact that immediately upon sitting up from a prolonged head-down position and upon returning to Earth after spaceflight, IOPs are lower than baseline.

Figure 18 depicts IOP values for eleven subjects over six Shuttle missions. The largest percentage of data is available for the first 6 days of flight and depicts a sharp rise in IOP over baseline values. Pre- and postflight data are not as well represented. Additional data is required to determine the effect of return to gravity postflight on IOP. Similarly, the last several days of flight is poorly characterized, with only four subjects represented, two with only a single data point. The IOP trend towards the end of a mission is of particular interest due to the insight it

would provide regarding physiologic effects and its application to longer-duration missions, for example, ISS increments [38-40].

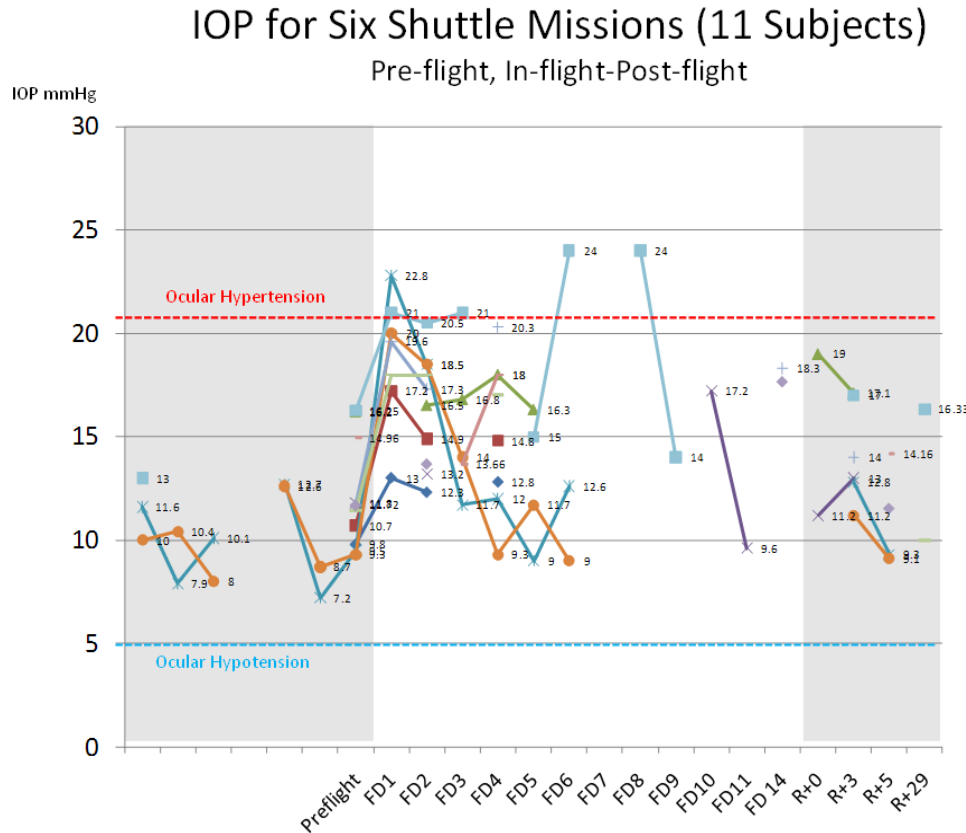


Figure 18: IOP values for eleven subjects over six Shuttle missions [38-40]. FD= flight day

g) Bed Rest and IOP

In normal Earth gravity, it is clear from a number of studies that IOP is influenced by changes in body posture[13, 14, 20, 39, 42-50], the most common of which is the transition from the upright, or seated, position to the supine posture. Bed rest studies, which are designed to simulate microgravity conditions in certain aspects of human physiology, have provided limited data on the long-term course of IOP.

In a study of four male subjects exposed to 120 days of horizontal bed rest, Kuzmin [50] found that IOP increased to 28 to 30 mm Hg. In two of the subjects, the increase in IOP was accompanied by visual disorders in the form of clouding of vision and a decrease in visual acuity. Kuzmin further concluded that it was possible that impaired regulation of IOP was occurring under prolonged bed rest, and that subjects over 45 years of age and those with autonomic dysfunction could be at increased risk. Similar changes in IOP were noted by Kuzmin et al. [50] in a previous 62-day horizontal bed rest study [50]. Mader et al. [42] examined IOP and visual acuity measured in nine men aged 19 to 29 during 48 hours of 10-degree head-down tilt (HDT). There was a diurnal variation in IOP, with values lowest early in the morning and highest at noon. Baseline IOP was 11.2 mm Hg seated, and rose to 17.9 mm Hg within seconds of subjects assuming the head-down position. Mader et al. [1] noted that an increase in episcleral

venous pressure would elevate IOP due to backflow resistance, yet aqueous flow is less than or equal to 3 $\mu\text{L}/\text{min}$ [16], so such a large increase in IOP would take at least several minutes to occur and would not lead to the observed rapid spike in IOP. This could however, be explained by an engorgement of intraocular uveal tissue, principally the choroid, secondary to cephalad-fluid shift. Normally, blood in the choroid is drained through the vortex veins. When the head remains in the recumbent position, venous blood may pool in the choroid due to the effects of gravity. As the choroidal blood flow lacks autoregulation, there is little resistance to fluid accumulation aside from the tamponade effect of rising IOP. As noted by [33], a sudden rise in choroidal blood volume of only 20 μL may result in an immediate rise in IOP of more than 20 mm Hg. Retinal circulation is characterized by a low blood flow while flow in the choroid is high. The choroidal circulation is mainly controlled by sympathetic innervation and is not autoregulated. Retinal circulation lacks autonomic innervation, shows an efficient autoregulation and is mainly influenced by local factors[51]. Therefore, small fluctuations in choroidal blood volume during positional changes may cause sudden and significant increases in IOP. Mader et al. [42] also noted that when subjects assumed the head-down position, IOP increased a mean of 4.7 mm Hg. When they sat up 48 hours later, IOP had decreased 6.7 mm Hg on average. Because these two IOPs were statistically different Mader's group concluded that a greater volume of blood was displaced at the end of the 48 hours than at time zero. In agreement with this observations, IOP monitoring of bed rest subjects in 6-degree HDT for 14 days at the NASA flight analogs unit revealed that IOP increased on average 1.8 mm Hg (+13.3%) at bed rest day (BR) 3 and 1.7 mm Hg (+12.6%) at BR 10 from baseline. By 2 days after bed rest, IOP decreased on average 1.1 mm Hg (-7.2%) from BR 10 [43]. If choroidal blood volume shifts are responsible for the IOP changes observed, a choroidal reservoir of increasing volume appears to develop over 48 hours of HDT. This phenomenon may explain the preponderance of choroidal folds seen in the affected ISS astronauts, reflecting vascular congestion.

Xu et al. [20] evaluated IOP in 65 males, with a mean age of 22.5 years, during 21 minutes of 15-degree HDT to assess whether myopic individuals were more sensitive to cephalad-fluid shifts than emmetropes and low myopic subjects. Baseline mean values of IOP in the low myopia eyes and emmetropic eyes were similar (15.09 \pm 3.20 mm Hg and 14.71 \pm 3.07 mm Hg, respectively) while those in the moderate myopic eyes appeared slightly higher (16.59 \pm 3.50 mm Hg). In the 15-degree HDT position, the mean value of IOP was increased in all subjects at every test point when compared to their respective baseline values. The IOP in the moderate myopic group was higher than the emmetropic and low myopic groups at 1, 6, and 11 minutes after the initiation of the 15-degree HDT test (P , 0.05), and reached a peak of 21 mm Hg at 6 minutes. The results suggested that IOP in the moderate myopia group was more sensitive to postural change. Jonas et al. [52] offered an explanation for the increased susceptibility to elevated IOPs in myopic individuals. The structure of the lamina cribrosa (LC) is explained in detail in its own section. Because the LC forms the border between the intraocular space with a higher pressure and the retrobulbar space with a lower pressure, a pressure gradient exists across the LC as the difference in IOP minus pressure in the retrobulbar cerebrospinal fluid space. This TLP is of importance in ocular diseases in which the pressure on one or both sides of the LC is either abnormally high or abnormally low [22, 23]. The TLP depends on the difference in pressure and the thickness of the LC, thus Jonas et al. suggested one may infer that the reduced thickness of the LC in highly myopic eyes is the histologic correlate of an increased susceptibility to glaucoma. In highly myopic eyes, as found in the work by Jonas et al. [52], the

LC is significantly thinner than in nonhighly myopic eyes that decreases the distance between the intraocular space and the CSF space and steepens the TLP at a given IOP, which may explain the increased susceptibility to glaucoma in highly myopic eyes. Taking into account that the myopic stretching of the globe and the secondary enlargement of the ONH increases with increasing axial myopia, Jonas et al. suggested that the susceptibility to glaucomatous optic nerve fiber loss is related to the degree of high axial myopia.

Chiquet et al. [44] measured IOP in 25 healthy female subjects using noncontact tonometer while seated as well as 1, 3, and 10 minutes after lying flat. IOP rapidly increased; IOP increased 2 mm Hg compared to sitting after 1 minute and was relatively stable at this level throughout the 10 minutes of monitoring. This observation of an elevation in IOP while supine is consistent with other studies [12, 45, 46].

The cephalad-fluid shift during the transition from an upright to a head-down posture would be expected to result in even greater elevations in IOP as the hydrostatic gradients are reversed compared to standing or sitting. In an extreme illustration, Draeger et al. [39] observed that IOP, measured with the same hand-held applanation tonometer as the one used during spaceflight studies, almost tripled in 20 healthy volunteers when they moved from the +90-degree head-up position (~12 mm Hg) to -90-degree head-down position (~34 mm Hg) in increments of 45 degrees. Similar increases were observed upon inversion by other investigators [47, 48]. As had been observed [53], IOP increased from head-up to the supine posture, but the elevation in IOP was more dramatic once subjects progressed beyond the supine posture to head-down positions. The influence of the respective height of the hydrostatic column relative to the gravity vector is clear when measuring local pressure changes during posture transitions; changes in leg arterial pressures appear to be concurrent and inversely related to the alterations in IOP [39]. It must be noted, however, that acute radical tilts do not reflect a spaceflight analog condition and these results should be taken for their own relevance.

Therefore, as spaceflight is not simulated by such extreme postures as inversion, it seems more reasonable to explore the effects of a more moderate head-down position on IOP. Draeger et al. [39] examined ten men during 90 minutes of 10-degree HDT. There was an immediate elevation of IOP with HDT that reached a maximum (~24 mm Hg) after 15 minutes. IOP decreased somewhat by 45 minutes of HDT and was stable through the end of the tilt, although still higher than the level observed during the seated posture. The effects of HDT on IOP also were present, although attenuated, when subjects were dehydrated by a sauna exposure that reduced their body weight by 2% before tilt. In this spaceflight model of induced plasma volume loss, the initial elevation of IOP was less severe and the peak pressure was acquired and resolved in a shorter time when subjects were dehydrated but the pattern of intraocular responses to tilt remained. In a similar investigation of the acute effects of HDT, IOP, blood pressure, and ocular perfusion pressure were elevated upon the assumption of 7-degree HDT and remained elevated through at least 90 minutes of tilt [14], resulting in a decrease in choroidal pulsatile ocular blood flow. A wide range of responses to HDT in these subjects suggest that some subjects may be more susceptible to the effects of the cephalic fluid shifts, in agreement with the observation that some but not all astronauts have indications of increased ICPs and visual disturbances[1].

While the cephalad-fluid shift with transient changes in posture and the resulting influence on IOP is not unexpected, the more chronic effects of head-down bed rest as a model of spaceflight may be more relevant to astronauts on board ISS. The well-recognized diuresis secondary to HDT might modify or attenuate IOP during the course of bed rest, although the continued hydrostatic gradient may result in filling of the choroidal vessels and increase of episcleral pressures [39]. Draeger et al. also observed that IOP decreased during lower body negative pressure used to reverse the cephalad-fluid shift, and the pressure was restored when the decompression of the lower body was released.

Data from short-duration bed rest studies appear to indicate that the transient elevation of IOP with assumption of the head-down position is resolved as the body adapts to the altered hydrostatic pressures. For example, Mader et al. [42] measured IOP, retinal vascular diameters, and visual acuity in nine men before, during, and after 48 hours of 10-degree HDT bed rest. As expected, the change from the seated posture to HDT resulted in an immediate increase in IOP, measured by pneumatonometer, and diurnal variation was noted using measurements repeated every 6 hours during bed rest. The short duration of this bed rest period did not result in any changes in IOP when comparing the HDT posture from the start to the end of bed rest (except for the diurnal variation), but the authors did report that seated IOP was less after than before bed rest. In a companion study of the same subjects during this 10-degree HDT period, Frey et al. [54] reported a 4% increase in the size of the optic disc. Retinal artery and vein diameters were greater and IOPs were lower during the seated rest period before assumption of the HDT posture, but there was no change in these during bed rest. Additionally, in these subjects, as bed rest progressed, thoracic fluid volume decreased concomitantly with tendency for middle cerebral artery velocity to decrease. The decrease in middle cerebral artery velocities was inversely correlated with the change in retinal vasculature caliber. This observation agrees with those made by Friberg and Weinreb [47] during inversion (hanging upside-down). In a slightly longer bed rest duration, Chiquet et al. [44] measured IOP and corneal thickness in eight women during and after 7 days of 6-degree HDT bed rest. In these subjects, IOP measured in the HDT position progressively decreased through the course of bed rest, becoming statistically significant after 5 days of bed rest. IOP recovered to pre-bed rest levels after just 2 days of normal activity. Concurrent increases in corneal thickness were reported in these subjects, after a similar time course during and after bed rest. The authors suggested that the decreasing IOP represents a physiologic adaptation to the HDT position, which is not fully explained by the bed rest-induced diuresis that would be expected to have occurred earlier in the bed rest period.

While not measuring IOP, an earlier study by Drozdova and Nesterenko is the first known study to examine the effects of simulated microgravity on ocular structure and function [55]. Sixteen healthy subjects were studied before, during, and after 70 days of bed rest. The specific conditions of hypodynamia studied were not clearly delineated in this report, but the effects reported were profound. After 45 days of hypodynamia, visual acuity had decreased by 21%, the visual field decreased by 11 degrees, and the near point of clear vision had been extended by 3.5 cm. Interestingly, IOP was reported to have decreased by 3 mm Hg from a prestudy level of 20 mm Hg. The authors reported that the visual function had decreased further at 67 days of hypodynamia, characterized by the visual field decreasing by 15 degrees and the near point of clear vision extended to 12.5 cm from prestudy. The authors failed to indicate the timing of their ophthalmic examinations relative to the study timeline, but they reported that changes in visual function appeared to be coupled with structural changes within the eye. The optic disc appeared

to have faded and the temporal borders were indistinct. Additionally, both the veins and the arteries of the eye appeared to be enlarged. In particular, the authors noted that the veins were distended and exhibited a deeper coloration.

Clearly, such longer-duration bed rest studies are more likely to be relevant to astronauts participating in the current long-duration missions on board the ISS. One other study has examined the effects of longer bed rest on IOP and vision. In the short report by Mekjavic et al. [56], the authors reported no changes in visual function in any of the 10 subjects who participated in 35 days of horizontal bed rest. Unfortunately, the authors failed to report whether IOP changed during this protocol, although they state it was measured. Interpretation of these results relative to other studies; however, is hampered by two important factors. First, the measurements were not made until the second or third day after bed rest had been completed, during which time some recovery from bed rest may have occurred. Second, this was a horizontal bed rest, which acute studies have suggested does not have as dramatic an effect on IOP.

Encouragingly, the changes in the visual function and structure after 70 days of hypodynamia in the study by Drozdova and Nesterenko recovered somewhat when subjects resumed their normal activities [55]. Twenty days after the end of the hypodynamia condition, ophthalmic examination revealed that the arteries of the eye had returned to their normal size, the veins were less distended, and the optic disk was pink with sharp boundaries. Concomitantly, visual acuity and the size of the visual field had recovered to some extent but these were not at prestudy baseline. Unfortunately, it appears that no follow-up examinations were completed beyond the 20 days post-hypodynamia therefore this study does not provide any clues as to whether these observed changes in vision and ocular structure were long-lasting or permanent. While it is difficult to correlate these changes to spaceflight-induced alterations in vision with any certainty, it is relevant to note that vision changes among long-duration astronauts do not consistently resolve after spaceflight either[1].

In conclusion, it is apparent that IOP is transiently elevated above the seated and supine pressures upon the assumption of the head-down posture as a model of spaceflight; this change in posture would correspond to the initial insertion into orbit. The rapid increase in IOP, concomitant with a cephalad-fluid shift, also has been observed during microgravity periods in parabolic flight [38]. However, available bed rest data suggest that elevated IOP resolves over time. Unfortunately, to-date, insufficient long-term spaceflight data are available to confirm whether these observations in bed rest can be used to better understand the effects during and develop countermeasures to microgravity. In-flight testing of IOP was initiated recently and as the data is available, it will be used in evaluation of the bed rest model for this risk. Of note, ocular hypotony has been recognized to result in optic disk edema, globe flattening, choroidal folds, and hyperopic shifts of similar magnitude to those observed in astronauts [1].

To reveal subtle morphological changes in the eye during simulated microgravity for spaceflights, Shinojima et al. measured subfoveal choroidal thickness and foveal retinal thickness during 10-degree HDT. They hypothesized that elevated ophthalmic vein pressure during simulated microgravity increases subfoveal choroidal thickness via enlargement of the choroidal vasculature and greater choroidal blood volume. Subfoveal choroidal thickness and

IOP were increased by HDT during simulated microgravity, although no change in foveal retinal thickness was observed [49].

h) Optic-Disc Edema

Optic disc edema, is typically associated with an increase in ICP (in which case it is referred to as papilledema), and is characterized by deformation of the ONH and swelling of the optic disc. It is also described as the dilatation or ‘ballooning’ of the ONH, causing it to protrude into the eye globe. Optic-disc edema has been observed in five American astronauts manifesting visual alterations after return from long-duration missions.

According to a study by Jinkins [21], certain features were frequently found in patients with papilledema compared to normal controls, irrespective of the cause of intracranial hypertension. These features included: a dilated optic nerve sheath seen in all 20 patients on IV-contrast thin-section orbital CT; a ‘bulging’ of the terminal optic sheath subarachnoid space into the posterior aspect of the globe at the ONH in eighteen of twenty patients with clinical papilledema; and depressed perfusion of the optic disk/nerve junction as measured by dynamic CT at the time of papilledema diagnosis in all six patients with chronic symptomatology (greater than 4-weeks duration). ICP can affect the optic-nerve head in diseases such as pseudotumor cerebri, a condition where the ICP is greater than IOP, resulting in swelling of the ONH. In addition to this protrusion, there may be a variable amount of associated intercellular fluid (true edema) accumulation within the optic papilla due to either primary tissue ischemia, an increased pressure gradient between the subarachnoid space and the vitreous of the globe with resultant transarachnoid transudation of fluid, and/or the extravascular extravasation of fluid secondary to this pressure gradient. A significant factor in the proximate cause of early edema is stagnant axonal transport (stasis) with added vascular congestion, leakage, and ischemia leading to disc swelling [57]. When severe dilatation of the distal optic subarachnoid space occurs, all of the regional neural as well as vascular structures are compressed and distorted to varying degrees. When such forces are applied to the sensitive retrolaminar area and contiguous disc, flow emanating from all vascular sources as well as the venous drainage is believed to be compromised, thus leading to stasis. Several investigators report that the demonstrated axonal swelling is a response to the increased pressure gradient and axoplasmic stasis [21, 58]. Similar swelling of the optic-nerve head can occur in ocular hypotony, where the translaminar pressure difference is produced by low IOP rather than elevated ICP. In both conditions optic-nerve head changes are caused by an increase in translaminar pressure. This biomechanical approach [59, 60] to understanding the stress (force/cross-sectional area) and strain (local deformation) on the ONH may yield clues as to the determinants of axonal, glial, and vascular dysfunction in the pathogenesis and progression of glaucoma and papilledema.

(1) Visual loss in papilledema

Visual symptoms frequently accompany papilledema that can lead to permanent visual loss if left untreated. The following are signs and mechanisms identified in the pathophysiology of papilledema [61]:

- a) The development of opticociliary shunt vessels and diversion of retinal venous outflow to the vortex/ciliary circulation, secondary to compressive forces causing progressive central retinal vein occlusion.
- b) Progressive and permanent loss of peripheral retinal nerve fibers: both small and large fibers are affected, but more peripheral fibers are affected earlier and to a greater extent, mainly superiorly, producing a visual field defect characterized by an arcuate shape. OCT analysis of astronauts with optic-disc edema has shown a distinct predilection for RNFL thickening in the superior and inferior distributions. Serial examinations of the RNFL may be a good indicator of stable or declining clinical course.
- c) Retinal nerve fiber layer infarcts and cotton-wool spots: retinal nerve fiber layer infarcts are seen in severe cases of papilledema and cotton-wool spots are sentinels of the axonal damage. Cotton-wool spots comprise localized accumulations of axoplasmic debris within adjacent bundles of unmyelinated ganglion cell axons. Their formation is widely held to reflect focal ischemia from terminal arteriolar occlusion.
- d) Enlargement of the blind spot: enlargement of the blind spot in patients with papilledema has been attributed to accumulation of peripapillary subretinal fluid and elevation of the surrounding tissue, thus changing the refractive status when measuring the blind spot during vision field testing. The accumulation of fluid is evidenced by a hyporeflective subretinal space in OCT scans. An additional effect is the reduction in the collection of light by the photoreceptors as they misalign with the line of propagation of the light rays.

(2) *Anatomical characteristics associated with papilledema*

- a) Crowded disc: Crowded disc refers to the tight crowding of fiber bundles at the disc border due to a smaller diameter of the ONH. The diameter of the scleral opening seems to be a determinant of this, so that eyes with smaller scleral openings tend to have more blurring of the disc margins by overlying nerve fibers. Of note, mean RNFL thickness is increased in both papilledema and congenital crowding of the optic nerve, for which a distinction between these two entities, especially on a case-by-case basis may not be possible by OCT alone. Thickening of the RNFL has been noted in VIIP affected astronauts postflight in comparison to their preflight baseline.
- b) Increased optic nerve sheath diameter (ONSD): With increasing ICP, the local compartment of the cerebrospinal fluid (CSF) predominantly in the retrobulbar portion of the optic nerve is distended by hydrostatic transmittance of CSF pressure within the SAS; thus, resulting in an increase in the local optic nerve sheath diameter (ONSD), even before papilledema appears. These phenomena precede the onset of papilledema and may reflect the accommodative capacity of the retrobulbar space. This was demonstrated in a study by Hansen et al., in which isolated human optic nerves preparations obtained from autopsies were submitted to predefined pressure alterations, and consecutive changes in ONSD were measured by B-scan ultrasound under defined conditions. It should be noted that papilledema can only develop when there is patency of the SAS surrounding the optic nerve.

In normal adults, the average length of the optic nerve is about 40 mm, and its average diameter, including the nerve sheath, is about 4 mm. Without the sheath the nerve has a

diameter of approximately 3 mm. This suggests that under normal conditions a minute total volume of CSF fluid is contained along the entire length of the optic nerve.

In another study on postmortem optic nerves from subjects without ocular disease, Killer et al.[62] concluded that "...the optic nerve cannot be regarded as merely a homogeneous space filled with cerebrospinal fluid, but rather a tubular, multi-chambered space subdivided by a distensible blind end (cul de sac) behind the ocular globe" (Figure 19). Structurally, the immediate retrobulbar space is more distensible due to the absence of pillars and septae found in the less distensible intraorbital and cannalicular portions of the optic nerve sheath. These features are believed to be important for pressure homeostasis. This arrangement facilitates the flow of CSF within the optic nerve SAS allowing a build-up of physiologic pressure within the retrobulbar space thereby facilitating periodic reverse flow and thus circulation of CSF. If the ICP rises because of an increase of cerebrospinal fluid, the pressure gradient will point unidirectionally from the chiasmatal cistern to the subarachnoid space of the optic nerve in the manner of a hydraulic pump, building up pressure in the small compartment that ends blindly behind the globe. Liu and Kahn have raised the doubt as to whether or not the pressure in the subarachnoid space can indeed be expected to be equivalent to the pressure in the ventricles, the cisterns, and the cranial subarachnoid spaces. Measurements made by Liu revealed decreasing pressure along the optic nerve SAS in a proximal to distal direction [63].

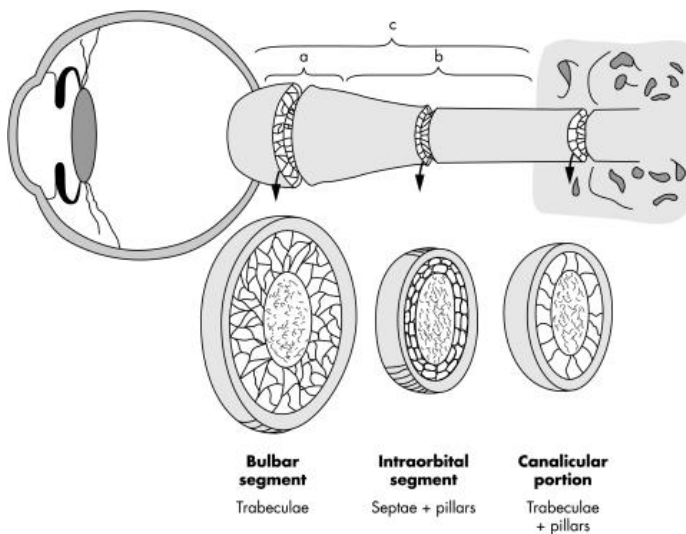


Figure 19: Schematic drawing of the optic nerve demonstrating the microanatomy of the ONS complex. Reproduced from Killer HE, and others [62] with permission from BMJ Publishing Group Ltd.

An important question is the relationship between the increase in ICP and the degree of distention of the ONS. Hansen and Helmke performed a study in twelve patients undergoing neurological testing that involved CSF absorption [64]. The ONS diameter was evaluated by serial B-mode ultrasound scans of the anterior optic nerve near its entry into the globe. The linear relationship between ONS diameter and ICP was only present within a certain CSF pressure interval. This interval differed between patients. ONS dilation commenced at pressure thresholds between 15 mm Hg (20.4 cm H₂O) and 30 mm Hg (40.8 cm H₂O) and, in some patients, saturation of the response (constant ONS

diameter) occurred between 30 mm Hg (40.8 cm H₂O) and 40 mm Hg (54.4 cm H₂O). Because of the variable pressure-diameter relationship, at higher CSF pressure levels the ONS may lose its ability for further dilation. Trabecular fibers and sheath collagen structure may determine this aspect of the sheath response. In Hansen's study, this certain threshold CSF pressure was, on average, 22 mm Hg (30 cm H₂O) in all patients. The largest diameters were observed in the subgroup with the highest ICP readings (6.5 mm ONS diameter equivalent to 30 to 55 mm Hg ICP or 40.8 to 74.8 cm H₂O).

Thus, the clinical relevance of this study relies on the demonstration of pathologically enlarged sheaths or ongoing enlargement on serial ultrasonography studies. The point at which the ONS loses its capacity to distend would be the saturation level at which the other papilledema-like features begin to manifest. Therefore, identifying the saturation level in astronauts might be of critical importance.

In their more recent work, Hansen et al. [65] showed that prolonged dysregulation of ICP led to persisting dilatation of the CSF compartment surrounding the optic nerve. As with any nonelastic behavior, ONSD returned to baseline only when SAS pressures did not exceed 35 mm Hg (47.5 cm H₂O). When decompression occurred from higher pressure levels (45 mm Hg or 61.2 cm H₂O and above), a clear residual dilatation remained (above 0.34 mm). In conclusion, there is a limited capability for retraction of the optic nerve sheath after pressure normalization, similar to a behavior known as 'hysteresis' (a time lag in the occurrence of two associated phenomena, as between cause and effect). When plastical deformation or trabecular damage-like over distension occurs, a pressure-dependent structural remodeling in the trabecular tissue and/or the dural elements takes place, reducing the retraction of the ONS to baseline levels when pressures are elevated above a certain threshold value and length of time. According to this study, direct correlation between distension and pressure exists for pressure values between 5 and 45 mm Hg (6.8 to 61.2 cm H₂O). Occupational surveillance analysis of the ISS astronauts who received ultrasound assessment of their ONSD revealed that VIIP cases had significantly greater ONSD (6.4 mm) compared to noncases (5.3 mm) $P < .02$. When the groups were examined for the number of days spent in microgravity before their ISS flight, the VIIP cases had more exposure compared to none among the noncases. Specifically, of the noncases, 57% had not flown before. Of the remaining noncases, 29% had short-duration flights and 14% had long-duration flight experience. Of the cases, 31% had not flown before while 53% had short-duration flights and 15% had long-duration flight experience. Therefore, the cases may have experienced elevated ICP on past missions, to the degree that the ONSD did not return to its original caliber. The difference in ONSD between cases (6.9 mm) and noncases (5.4 mm) persisted in flight, and was significantly different, $P < .01$. The cases also demonstrated a significant rise in ONSD from preflight to in flight $P < .05$, and from in flight to postflight, $P < .03$. The noncases did not show a significant change from preflight to in flight or postflight (Figure 20).

Optic Nerve Sheath Diameter Cases vs non-Cases Preflight-Inflight-Postflight ISS

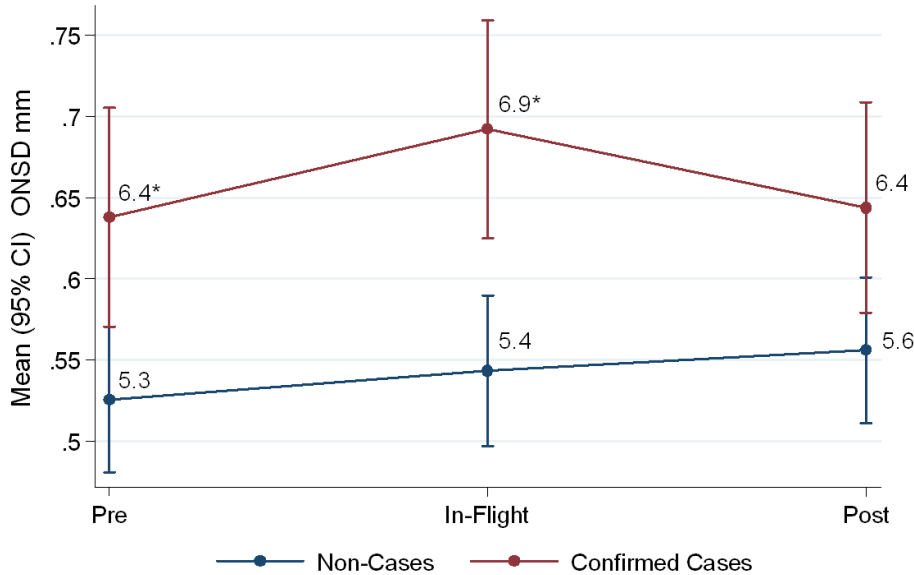


Figure 20: ONSD (in cm) in astronauts: VIIP cases versus noncases preflight/in-flight/postflight. Data from the NASA Lifetime Surveillance of Astronaut Health (LSAH).

- c) Choroidal folds and hyperopic shift can be associated with papilledema and are discussed in detail below.
- d) Other features that may present with papilledema include disc elevation in cases of more advanced disc swelling and hemorrhages. Asymptomatic papilledema at presentation is not uncommon.

In summary, development of papilledema apparently depends on increased pressure in the distal optic nerve sheath, decreased perfusion of the axons exiting through the LC, and, possibly, elevated central retinal venous pressure.

i) *The Choroid and Choroidal Folds*

Choroidal folds involve Bruch's membrane and the adjacent retinal pigment epithelium (RPE) while the overlying retina is not involved, which explains the absence of visual symptoms in the presence of choroidal folds. Any factor causing congestion within the choroicapillaris will lead to folding.

In a microgravity KC-135 parabolic flight experiment, choroidal blood flow increased 75%, while choroidal blood volume increased 100% during simulated microgravity compared with the baseline measures (1 G) [66]. It is hypothesized that the choroidal engorgement may be responsible for anterior displacement of the macula, contributing to the hyperopic shift.

If the retrobulbar pressure becomes elevated beyond physiologic levels, the pressure exerted may compress the posterior globe causing posterior sclera flattening thereby moving the macula anteriorly. Hence, posterior globe, or sclera flattening may be a secondary mechanism contributing to the hyperopic shift. Scleral flattening may also contribute to choroidal fold development by decreasing the available surface area supporting the choroidal vasculature. As a consequence, the choroidal vessels become compressed, precipitating folding.

In some cases of idiopathic intracranial hypertension (IIH), choroidal folds have been found to precede the development of papilledema. In others, choroidal folds have been the only presenting sign of raised ICP from any source (that is, pseudotumor cerebri, venous sinus thrombosis, or intracranial mass). This suggests that either: 1) elevated intrasheath pressure and indentation of the globe, or 2) elevated venous pressures transmitted to the choroid; may cause choroidal folds before the onset of papilledema. It may be possible that variation of elastic properties of the sclera in different individuals could have some influence on how readily globe flattening occurs. Raised ICP may cause retrolaminar ONS enlargement and posterior globe flattening without causing obvious ONH swelling, if the critical pressure required to cause axoplasmic stasis within the individual is not reached. Figure 21 is a detailed schematic of the ocular anatomy for reference.

The notion of inter-individual variability of the elastic properties of the ONS has been demonstrated by Hansen et al. [65], while Lavinsky et al. [67] showed variability among subjects in scleral rigidity as a determinant of the visible effects of the transmission of an increased ICP to the globe. In their study, they described the most frequent sonographic findings in IIH cases: flattening of the posterior ocular wall, thickening of the retinochoroid layer, and distension of the ONS. It is likely that in some individuals, retrobulbar pressure becomes great enough to cause some globe flattening, but, not so high as to cause axoplasmic stasis (choroid is engorged due to ICP elevation, but the sheath and lamina are flexible enough that axonal compression does not block axoplasmic flow and cause swelling and disc edema).

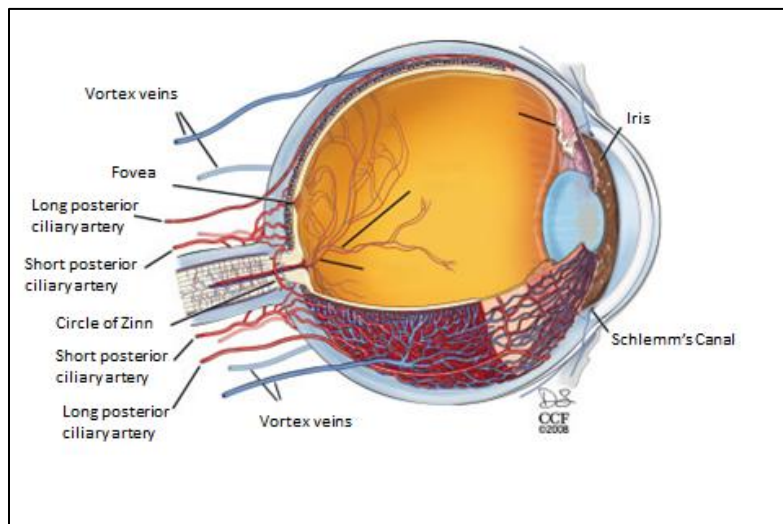


Figure 21: *Vascular anatomy of the eye. Reproduced from Anand-Apte B, and others. [68] with permission of Elsevier.*

j) *Biomechanical Modeling of the ONH and ONS*

Strain is a measure of the local deformation in a material or tissue induced by an applied stress, and is usually expressed as the percentage change in length of the original geometry. Stress is a measure of the load applied to, transmitted through, or carried by a material or tissue, and can be defined as the amount of force applied to a tissue divided by the cross-sectional area over which it acts. It is important to recognize that strain, unlike stress, may be observed and measured and it is strain, not stress, which causes damage to tissues [69]. Stiffness is a composite measure of the entire structure's resistance to deformation that incorporates both the material properties and geometry of a complex load bearing system. In the posterior pole of the eye, both the geometry and material properties of the sclera and LC contribute to their structural stiffness, and hence determine the ability of the ONH and peripapillary sclera to withstand strain when exposed to IOP or ICP. The ONH biomechanics are therefore determined by the geometry (size and shape of the scleral canal, scleral thickness, regional laminar density, and collagen beam orientation) and the material properties (stiffness) of the LC and sclera. As a consequence, eyes with identical IOPs may exhibit very different strain fields due to differences in their structural stiffness [70].

Three tissue types are found in the ONH [70]: load-bearing connective tissues of the peripapillary structures (sclera, scleral canal wall, and LC), axonal tissues (retinal ganglion cell axons), and cellular elements (astrocytes, glial cells, endothelial cells, and pericytes along with their basement membranes).

When mechanical failure of the load-bearing connective tissues of the ONH occurs, then progressive damage to the adjacent axons (with eventual retinal ganglion cell death) ensues from a combination of both compressive and ischemic mechanisms. The stress generates strain (tissue deformation in response to load) within the tissues that experience the load. The magnitude of strain is based on the material properties of the tissues, including how well the tissues are able to resist deformations induced by the applied stress.

Inter-individual variation in peripapillary scleral thickness can result in significantly different biomechanical responses to IOP. The principal load bearing tissue of the eye is the sclera, mostly, the peripapillary area. According to a study by Norman et al. [71], thickness over the whole sclera was $670 \pm 80 \mu\text{m}$ (mean SD; range: $564 \mu\text{m}$ to $832 \mu\text{m}$) over the 11 eyes studied. Maximum thickness occurred at the posterior pole of the eye, with mean thickness of $996 \pm 181 \mu\text{m}$. Thickness decreased to a minimum at the equator, where a mean thickness of $491 \pm 91 \mu\text{m}$ was measured. Eyes with a reported history of glaucoma were found to have longer axial length, smaller ONH canal dimensions and thinner posterior sclera. The posterior radius had a smaller but still significant effect, suggesting that the shape of the posterior of the eye can alter its biomechanical response. The positive correlation of increased posterior radius with increased strain and displacement suggests that a flatter posterior sclera (that is, one with lower curvature) may lead to higher biomechanical loads in the ONH.

Finite element modeling for a range of normal and elevated IOPs predicted that strains in the LC were more dependent on scleral stiffness, scleral thickness, and scleral canal diameter than on LC stiffness and optic cup shape [72]. The fact that neural tissue is two orders of magnitude more compliant than the sclera is consistent with the expectation that neural tissue is unlikely to bear significant load. Mechanical modeling of the LC is complex because it is a composite of

connective tissue with pores through which glial cells and nerve fibers pass. This modeling suggests that average laminar strains depend more on scleral compliance than on laminar compliance.

The five input factors that had the largest influence across all outcome measures were, in ranked order: stiffness of the sclera, radius of the eye, stiffness of the LC, IOP, and thickness of the scleral shell [60]. Their modeling predictions indicate that scleral properties have the largest effect when the sclera is more compliant. Increased scleral compliance occurs, for example, in myopia, either because of scleral thinning or due to alterations to the scleral extracellular matrix, which could help explain the higher incidence of glaucomatous optic nerve damage in highly myopic eyes at a given IOP.

Downs et al. [69] considered a physiologic level of strain in the sclera to be between 0% and 1% and suggested that levels above 3.5% could be pathophysiologic, because they result in detectable changes in scleral material properties (stiffening). Slightly higher strain levels (5% to 6%) have been observed to be the threshold for axonal injury [73]. Axons are damaged through a variety of mechanisms: either external compression by intact laminar beams, spontaneous compression (in which differences in tissue pressure across the lamina cause axons to collapse spontaneously), and both acute and chronic ischemia. Because the sclera is the stiffest ONH tissue, it supports much of the overall load. In particular, the peripapillary sclera must support relatively high stresses, which are compounded by peripapillary scleral thinning. Scleral thinning confers a biomechanical disadvantage, because it produces higher strains in the LC.

k) Lamina Cribrosa (LC)

The LC is a lattice-like structure, consisting of successive perforated cribriform plates across the optic nerve canal, through which pass bundles of nerve fibers. The plates are lined by basement membranes and their cores are filled with significant amounts of fibrillar collagens and elastic fibers. All of the axons passing through the LC depend on slow and fast axoplasmic transport for viability and synapse production. The main functions of the LC are to allow the retinal ganglion cell axons and the central retinal vein to leave the eye, to allow the central retinal artery to enter the intraocular space, and to stabilize the IOP by forming a barrier between the intraocular space and the extraocular space (Figure 22).

Because of its barrier function, the LC prevents major leakage of aqueous humor from the intravitreal space into the retrobulbar cerebrospinal fluid space surrounding the retrobulbar part of the optic nerve. Because the LC forms the border between the intraocular space with a higher pressure and the retrobulbar space with a lower pressure, a pressure gradient exists across the LC as the difference in IOP minus pressure in the retrobulbar cerebrospinal fluid space.

During aging, the constituents of these cribriform plates are altered including an increase in nonenzymatic glycation, a process that weakens collagen; in addition, there are changes in the amounts of types I, III, and IV collagen [74, 75]. Such changes alter the mechanical behavior of the aging LC and therefore compromise its ability to support the nerve axons that pass through it. Albon et al. [76] noted that the reversibility of the LC towards its original volume upon reduction of pressure, decreased with age, which indicated a decrease in resilience. These alterations in

mechanical properties of the aging LC are likely to influence the susceptibility of the retinal ganglion cell axons to damage due to the close anatomical arrangement of the cribriform plates and the nerve axons that pass through them. In a young eye, the stress exerted on the nerve axons during the compression and rearrangement of the cribriform plates may be effectively much less than in the more rigid structure of the elderly LC. The change in mechanical compliance appears to be most marked after 40 to 50 years, the age at which the incidence of primary open angle glaucoma (POAG) is increased. This corresponds with the age range for astronauts affected with the VIIP syndrome.

Simple considerations of the eye as a pressurized globe show that the stress in any part of the ocular shell, including the LC, is related to both IOP and the radius of the structure; $\sigma = PR/2t$, where σ = circumferential stress, P = IOP, R = radius of curvature at that part of the globe and t = thickness. Thus in large eyes or when the LC is cupped (that is, in glaucoma or the elderly), the effective radius of the entire pressure vessel is greater at this point, and therefore the stress is greater. This places myopic individuals at greater risk for glaucomatous damage.

The LC shows regional variations. Pore size increases with increasing distance from the center of the LC (Figure 22B); the largest pores are located close to the lamina margin, with the least amount of inner pore connective tissue in the inferior, superior, and temporal disc regions, and higher retinal nerve fiber count in the inferior and superior disc regions. The structurally weaker areas of the LC correspond with the appearance of RNFL thickening in astronauts seen most prominently in the superior and inferior portions of the optic disc followed by the temporal region.

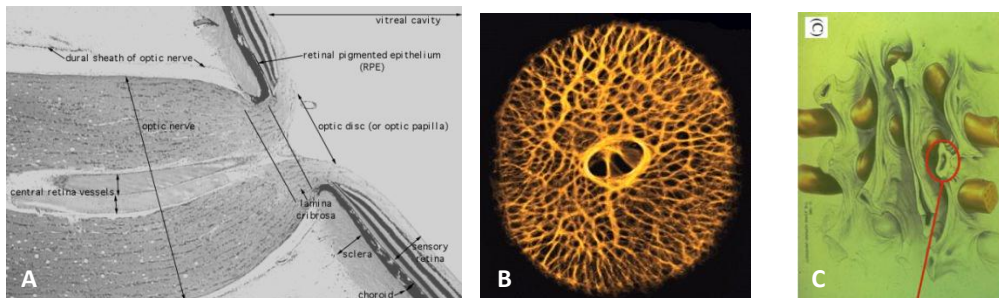


Figure 22: A. Optic nerve and ONH X-Section. Reproduced with permission from Vaughan DW [77]. B. Anterior view LC. C. Arrangement LC plates and axonal passage. B and C - Reproduced from Burgoyne CF, et al. [59], with permission of Pergamon, obtained via Copyright Clearance Center, Inc.

(1) *The Translaminar Pressure (TLP) Gradient*

In a 1-G environment under normal physiologic conditions, the difference between IOP and the retrolaminar cerebrospinal fluid pressure is the TLP gradient that generates both a net posterior force on the surface of the LC and a hydrostatic pressure gradient within the neural and connective tissues of the prelaminar and laminar regions.

In a modeling experiment, Bellezza et al. [70] found that maximum LC insertion zone stresses are approximately twice the magnitude of peripapillary scleral stresses in each of three ocular models, and are also influenced by changes in canal geometry, inner canal radius, and scleral

wall thickness. Progression of the neuropathy within an individual ONH is very much influenced by the physiologic age of the tissues in which it occurs. Once the load-bearing connective tissues are damaged, further damage to the connective tissues themselves and damage to the adjacent axons and living cells can be expected to occur. Burgoyne et al. [59] reported that once the load-bearing connective tissues are physically damaged, secondary pressure-related damage to axons would be expected to occur at lower levels of IOP. When individual connective tissue trabeculae of the anterior LC mechanically fail, the load they were supporting is transferred to the immediately adjacent trabeculae thus increasing their load for the same level of IOP. Hence, even under a constant level of IOP, the adjacent laminar trabeculae progressively fail as the same level of overall IOP-induced load is spread over a continually decreasing cross-sectional area of connective tissue. More trabeculae increasingly fail, and increased pressure is exerted on the ones that remain.

Axonal damage occurs by these main mechanisms:

- (1) axonal ischemia through the traditional vascular hypothesis (acute compressive effects on laminar capillary volume flow within the LC, which decreases axonal viability because of inadequate delivery of nutrients, secondary to reduced laminar capillary volume flow) [78]
- (2) physical compression of the axons secondary to the deformation of intact laminar trabeculae (the traditional mechanical hypothesis) [78]
- (3) spontaneous axonal compression secondary to tissue pressure differences across the intact LC (Yablonski's theory of spontaneous axonal compression) [79]

Overall, connective tissue strain within the LC has both direct and indirect effects on axonal nutrition. Axonal ischemia can be the result of either IOP-induced occlusion of the laminar capillaries (direct effect) or decreased diffusion of nutrients (indirect effect), or both.

In a study by Yan et al. [80], it was observed that most of the posterior displacement due to pressure elevation occurred within the peripheral areas of the LC. Yan found that deformation of the LC by elevated IOP stresses were maximal at the periphery and minimal at the centre of the ONH, owing to the greater curvature at the periphery, which is more prominent in myopic eyes. This is also consistent with a mechanical model in which shear forces within the LC dominate compressive or tensile stresses. Shear stresses are maximal at the border between the sclera and the LC, and decrease as moving away from the scleral boundary until they are negligible at the centre of the LC, consistent with clinically observed patterns of visual field loss in glaucoma (Figure 23). In highly myopic eyes, the LC is significantly thinner than in nonhighly myopic eyes, which decreases the distance between the intraocular space and the cerebrospinal fluid space and steepens the TLP gradient at a given IOP. This may imply that in highly myopic eyes, clinically, the target IOP may be set at a lower level than in emmetropic eyes. The periphery of the ONH was the region with the shortest distance between the intraocular space and the cerebrospinal fluid space. Jonas et al. [52] also suggested that a short distance between the cerebrospinal fluid space and the intraocular space steepens the pressure gradient and that a steep pressure gradient increases the susceptibility of optic nerve fibers to glaucoma. One may infer that optic nerve fibers located in the optic disc periphery would be more susceptible to glaucoma than fibers running through the optic-disc center.

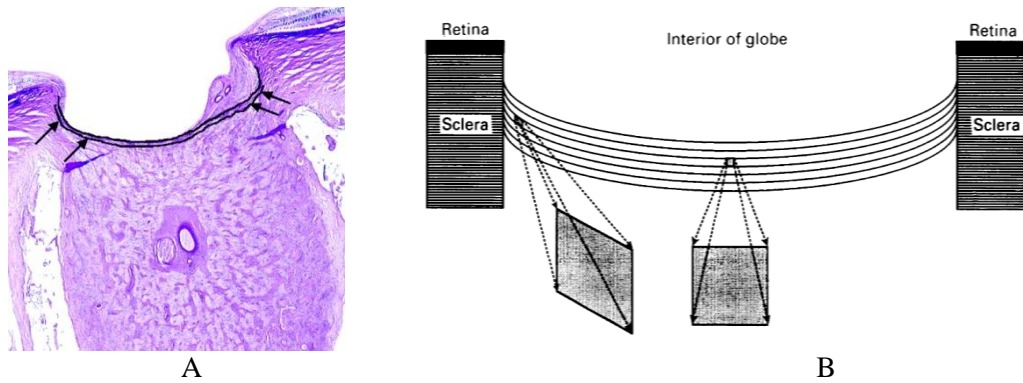


Figure 23: A. ONH cross section, high shear stress at arrows. B. Schematic showing greater shear stress at periphery of LC. Reproduced from Yan DB, et al. [80] with permission from BMJ Publishing Group Ltd.

1) ***Altered IOP/ICP Relationship: A Precipitant of Optic-Disc Edema?***

In healthy individuals, normal mean IOP is 16 mm Hg (22 cm H₂O). The normal mean ICP in the recumbent position is 15 cm H₂O (11 mm Hg). On average, there is a small pressure gradient (mean 5 mm Hg) directed posteriorly across the LC in normal eyes. The TLP gradient increases with elevation of IOP or reduction of ICP. The distance through which the TLP difference is exerted becomes critically important. While the thickness of the normal-LC is around 450 μ m, the LC is thinner (or becomes thinner) in glaucomatous eyes or myopic eyes.

Reducing ICP could have the same effect as increasing the IOP for the development of glaucoma, which in effect is altering the TLP gradient. This has been demonstrated by Yablonski et al. [79] using a cat model. ICP was decreased to 3.7 mm Hg (5 cm H₂O) below the atmospheric pressure by cannulation of the cisterna magna. The IOP of one eye was reduced to slightly above atmospheric pressure by cannulation of the anterior chamber, whereas the other eye was left unchanged. After 3 weeks, the ONHs of the eyes, in which the IOP was unaltered and therefore had a higher TLP gradient, showed typical features of glaucomatous optic neuropathy. In contrast, in the eyes in which the IOP was also lowered, thereby maintaining a normal TLP gradient, no ONH changes occurred. The authors hypothesized that reducing ICP would have the same effect as increasing the IOP for the development of glaucoma. This underscores the importance of the TLP gradient as a source of axonal damage.

In a recent series of human studies [58, 81], differences in ICP among subjects have been found to alter the TLP gradient and are correlated with visual field loss even in subjects with normal IOP (Figure 24). This relationship may have a primary role in the etiology of the VIIP ocular symptoms of spaceflight. In a prospective study, Berdahl et al. [58] reported that ICP is lower in patients with glaucoma and normal-tension glaucoma (9.1 mmHg or 12.4 cm H₂O and 8.7 mmHg or 11.8 cm H₂O, respectively, versus ICP in nonglaucoma subjects, 11.8 mm Hg or 16 H₂O). Conversely, ICP appears to be elevated in patients with ocular hypertension (12.6 mm Hg or 17 H₂O versus 10.6 mm Hg or 14.4 cm H₂O in healthy individuals). In a prospective study by Ren et al. [81], the extent of glaucomatous visual field loss was positively correlated with the trans-LC pressure difference (Table 2). A surprising finding was the lower than average ICP in the normal pressure glaucoma patients, those with normal IOP. Thus, their reduced ICP resulted

in an abnormal TLP gradient and resultant visual field loss. In the more typical high pressure glaucoma patients an elevated TLP is to be expected due to the high IOP, however, a lower than expected ICP also contributed to the increased TLP gradient.

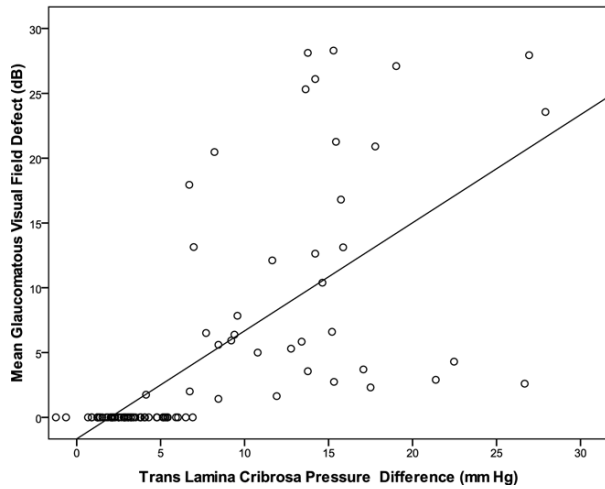


Figure 24: Amount of glaucomatous visual field defect correlated positively with the TLP pressure difference ($P < 0.005$) $r = 0.69$. Reproduced from Ren R, et al. [81], with permission from Elsevier, obtained via Copyright Clearance Center, Inc.

Table 2: The Extent of Glaucomatous Visual Field Loss was Negatively Correlated with CSF Pressure and Positively Correlated with the TLP Difference. Reproduced from Ren R, et al. [81], with permission from Elsevier, obtained via Copyright Clearance Center, Inc.

Measure (pressure in mm Hg)	Control group (N = 71)	Normal Pressure Glaucoma(N = 14)	High Pressure Glaucoma(N = 29)
IOP	14.3 +/- 2.6	16.1 +/- 1.9	24.3 +/- 3.2
CSFp (ICP)	12.9 +/- 1.9	9.5 +/-2.2	11.7 +/-2.7
TLP Difference	1.4 +/-1.7	6.6 +/-3.6	12.5 +/-4.1

The central role that CSF pressure plays in the TLP gradient has been investigated by Morgan et al. [22, 23, 82] with in vivo measurements using a dog model. It was found that cerebrospinal fluid pressure largely determines the retrolaminar tissue pressure, that is, the retrobulbar pressure. Hence, along with IOP, CSF pressure is of major importance in setting the translaminar tissue pressure gradient (TLPG). Furthermore, Morgan showed that there is a strong linear correlation between the TLP gradient and the difference between IOP and CSF pressure (CSFp), when CSFp is 0 mm Hg or higher (Figure 25).

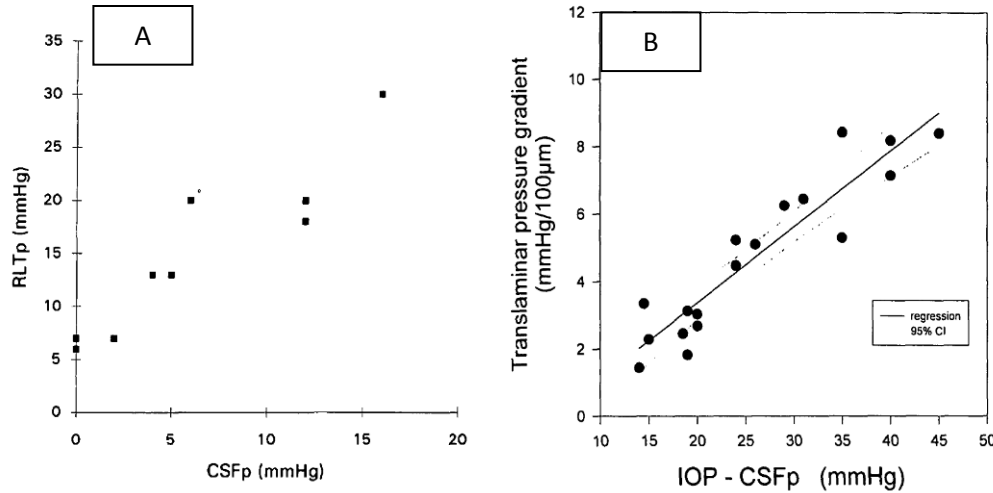


Figure 25: **A.** Correlation of CSF pressure with RLT gradient. Reproduced from Morgan WH, Yu DY, Cooper RL, et al. [80], with permission of The Association for Research in Vision and Ophthalmology. **B.** Correlation of IOP-CSFp with TLP gradient. Reproduced from Morgan WH, Yu DY, Alder VA, et al. [23], with permission of The Association for Research in Vision and Ophthalmology.

Optic nerve axons experience an abrupt pressure change as they leave the eye at the level of the LC. A pressure gradient, if present, will induce mechanical stress transverse to the pressure gradient (LaPlace's Law). Determinants of the TLP gradient are IOP, retrolaminar tissue pressure (ICP), and the axial thickness of the LC. Although peripheral nerves can withstand very high absolute pressures of up to 3800 mm Hg, pressure gradients are poorly tolerated. For instance, a gradient as low as 4.5 mm Hg/100 µm will reduce axonal transport [58]. Mechanical forces applied to nerves are known to cause ischemia and cytoskeletal disruption in association with axonal transport inhibition. Within the LC, the axonal cytoskeleton is subject to the pressure gradient, which may be increased in regions adjacent to the LC connective tissue beams.

Morgan et al. [22] also found that for a given degree of pressure change, an increase in CSF pressure resulted in larger changes in ONH disc displacement than a corresponding increase in IOP and that most displacement occurred at low TLP differences, with little extra movement at TLP differences higher than 15 mm Hg or 20.4 cm H₂O (Figure 26).

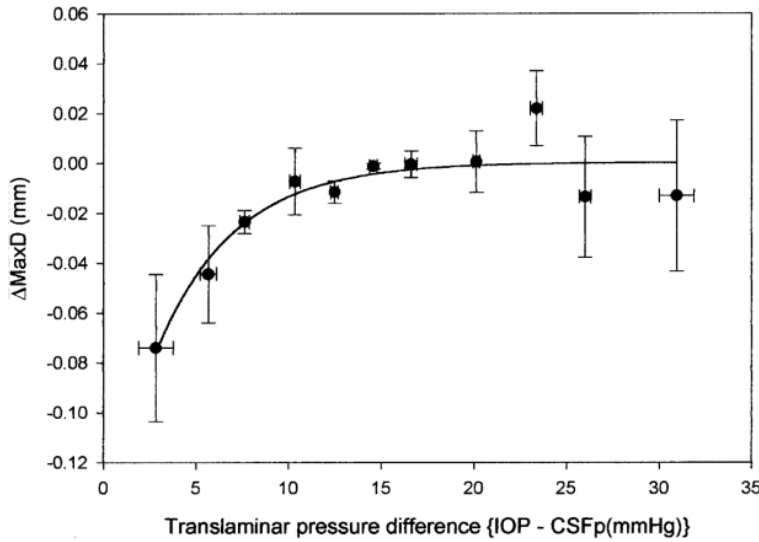


Figure 26: ONH disc depth displacement as a function of TLP difference. Reproduced from Morgan WH, Chauhan BC, Yu D, et al. [22], with permission of The Association for Research in Vision and Ophthalmology.

Large movements of the central and deepest parts of the LC were seen with some small areas moving more than 128 μm with an increase in CSF pressure of only 2 mm Hg (2.7 cm H₂O), or a decrease in IOP of only 5 mm Hg. Small increases in CSF pressure had a much greater effect than equivalent increases in IOP. This maximum displacement was stable at TLP differences greater than 15 mm Hg (20.4 cm H₂O). This would suggest that at pressure differences of more than 15 mm Hg (20.4 cm H₂O), almost no further posterior laminar movement occurred. This nonlinearity is consistent with the known nonlinear stress–strain relation of collagen, whereby the change in strain decreases with increasing stress.

What does all of this mean for astronauts and the spaceflight VIIP syndrome? If one reverses the pressure relationship in glaucoma (IOP>ICP), the result is papilledema (ICP>IOP). And, if the TLP gradient determines the degree of axonal damage, it stands to reason that any increase in ICP (as is hypothesized to occur in the VIIP syndrome), and any decrease in IOP would exacerbate the TLP gradient and the expectation would be increased severity of VIIP. Interestingly, recent occupational surveillance work has revealed that IOP declines in ISS astronauts from preflight to postflight on average 1mmHg for both VIIP cases and noncases. Further analysis of the data is needed because of the small sample size and the unclassified cases. However, VIIP cases have a preflight IOP that is 1 mm Hg less than noncases. Furthermore, their postflight IOP is also 1 mm Hg lower than noncases (Figure 27). These data should be taken with caution when one considers that an IOP difference of 1 mm Hg is within the typical error of measurement (1.5 mm Hg) and the sample size is small.

NASA’s Clinical Practice Guideline (CPG) for the VIIP syndrome, which is elaborated on in section VI of this report, divides cases into class 0 through 4, with class 4 being the most severe. When the IOP of the CPG VIIP cases is examined more closely, the most severely affected cases in CPG class 3 and 4 exhibit the lowest IOPs, both preflight (mean value of 13.2 mm Hg), as well as postflight (mean value of 11.8 mm Hg) (Figure 28). They also exhibit the greatest drop in IOP from preflight to postflight, nearly 50% more than any other classification.

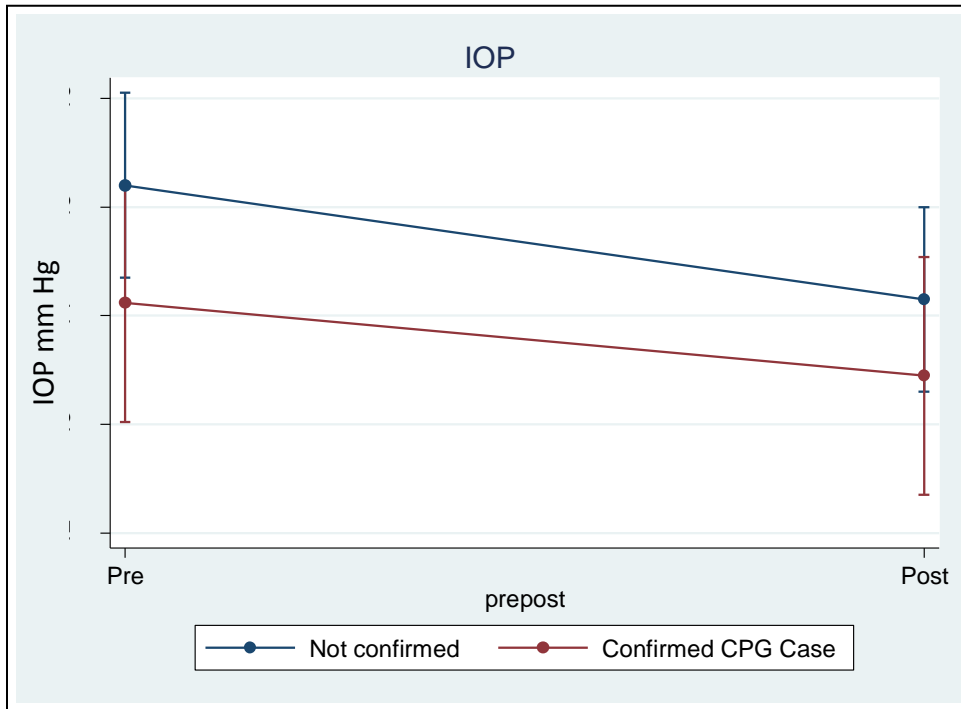


Figure 27: Preflight and postflight IOP in VIIP cases and noncases.

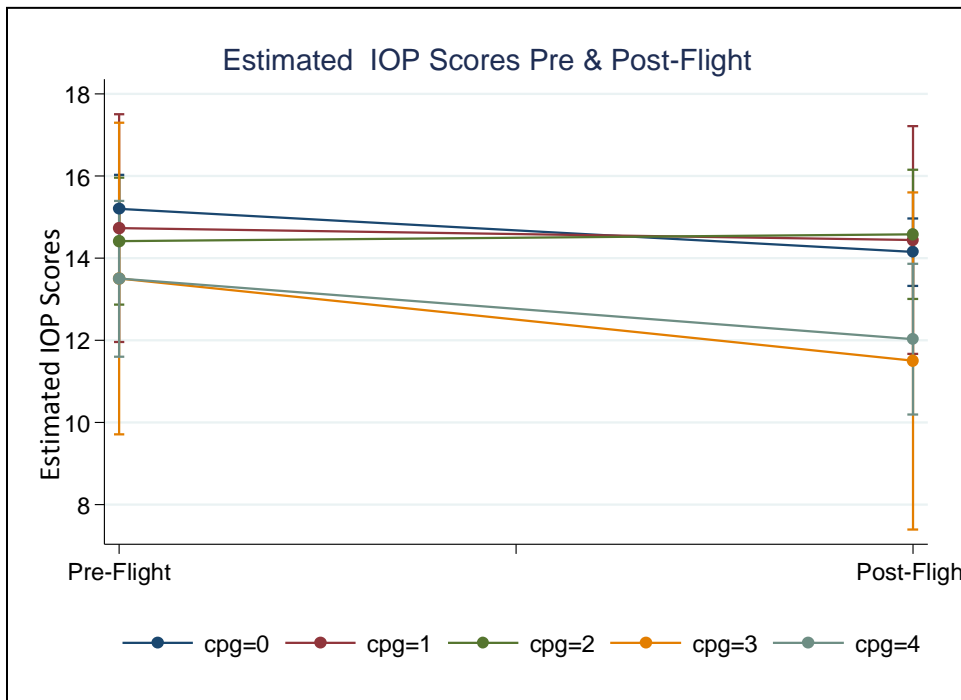


Figure 28: Preflight and Postflight IOP in CPG-defined VIIP cases versus noncases.

In addition to the acquired globe flattening seen in the documented cases (a known correlate with increased ICP in IIH patients), several of the astronauts diagnosed with the VIIP syndrome have also been found to have optic-disc protrusion on MRI analysis. This is suggestive of a pressure

differential where ICP is greater than IOP. The characteristic feature is shown in astronaut ultrasound and MRI images presented in an earlier section of this document (Figures 5 and 9).

In a recent clinical study using OCT, Kupersmith et al. [83] found that papilledema with raised ICP in patients with IIIH resulted in an inward bowing of the retinal pigmented epithelium and basement membrane (RPE/BM), reflecting deformation of the underlying LC in response to a TLP gradient favoring ICP over IOP. This study confirms the animal work of Morgan et al. and demonstrates, in human subjects, an association between an elevated ICP/IOP gradient, papilledema and anterior displacement of the RPE/BM angle in severe cases of disc edema. Kupersmith et al. [83] prospectively examined 30 eyes with papilledema. The angle of the RPE/BM in the peripapillary retina furthest from the ONH and the altered border adjacent to the neural canal opening NCO was measured on the nasal and temporal sides of the optic nerve (Figure 29).

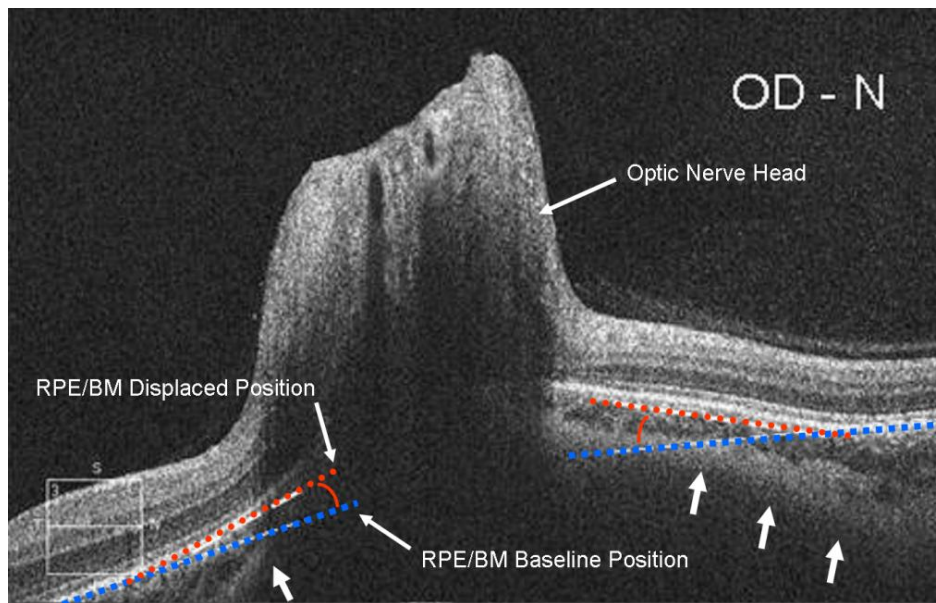


Figure 29: RPE/BM angle measurement: red line denotes angular deflection from blue baseline indicating positive or anterior protrusion of ONH. Note inward bowing of the sclera (short arrows). Image adapted from Kupersmith MJ, Sibony P, Mandel G, et al. [83], with permission of The Association for Research in Vision and Ophthalmology.

The relative RPE/BM angulation inward, or towards the vitreous of the globe, was measured as a positive angle, and outward was measured as a negative angle. For each eye, the angulation was considered positive if there was > 5 degrees inward angulation, and deemed negative if less than or equal to 5 degrees. Positive angulation of the RPE/BM borders was found in 20/30 eyes (67%) among 10 of the 15 patients with papilledema. Notably, no patient had an IOP > 20 mm Hg. Mean inward RPE/BM angle was +1.5 degrees temporally and +2.5 degrees (SD 1.8 degrees) nasally. For individual patients with papilledema, positive angulation was correlated with RNFL thickness. For all 30 papilledema eyes, the amount of change in the nasal RPE/BM angle correlated with the change in average RNFL (Spearman $r = 0.63$, $P = 0.01$), but no such correlation was seen at the temporal angle ($r = 0.13$, $P = 0.51$). Notably, when medical therapy failed to decrease ICP and relieve papilledema, surgical optic nerve fenestration was performed (incision of the optic nerve sheath to release CSF pressure) that resulted in a decrease in

papilledema and RNFL thickening (Figure 30). Such a finding supports the role of onboard OCT as a means to monitor VIIP severity in astronauts via regular assessment of RNFL.

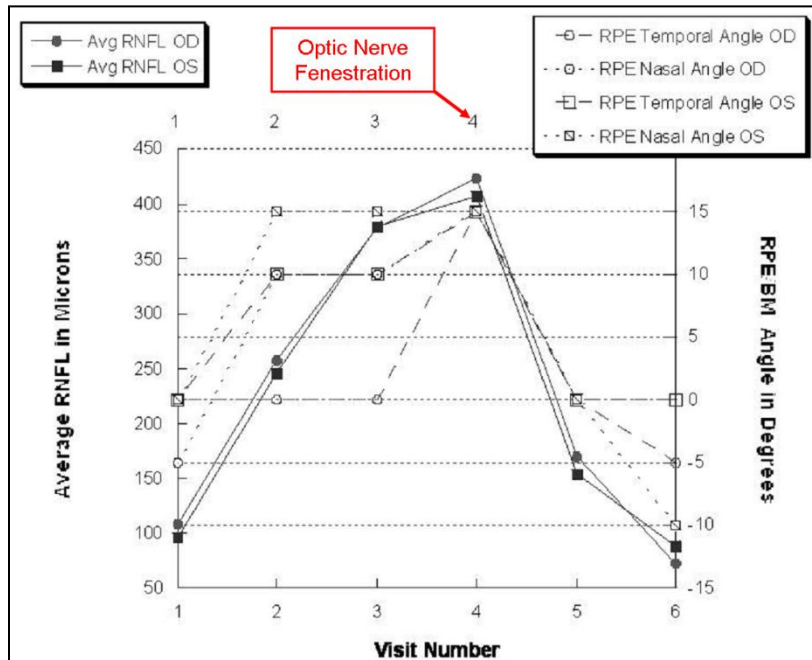


Figure 30: Positive RPE angle associated with RNFL thickening. Note, upon relief of CSF pressure via optic nerve fenestration, RPE angle and RNFL thickness decreased. Reproduced from Kupersmith MJ, Sibony P, Mandel G, and others [83] with permission of The Association for Research in Vision and Ophthalmology.

m) Manipulation of ICP and IOP to Prevent Optic-Disc Edema and Visual Loss

Potentially, one could utilize the TLP gradient to guide treatment of optic-disc edema, by monitoring and modulating IOP and ICP. Pharmaceutical treatments aimed at ICP and IOP could rebalance the TLP gradient thereby reversing axonal compression and edema formation. However, at present there is no validated method of noninvasively measuring ICP during flight.

In summary, changes in ocular system structure and function that have been documented to occur as a result of space flight include, choroidal folds, cotton wool spots, scotomas, hyperopic shifts, RNFL thickening, retinal hemorrhage, globe flattening, optic nerve sheath distention and optic-disc edema. Notably, the latter three findings: globe flattening, optic nerve sheath distention and optic-disc edema have documented associations with elevated ICP. Data collected during short-duration space flight has shown that IOP increases by 20-114% in the first hour of spaceflight, decreases to preflight values for the duration of the flight thereafter, and then decreases to below baseline values postflight. IOP from long-duration spaceflight is being collected, but there are insufficient data points at present to allow a meaningful analysis. Evidence from parabolic flight includes an increase of 5-7 mmHg in IOP, while evidence from bed rest studies shows an almost immediate rise in IOP with horizontal and head-down tilt (6, 7, 10, and 15 degrees), and lower than baseline IOP upon rising from prolonged head-down position, Bed rest has also been shown to cause a decrease in visual acuity, an increase in subfoveal choroidal thickness, and hyperopic shifts.

2. Spaceflight-Induced Cardiovascular Adaptations

In this section several hypothesized cardiovascular system contributors to the development of spaceflight-induced visual impairment and potential interactions with IOP are discussed (Figure 31). Outlined are known, investigated, and hypothesized effects of spaceflight on the cardiovascular system in the hopes that this review will elucidate the relationship among these spaceflight-induced adaptations and their influences upon the changes in vision impairment and IOP in astronauts during and after exposure to weightlessness.

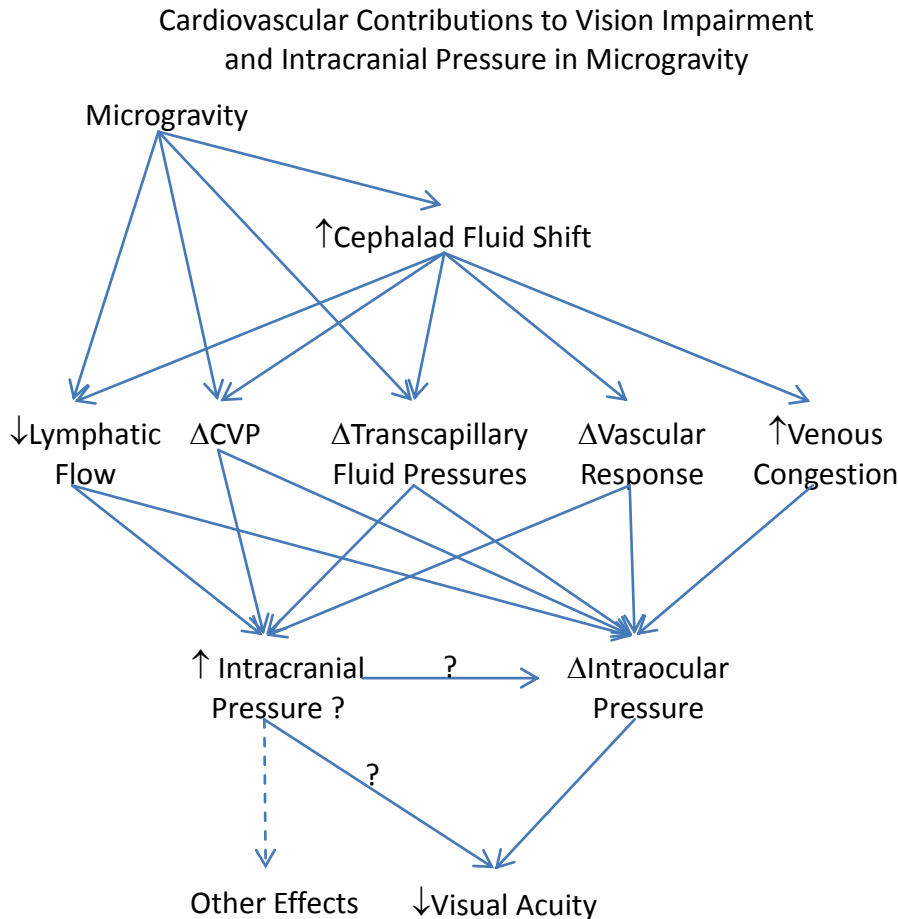


Figure 31: Known, investigated, and hypothesized cardiovascular contributions to vision impairment, ICP and IOP in microgravity.

In a review of the astronaut cases, Mader et al. [1] extensively discussed a number of hypotheses that might explain changes in vision during microgravity exposure but, in general, did not emphasize the potential role of elevated ICPs. While acknowledging that the cephalad-fluid shift may result in venous congestion, as observed from jugular vein distension [84-86], and facilitate increasing ICPs, they outlined arguments against the development of intracranial hypertension and the potential role it might have. Perhaps the most compelling arguments were that no classical clinical symptoms of intracranial hypertension were reported (such as, chronic headaches, diplopia, transient visual obscurations, pulse synchronous tinnitus), and the degree of

ocular manifestations were disproportionate to the borderline elevated measures of ICPs available in these cases. Additionally, it is hard to directly ascribe the changes in vision to an increase in ICP as there currently are no in-flight measures of ICP that temporally correspond to the onset of symptoms; all lumbar punctures were performed after landing. However, Mader et al. [1] suggest that changes in vision and ocular structures with spaceflight might be related to altered IOPs.

a) *Spaceflight-Induced Fluid Shift*

Spaceflight is known to cause a cephalad-fluid shift secondary to the loss of the hydrostatic pressure gradient normally experienced on Earth. Moore and Thornton suggest a 2000 mL shift from the legs to the upper body [87]. Ground-based analogs of spaceflight, such as head-out water immersion and head-down bed rest, suggest that the fluid shift is between 700 to 3000 mL [87-89]. This fluid shift leads to transient increases in stroke volume [90, 91] and cardiac output [92] and possibly increases in ICP and IOP [40]. It is likely that there is significant variability across astronauts in the type and volume of the fluid shift experienced in spaceflight [89]. While fluid shift seen in bed rest results in a reflex diuresis, the mechanisms of fluid redistribution are far less clear during spaceflight [93].

It is clear that the distribution of fluids in the body is influenced by the direction and magnitude of gravity and the resulting hydrostatic gradients. On Earth, standing up from a supine position in a gravity field imposes a substantial challenge to the human cardiovascular system. Due to the increase in hydrostatic pressure gradient acting along the length of the body, venous volume increases by approximately 500 mL [94]. This redistribution of fluid from the central circulation is immediately detected by baroreceptors (pressure) and, in time, by volume (osmolarity) receptors, activating reflex responses to increase heart rate, contractility, and vascular resistance to maintain blood pressure. When astronauts enter the microgravity environment of spaceflight, the opposite effect occurs. It has been well documented that microgravity leads to a cephalad-fluid shift in the absence of the hydrostatic pressure gradient [86, 87, 95-97].

One of the first physiologic changes noted during the Apollo program was the decrease in plasma volume, exhibited by the decrease in weight of the crewmen [98]. It was initially hypothesized that this decrease in plasma volume was a reflex response to a cephalad-fluid shift, although the etiology of this plasma volume decrement was never clearly characterized. Although the time course of the plasma volume losses was unknown due to the lack of in-flight measurements, the degree of plasma volume loss was independent of the duration of the Apollo mission [98].

Initially, the cephalad-fluid shift upon entry into microgravity was documented using anthropometric measures. Pre and postflight anthropometric measures were easily obtained by astronauts and flight surgeons, but the surgeons lacked the ability to distinguish between changes in fluid status and tissue loss. It was assumed that the rapid recovery of anthropometric measures postflight represented fluid shifts and plasma volume recovery, while the more gradual recovery was the result of lean tissue and fat mass accretion. For example, 16 of 24 Apollo astronauts had a decreased calf circumference after spaceflight, which amounted to a mean decrease of 3% immediately postflight that was not fully restored 5 days later, indicating that this loss was a combination of fluid and muscle atrophy [99]. In the last two Apollo missions, leg volume was

reduced by 6% post-landing and did not change appreciably over the next 90 to 160 hours after splashdown. Similar results were obtained in the three U.S. astronauts participating in the Apollo-Soyuz Test Project [100].

Anthropometric observations made during the Skylab 2 and 3 missions demonstrated a decrease in thigh circumference suggesting that these astronauts experienced a significant fluid shift and muscle atrophy during the course of their missions. More extensive circumferential measures were obtained during Skylab 4 [86], when it was found that astronauts experience a rapid loss in leg volume early during their flight, too rapid to be explained by fat or lean tissue loss, but the change was consistent with the cephalic fluid shift that occurs during spaceflight. These measures were performed every 3 cm along the leg and the arm, around the neck, chest, abdomen, and hip (Figure 32).

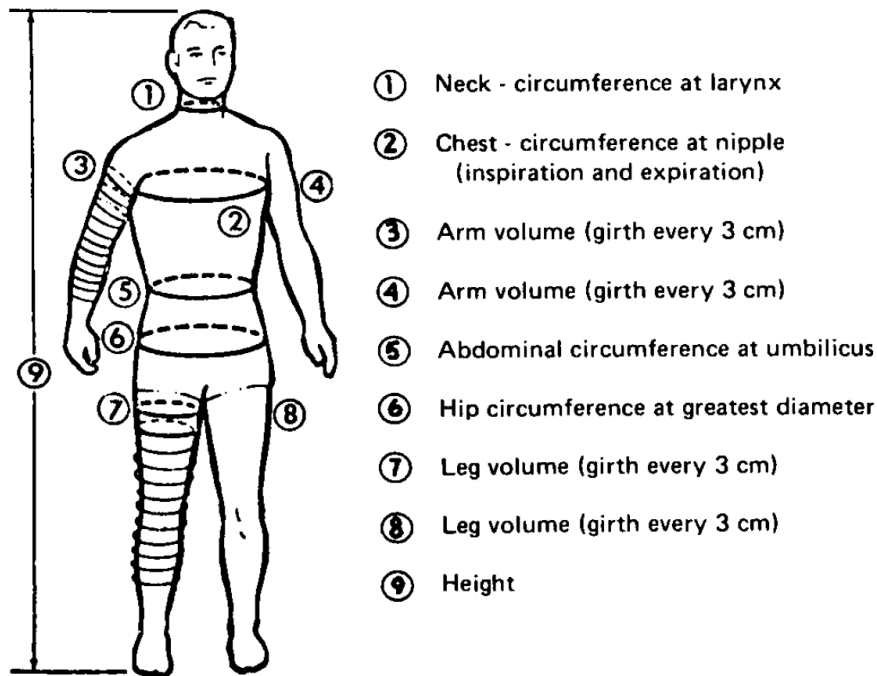


Figure 32: Circumference measures used to calculate volume of fluid shift during Skylab 4 [86].

Interestingly, there was little to no change in arm volume in these subjects from pre to in flight and from in to postflight, suggesting that neither arm fluid volume nor tissue volume changed during the course of their mission (Figure 33). Furthermore, they noted lower limb veins were not distended, while the veins of the upper body, including the jugular, temple and forehead veins were completely full and distended. They concluded that intra and extravascular fluid shifts to above heart level had occurred and hypothesized that increased transmural pressure led to cephalad edema (puffy face).

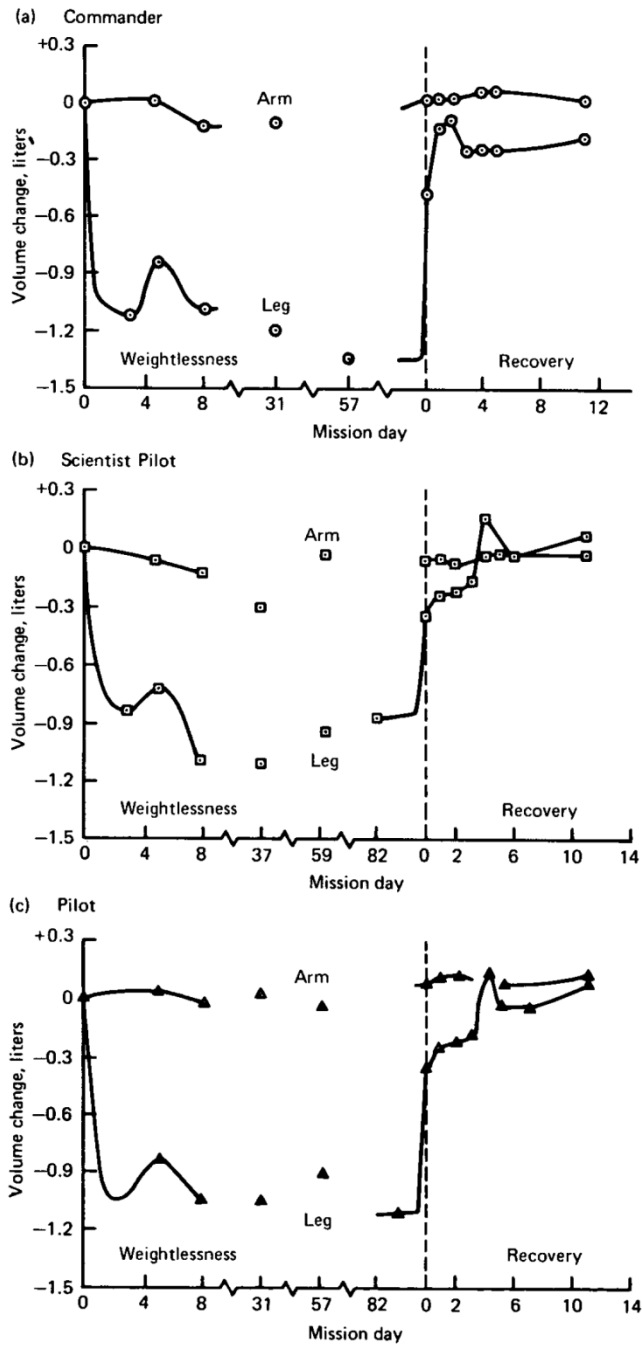


Figure 33: Volume changes pre, in, and postflight from Skylab 4 [86]

Anthropometric measurements of the thigh and calf also were obtained in eleven astronauts during and after five early Shuttle flights (STS-7, 8, 51D, 51B, 61B) using stocking plethysmography [86, 87] (Figure 34). As expected, upon entry into microgravity, leg volume decreased by 11.6% and was explained by the authors to result from a rapid shift in fluid volume to the upper body, which could be seen in photographs of puffy faces, and reports of nasal congestion and 'full headedness'. The total fluid shift was measured to be 2 L, 1 L from each leg, with the majority of the volume coming from the thigh, not the calf. The majority of this fluid

shift occurred in the first 6 to 10 hours after entering microgravity, with a subsequent slow negative decline or plateau. Similar to observations after Skylab missions, when measurements were repeated within 1.5 hours of landing with the astronauts standing, the difference between pre and postflight leg volume was less than in flight, amounting to only an average decrease in leg volume of 4%. The decreased volume upon landing was likely the combined result of lower plasma volume, decreased fat mass, and lower muscle mass. As in Skylab, 1 week after Shuttle landing, leg volume had recovered somewhat towards the preflight value; leg volume was 3% lower than preflight at this time when plasma volume would have been recovered. Using a similar method, Kas'ian et al. [95] measured leg changes on two cosmonauts during the 120-day Salyut-6 mission. They noted a decrease in leg volume of 6% to 7% within the first week of flight in both cosmonauts, which continued to decrease to 18% to 23% reduced leg volume by flight day 120. The absence of postflight tests makes interpretation of these volume changes difficult, as it is unclear how much of the volume loss was due to muscle atrophy from hypokinesia.

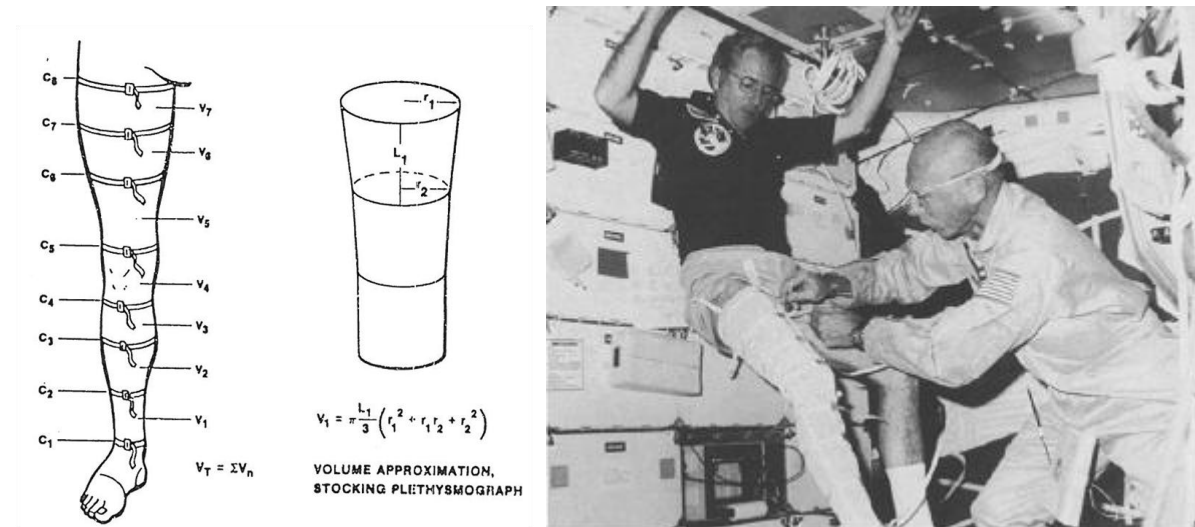


Figure 34: Schematic of leg plethysmograph and Dr. William Thornton making measurements on Commander Richard Truly on STS-8. Reproduced from Moore TP, et al. [87] with permission of the Aerospace Medical Association.

Kirsch et al. [96] were able to use A-mode ultrasound to quantitate the spaceflight-induced fluid shift in one cosmonaut on the Mir 1992 mission. Interstitial thickness measures over the forehead and tibia were used to quantify the hydration or dehydration preflight (supine and head-down), eight times during flight and after 7 days of flight. Facial tissues swelled during the first 3 days but then may have been impacted by a lower body negative pressure session on day 4 of this mission. Tibial interstitial thickness was reduced by 20% and remained low for the duration of the flight and immediately upon landing as well. Body weight did not fully recover within the first 4 days after landing, suggesting that only a portion of the interstitial thickness changes were fluid dependant.

b) Plasma Volume Losses

It is well documented that plasma volume decreases with spaceflight [93, 101-103] although the exact mechanism of this plasma volume decrease is not completely understood. Red cell mass is decreased in spaceflight [103-105] appropriately as a reflex response to hemoconcentration after reduced plasma volume. Leach and coworkers initially reported that total body water is decreased after short-duration Shuttle flights [106] yet suggested that this number may have been enhanced by a space motion sickness-induced reduction in water intake. Several years later, they published the results of SLS-1 and SLS-2 studies in which they measured plasma volume, total body water, and extra and intracellular fluid volumes in seven astronauts. In this report, Leach and coworkers reported that plasma and extracellular fluid volume were decreased, while total body water was unchanged, suggesting that the intracellular fluid volume was increased. This reduction occurred despite no report of natriuresis or diuresis, similar to results from Drummer et al. [107]. It is generally accepted that diuresis is not the cause of reduced plasma volume during spaceflight, but rather a combination of decreased water balance (that is reduced intake) and extravasation into intracellular and interstitial compartments [108]. Leach et al. [93] reported a negative water balance and reduced total circulating protein in the astronauts. They suggest that a rapid filtration of protein out of the vascular space is responsible for the early plasma volume loss and a negative water balance perpetuates this hypovolemia. Norsk also reported that a negative water balance exists in spaceflight and is more pronounced than that seen in bed rest [109]. In his review of Shuttle, Mir, and bed rest data, he reports that intravenous infusion of isotonic saline resulted in an attenuated diuresis compared to bed rest. Similarly, oral water load during a Mir mission resulted in an attenuated diuresis compared to an identical oral water load in bed rest.

c) Central Venous Pressure (CVP)

In the early days of the Shuttle era, the spaceflight-induced cephalad-fluid shift was well-known and assumed to cause an increase in CVP. Norsk et al. [110] measured CVP in 14 subjects while seated upright during parabolic flight and determined only a slight (1.8 mm Hg) increase in CVP during short periods of weightlessness. When seven subjects were studied in a separate parabolic flight study in which CVP was measured in the supine posture, Foldager and coworkers reported a decrease from 6.5 +/- 1.3 to 5.0 +/- 1.3 mm Hg during weightlessness [111]. They were also able to measure CVP in one Spacelab D-2 astronaut, and concluded that CVP in microgravity is close to or below measured values in 1g, supine position. Earlier, Kirsch and co-workers measured peripheral venous pressure in four Spacelab 1 astronauts and suggested that these measures would be analogous to central venous pressure [112]. All four astronauts were reported to have reductions in venous pressure measures; however, only data for two of the astronauts were reported. One astronaut was reported to experience a reduction in CVP from 9.5 cm H₂O (7 mm Hg) on the day before flight to 6.5 and 2.6 cm H₂O (4.8 and 2 mm Hg) on the first and sixth days of flight, respectively. CVP in a second astronaut was reduced from 15.2 cm H₂O (11.2 mm Hg) on the day before flight to 6.5 and 7.7 cm H₂O (4.8 and 5.7 mm Hg) on days 1 and 6 of flight, respectively [112]. These findings were supported by two separate studies by Buckley et al. [113, 114]. The first report was from a Spacelab Life Sciences (SLS-1) flight in which CVP was measured preflight while seated and while in the launch position in the orbiter, during launch and during the initial moments upon reaching microgravity. CVP was elevated from 5 to 6 cm H₂O (3.7 to 4.4 mm Hg) while seated to 10 to 12 cm H₂O (7.4 to 8.8 mm Hg) in the launch

position. It increased further during the launch, presumably from the G_x forces, to 15 to 17 cm H₂O (11 to 12.5 mm Hg) before decreasing to 0 to minus 3 cm H₂O (0 to minus 2.2 mm Hg) upon entering microgravity. This reduction was rapid, occurring during the first minute of microgravity, and remained within 1 to 2 cm H₂O (0.7 to 1.4 mm Hg) until the catheter was removed [113]. This was one of the first reports to refute the hypothesis that CVP increased with the cephalad-fluid shift experienced in microgravity. Interestingly, heart size in this astronaut increased at the same time that CVP decreased. In a second report of two SLS-2 crewmembers, similar results were obtained [114]. Mean CVP (two SLS-2 crewmembers and one SLS-1 crewmember) increased from 8.4 cm H₂O (6.2 mm Hg) preflight to 15 cm H₂O (11 mm Hg) in the launch position to 2.5 cm H₂O (1.8 mm Hg) after 10 minutes in microgravity (Figure 35). They further reported that cardiac filling was increased, despite the reduction in CVP, hypothesizing that effective filling pressure was elevated due to the reduced transmural pressure applied from the lungs and abdominal organs in microgravity.

Despite a decrease in central venous pressure, elevated filling pressure may impede the emptying of the large thoracic veins, such as the jugular and superior vena cava. Herault et al. [85] reported significant engorgement of the jugular and femoral veins during spaceflight. Arbeille and coworkers examined both lower and upper body veins during bed rest and long-duration spaceflight [115]. During bed rest, only the jugular vein was distended, while the femoral vein was smaller. During spaceflight; however, both veins were distended upon exposure to microgravity and remained distended by as much as 40% after 6 months of spaceflight (Figure 36). Arbeille suggests that the marked enlargement of the jugular vein may be indicative of blood pooling in the brain [115]. This study highlights an important deficiency of HDT bed rest as an analog of spaceflight. Despite the cephalad-fluid shift in bed rest, hydrostatic pressure tissue gradients still exist, which explain the divergent femoral vein responses in Arbeille's study. Spaceflight causes more than a fluid shift due to the removal of the G_z hydrostatic gradient. Removal of all gravitational gradients results in a fluid shift and a response to the fluid shift that is unique to the microgravity environment.

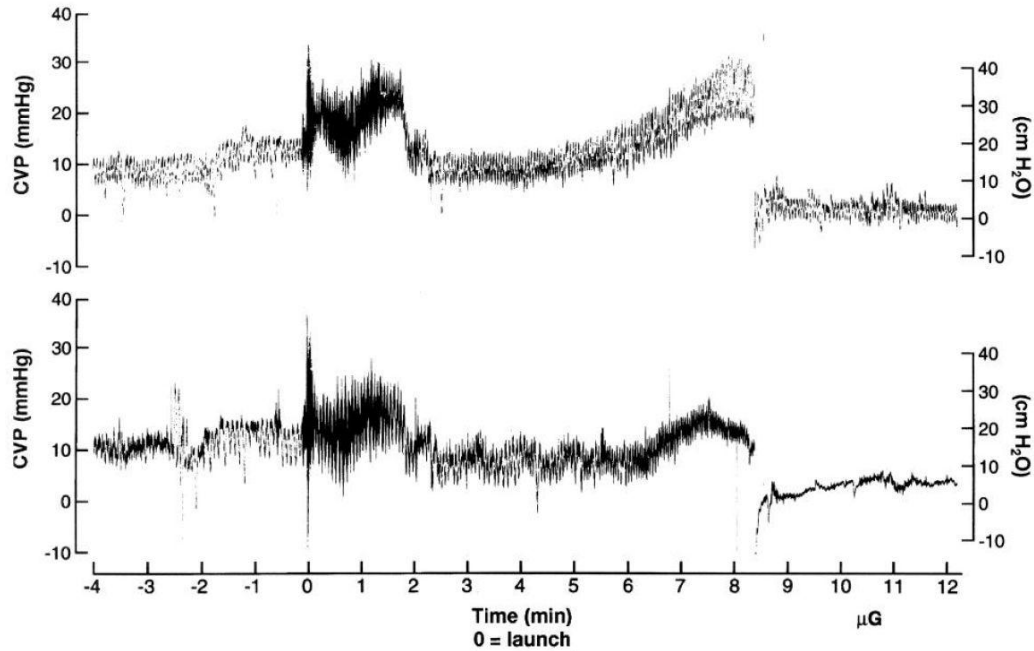


Figure 35: CVP tracing from two SLS-2 astronauts showing the decrease in CVP upon exposure to microgravity 8.5 minutes post-launch. Reproduced from Buckley JC Jr, et al. [114] with permission from The American Physiological Society, obtained via Copyright Clearance Center, Inc.

Videbaek and coworkers tested this hypothesis by measuring central venous pressure, esophageal pressure (EP – a surrogate of intrathoracic pressure) and atrial distension in seven men during parabolic flight [116]. The CVP decreased during the microgravity period of parabolic flight from 5.8 ± 1.5 to 4.5 ± 1.1 mm Hg and esophageal pressure decreased from 1.5 ± 0.16 to -4.1 ± 1.7 mm Hg. Left atrial diameter increased from 26.8 ± 1.2 mm to 30.4 ± 0.7 mm. Despite the decrease in CVP, the left atrial filling pressure was elevated (as demonstrated by left atrial distension). Videbaek suggests that the difference in CVP and EP results in an increased ‘transmural’ central venous pressure, which explains the increased cardiac filling despite the reduced CVP. Furthermore, they report increased left ventricular end diastolic volume, stroke volume, and cardiac output, likely the result of the chest wall changing shape and expanding in the absence of gravity. White and Blomqvist used a three-compartment cardiovascular model to simulate the relaxation of the chest in microgravity [117]. Their results indicate that this would increase the transmural filling pressure of the heart, increase left ventricular end diastolic volume, stroke volume, and cardiac output, similar to the results obtained by Videbaek in parabolic flight. Prisk et al. [118] also reported elevated stroke volume and cardiac output in four SLS-1 astronauts. In their report of pulmonary diffusing capacity, they also suggest that improved membrane diffusing capacity is a function of microgravity-induced mechanical changes in pulmonary blood flow and not an adaptive response.

These data regarding CVP have been collected and evaluated largely in the context of cardiac filling and the progression of post-spaceflight orthostatic intolerance. It is important to point out that the apparent disagreement in the field regarding the effects of microgravity on CVP may largely be perceptual. While changes in transmural pressure will have a significant effect on venous return and thus cardiac output, it is far less clear if there would be any effect on venous or

lymphatic drainage from the head. This is due to the fact that driving pressures are thought not to change in microgravity as both sides of the vascular tree are influenced by gravity. It may be that peripheral venous pressures in the neck will provide more applicable information regarding blood and lymph drainage.

d) *Transcapillary Fluid Pressure*

In support of the many anecdotal reports of puffy faces, sinus congestion, and feeling of a full head during spaceflight, Kirsch et al. [96] were one of the first to clearly show interstitial swelling in the forehead during flight. However, there is little spaceflight evidence of filtration into the extravascular space in the head and neck. Using a ground-based analog of 10-degree HDT, Diridollou and coworkers [119], showed that after 24 hours, subjects presented with a similar forehead interstitial swelling to that seen by Kirsch [96]. Linnarsson et al. [120] using tetrapolar bioimpedance, measured segmental fluid shifts during 7-degree HDT bed rest. The authors suggest that the initial interstitial swelling is a result of a rapid blood shift, which is detected as a plasma volume expansion and is followed by a more gradual extravascular shift from the legs over the course of 2 hours. Bioimpedance detected extravascular volume leaving the thigh and the calf, but not entering the chest, suggesting that this volume was being absorbed into the vascular space. This would result transiently in decreased plasma oncotic pressure. This is supported by a study by Hsieh et al. [121] who reported an initial decreased oncotic pressure in the time frame reported by Linnarsson [120], but ultimately resulting in an elevated colloid osmotic pressure. Similarly, Parazynski et al. [122] reported an initial decrease in colloid oncotic pressure from 21.5 +/- 1.5 mm Hg to 18.1 +/- 1.9 mm Hg within the first 4 hours of HDT. They suggest that this decrease in plasma oncotic pressure is a result of the change from filtration to absorption in the capillary beds below the heart. This colloid oncotic pressure is thought to gradually return to baseline and is described by the Starling-Landis equation

The Starling-Landis equation describes fluid movement in the microvasculature:

$$J_v = K_f[(P_c - P_i) - \sigma(\pi_c - \pi_i)]$$

- J_v = Net fluid movement
- K_f = Filtration coefficient
- P_c = Capillary fluid pressure
- P_i = Interstitial fluid pressure
- σ = Reflection coefficient
- π_c = Capillary oncotic pressure
- π_i = Interstitial oncotic pressure

Fluid movement into or out of the capillaries is dependent on the hydrostatic pressure drop ($P_c - P_i$) minus the colloid osmotic pressure drop ($\pi_c - \pi_i$). The filtration coefficient (K_f) takes into account the permeability of the capillary membranes to water that is dependent on surface area and hydrostatic conductance. The reflection coefficient (σ) is used to correct for the fact that not all plasma proteins are effective in retaining water, and is different in various vascular beds.

Parazynski et al., were the first to quantify all four Starling-Landis pressures during HDT [122]. They measured upper body capillary and interstitial fluid pressures, as well as plasma and tissue oncotic pressures in seven men during 8 hours of 6-degree HDT. Capillary fluid pressure increased from

27.7 +/- 1.5 mmHg to 33.9 +/- 1.7 mm Hg at the end of bed rest, while interstitial fluid pressure did not significantly change (Figure 36). Although plasma oncotic pressure initially decreased, it returned to baseline by the end of 8 hours of bed rest. Subcutaneous and intramuscular colloid osmotic pressure in the face and neck did not change. Parazynski and coworkers suggest that the significantly elevated net Transcapillary pressure gradient in the head and neck is the reason for cephalic edema during bed rest and spaceflight. They further suggest that capillaries above the heart may be more permeable to protein filtration than those below the heart, similar to the report by Leach et al. [93]. Hargens measured interstitial pressure in the lower leg muscles and subcutaneous tissues and reported a decrease in tissue pressure of 7.4 and 4.4 mm Hg, respectively [123]. He also hypothesized that lower leg vascular absorption results in decreased vascular oncotic pressure and, coupled with increased cephalic capillary pressure, results in filtration in the upper body. Several years later, in a separate review, Hargens further postulated that the reduced tissue weight in microgravity results in lower interstitial fluid pressure, further shifting the Starling balance to net filtration during spaceflight [124].

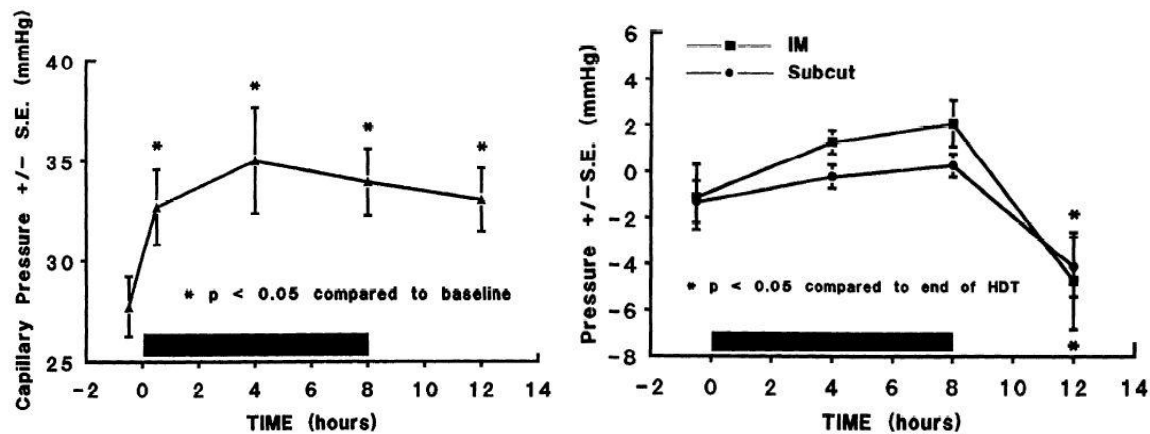


Figure 36: Capillary (left) and interstitial fluid pressure (right) during 8 hours of HDT bed rest. Capillary pressure is significantly elevated and interstitial fluid pressure does not significantly change. Reproduced from Parazynski SE, et al. [122] with permission from The American Physiological Society, obtained via Copyright Clearance Center, Inc.

Cephalad edema may further be exacerbated in spaceflight by changes in microvascular water permeability. In a lumped parameter cardiovascular model, Lakin et al. [125] postulated that cerebral fluid filtration is increased if the space between endothelial cells of the cerebral blood vessels is increased. This would be possible in spaceflight if the gravity-induced hydrostatic pressure gradients in the cerebral interstitium were removed. They also suggest that radiation exposure during spaceflight may alter endothelial protein structure such that cells shrink, increasing permeability between cell junctions. Christ et al. [126] showed that fluid filtration capacity (capillary permeability) is increased during long-duration bed rest, and this may be enhanced in the presence of free O₂ radicals and activated leukocytes, such as during exposure to spaceflight radiation and other oxidative stressors.

Diedrich et al. [127] nicely summarizes the current model of spaceflight-induced fluid volume changes (Figure 37). Exposure to microgravity causes a cephalad-fluid shift secondary to the removal of the hydrostatic pressure gradient. Central venous pressure is reduced due to expansion of the chest and decreased pressure from tissue and organs. This reduction in tissue compression likely plays a role in extravasation of fluid, resulting in overall reduced plasma volume and cephalic edema.

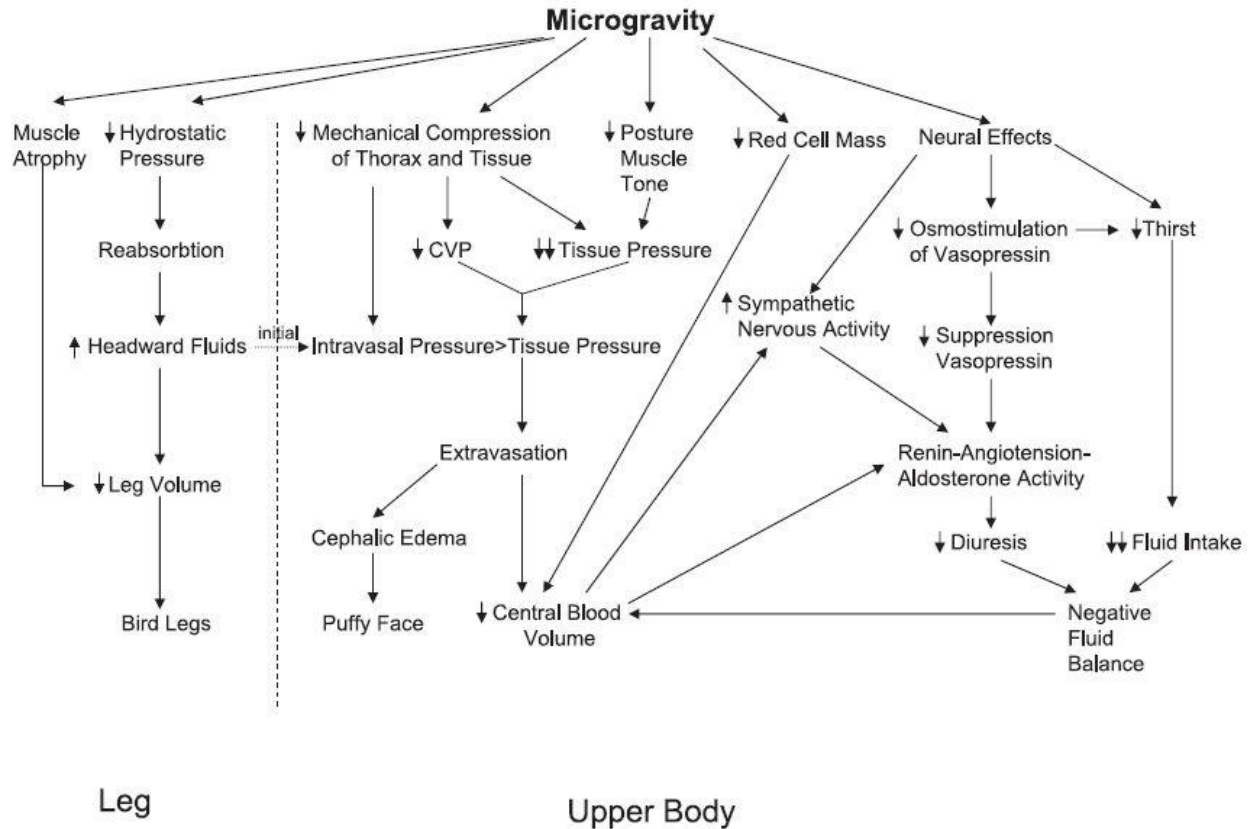


Figure 37: Flow diagram of predicted blood and fluid volume changes during spaceflight. Reproduced from Diedrich A, et al. [127] with permission of Wolters Kluwer Health, obtained via RightsLink.

e) Venous Distension

Arbeille and coworkers examined both lower and upper body veins during HDT bed rest [115] (Figure 38). Spaceflight causes more of a fluid shift due to the removal of the G_z hydrostatic gradient. Removal of all gravitational gradients results in a fluid shift and a response to the fluid shift that is unique to the microgravity environment.

Risk of Microgravity-Induced Visual Impairment/Intracranial Pressure (ICP)

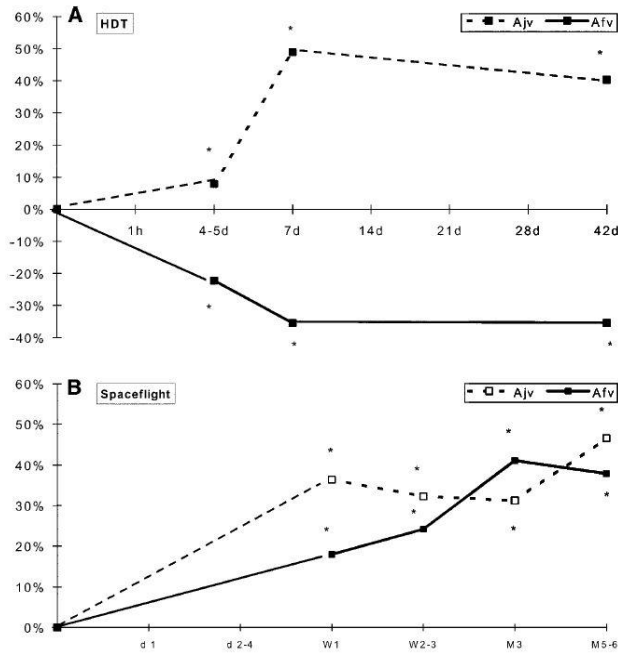


Figure 38: Divergent vein diameter responses between HDT bed rest (panel A) and spaceflight (panel B). The panels show percentage change of the preflight values, measured at 1h, and days 4-5, 7, 15, 21, 28 and 42 during HDT, and at days 1 and 2-4, weeks 1 and 2-3, and months 3 and 5-6 during spaceflight. The jugular vein is distended in both real and simulated microgravity, while the femoral vein is only distended in real microgravity. A_{jv} - Jugular vein cross-sectional area. A_{fv} - Femoral vein cross sectional area. * P<0.05, significantly different from preflight or pre-HDT values. Reproduced from Arbeille P, and others [115] with permission of Springer-Verlag, obtained via Copyright Clearance Center, Inc.

f) Vascular Adaptations to Spaceflight

Normal blood vessel function is necessary for sustaining and adapting to the metabolic demands of individual organs. To meet the blood flow requirements of organs and local tissue beds, arteries and veins must be able to respond rapidly to diverse physical and chemical signals by changing either vessel caliber (diameter) or altering the density of the vascular network. Several factors regulate how vessels respond to modifications in demand including humoral, neural, and autoregulatory. Importantly, changes to any of these systems such as in response to chronic activation from environmental stimuli or injury may result in impaired vascular control and contribute to numerous pathologies.

Medical data from as early as the Mercury and Gemini missions indicate that exposure to microgravity results in cardiovascular deconditioning presenting as orthostatic intolerance upon return to Earth's gravity [128]. While many researchers agree that the space-related deconditioning is likely triggered by a headward fluid shift and a reduced plasma volume, a preponderance of evidence indicates that the loss of vascular control, indicated by lower peripheral resistance and increased blood pooling in the lower limbs, is a primary mechanism for postflight orthostatic hypotension and is independent of volume status [101, 102, 129-132]. For example, flight data from both Buckey [101] and Fritsch-Yelle et al. [131] demonstrated that astronauts who finished a postflight stand test, compared to those who became presyncopal, had a significantly greater vasoconstrictor response with higher total peripheral resistance. Fritsch-Yelle et al. suggested that the lower level of peripheral resistance, associated with an increased incidence of postflight orthostatic hypotension, is likely due to decreased circulating levels of norepinephrine and is less likely related to volume status as there were no differences in plasma volume levels between presyncopal and nonpresyncopal subjects. Ground-based studies using HDT bed rest to simulate microgravity overwhelmingly confirm a significant relation between

orthostatic intolerance and a decreased vasoconstrictor response that is evidenced by increased lower limb venous compliance [133-136].

Along similar lines of thought, differences between astronauts who become presyncopal and those that are nonpresyncopal on landing day may provide additional insight into the effects of spaceflight that might contribute to in-flight vision changes. Specifically, Taday et al. [137] observed that although vascular compliance, calculated as stroke volume divided by pulse pressure, was not different between the astronaut groups before flight, vascular compliance was lower in the nonpresyncopal astronauts than in the presyncopal astronauts on landing day. Perhaps increased stiffness may reflect remodeling of the vascular wall, including increased collagen: elastin ratio, collagen cross-linking, and modifications of the vascular matrix. Although this response to spaceflight may be to protect against postflight orthostatic intolerance, assuming that the decrease in vascular compliance is similar across all vessels in the body, then perhaps these observed changes may be suggestive of changes in the cerebrovasculature. However, using the hind-limb suspension model in rats, Taday et al. [137] provided some of the first ground-based experimental evidence demonstrating that a reduction in large artery hydrostatic forces results in greater vessel distention and is accompanied by an impaired vasoconstrictor response to the sympathetic neurotransmitter norepinephrine. Since then, considerable attention has been focused on understanding the mechanisms that underlie many of the microgravity-induced vascular adaptations in relation to orthostatic intolerance. Much of this data has recently been reviewed in-depth by Zhang, who reported that changes in arterial compliance were a local effect resulting from regional changes in blood pressures. A number of other probable explanations may include, a reduced adrenergic receptor sensitivity [138], less vasoconstrictor reserve [139, 140], and an enhanced flow-dependent vasodilator response [141].

The effects of gender on postflight orthostatic tolerance, or the ability to regulate blood pressure during standing or upright tilt, may be of interest in the investigation of VIIP as men appear better able to maintain blood pressure during orthostatic challenges than women, and men also seem to be more susceptible to vision changes during long-duration spaceflight. However, as noted by Fritsch-Yelle et al. [131], differences in postflight orthostatic tolerance in the astronaut population may be the result of selection bias. That is, the large majority of astronauts who did not experience orthostatic intolerance on landing day were career military pilots or had high performance aircraft training [131, 142]. To further illustrate this potential bias, the study with the highest incidence of orthostatic intolerance also has the highest proportion of payload specialists [101].

g) *Radiation Effects on Vascular Function*

Our present level of knowledge of the vascular effects of radiation, in particular space-like radiation, greatly lags that of the microgravity-related vascular alterations. Until recently, the majority of evidence suggesting radiation-induced changes in vascular function was substantiated only by epidemiologic studies such as those reporting data on cardiovascular disease rates in the Hiroshima/Nagasaki atomic bomb survivors [143] or the similar findings from the Chernobyl emergency workers [144]. The vascular effects of exposure to radiation are generally focused around cardiovascular disease formation, most notably atherothrombotic vascular disease. Unlike the deconditioning effects of microgravity, radiation is thought to

produce damaging cellular effects either directly [145-147] or indirectly [148-151]. Aside from programmed cell death (apoptosis), several studies suggest that exposure to radiation impairs endothelial function shifting the regulatory balance towards increased vasoconstriction through impairment in the nitric oxide pathway [151-153]. While a healthy endothelium is primarily associated with maintaining normal vascular function through the production and secretion of several vasoactive substances such as nitric oxide, it also serves as a selective permeable barrier, regulating the exchange of fluids and blood constituents (such as plasma proteins and cells) between the circulation and the surrounding tissues. The impaired trafficking of substances from the intravascular space to the extracellular region could have significant implications on the delivery of nutrients and fluid distribution to surrounding tissues and organs. In addition, questions remain as to whether the combined vascular effects of exposure to microgravity and space-like radiation will be additive contributing to an even greater pathogenesis or whether the increase in vascular compliance resulting from the microgravity-induced deconditioning will be offset by the increase in vasoconstrictor tone due to impairment in the nitric oxide pathway.

h) Microgravity Effects on Cerebral and Ocular Circulation Vascular Function

Often overlooked, but critically important toward producing orthostatic intolerance is a decrease in cerebral perfusion. In general, cerebral blood flow is well protected against systemic changes in pressure or flow without compromising the high demands of brain tissue. However, with a reduction in central volume from both a decrease in plasma volume and blood pooling in the lower limbs, it is reasonable to assume that cerebral blood flow may be impacted after spaceflight.

Blood flow to the brain is supplied by the two carotid and two vertebral arteries that communicate with each other through the arterial anastomoses that form the circle of Willis. Under normal conditions the circle of Willis acts only to communicate need and not as a central station where supply is mixed and then delivered to the smaller collateral circulations [154, 155]. Three pairs of arteries form the circle of Willis and feed specific regions of the brain, the anterior, middle, and posterior cerebral arteries. Extending beyond the larger arteries are dense networks of capillaries where nutrient exchange takes place with a 2 to 3 fold greater density in the gray compared with white matter. The blood is collected and drained by two systems of veins, including the deep venous system within the brain and the internal jugular and other veins outside of the skull. Unique to the circulation within the skull is that it is tightly regulated by the blood-brain barrier and is therefore protected against ionic and humoral factors. The cerebral vasculature undergoes fine adjustments primarily through autoregulatory processes such that under normal healthy conditions on Earth, the cerebral blood vessels have an intrinsic ability to keep blood flow constant over a wide range of arterial blood pressure levels via myogenic, metabolic and tissue pressure mechanisms.

Data indicate that upon entry into space, the mean arterial pressure in the head increases from approximately 70 mm Hg to 100 mm Hg. The higher cerebral perfusion pressure in turn leads to elevations in both cerebral artery and capillary blood flow which contributes to elevations in ICP [124]. It is widely held by some that the product of these microgravity-induced alterations in perfusion pressures and blood flow, and elevations in ICP over time contributes to pronounced changes in cerebral responsiveness [101]. However, a number of studies suggest that cerebral

blood flow is lower in response to spaceflight and head-down bed rest [131, 156, 157]. Specifically Kawai et al. [156], demonstrated that after 24 hours of HDT bed rest peak cerebral blood flow velocity was significantly lower compared to before HDT and remained lower up to 6 hours of recovery (Figure 39). These differences in the literature highlight the need for additional research in this area.

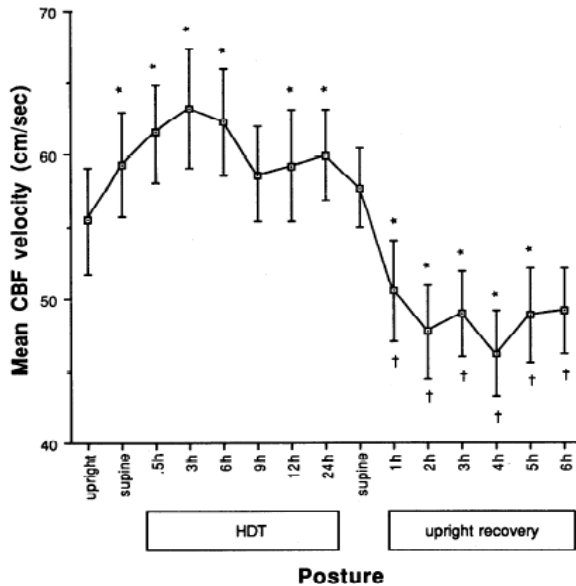


Figure 39: The time course of mean cerebral blood flow velocity in subjects after 24-hours HDT bed rest. Reproduced from Kawai Y, and others [156] with permission from The American Physiological Society, obtained via Copyright Clearance Center, Inc.

Controversy exists as to whether regulation of blood flow is altered in response to stress (such as, going from a supine to a standing position) or whether the lower values are simply a factor of hypovolemia. Data against a change in regulation include that from Fritsch-Yelle et al. [131] who measured blood flow velocity in the middle cerebral artery using ultrasound and did not find a difference in tilt response between presyncopal and nonsyncopal astronauts. In another study that measured cerebral blood flow, velocities and beat-to-beat changes in arterial pressure, it was found that after 16 days in space static autoregulation was not impaired and moreover dynamic regulation (changes occurring during stress) was actually improved [158]. Interestingly, Greaves et al. [159] also reported on improved autoregulation in a set of subjects who participated in 60 days of HDT bed rest. Taken together, these data and recent findings from Jeong and colleagues [160] suggest that autoregulation is in fact not impaired and that the alterations in blood flow after spaceflight are related to volume status .

While the human data appear undisputable, evidence from several ground-based studies using the rat hind-limb tail suspension model suggests that the reduction in cerebral blood flow is associated with a decrease in autoregulation and that it is due to alterations in cerebral arterial structure and function. Indeed, data from Geary et al. [161] and Wilkerson et al. [162, 163] indicate that myogenic tone and vascular resistance is increased, and that the difference in tone (suspended versus control rats) is related to changes in nitric-oxide-mediated vasodilation. Interestingly, the overall functional consequence of increased tone appears to lead to reduced blood flow and the stimulus does not appear to be an increase in arterial pressure but rather increases in transmural pressure caused by the elevation in the extravascular pressure in the cranium [162].

However, as noted previously, data from similar investigations on cerebral autoregulation in human spaceflight do not corroborate the findings in the ground-based analogs. These data are in line with evidence from modeling steady-state ICP differences between HDT bed rest and long-duration microgravity exposure [164]. It was concluded that ICP should be less in crew exposed to actual microgravity compared to subjects in long-term HDT [164]. The reason for the profound differences in findings between actual spaceflight and its analogs remains unclear; however, it has been speculated that the central volume shift in fluid, and subsequent redistribution of fluid between compartments and tissues, is not comparable.

Evidence suggests that most spaceflight-related cardiovascular adaptations return to preflight values within 7 to 14 days of re-exposure to Earth's gravity. However, there are no surveillance data to confirm this. Moreover, no data exist that directly compare measures of cardiovascular regulation in astronauts who have participated in the ISS missions that may identify individuals at risk for visual disturbances after long-duration spaceflight. Towards this end, a retrospective analysis was performed on Medical Operation tilt/stand test data collected pre and immediately postflight on 20 astronauts that flew on both Shuttle and the ISS (Figure 40). It was found that pulse pressure most clearly differentiated the two mission types compared to other cardiovascular measures (for example, total peripheral resistance and stroke volume). Statistical analysis confirmed that mean pulse pressure across the first 5 minutes of the postural stress test was significantly higher before (45.6 [42.1 to 49.1] mm Hg) and after (50.7 [46.9 to 54.6] mm Hg) time on the ISS compared with their most recent Shuttle flight (31.6 [27.8 to 35.4] mm Hg, and 32.2 [28.3 to 36.0] mm Hg respectively), even after correcting for differences in age and cumulative number of mission hours. Examination of the relation between stroke volume and pulse pressure, an indicator of change in arterial compliance, demonstrated that the range of pulse pressures, for a similar change in stroke volume, was greater immediately after Shuttle flight (lower compliance) compared to before flight. Interestingly, the range of pulse pressure remained greater in astronauts (no difference in stroke volume) before their time on the ISS (Figure 41). These results suggest that measures of arterial compliance (the relation between stroke volume and pulse pressure) are lower after a Shuttle mission and do not resolve in astronauts who also participate in long-duration spaceflight and thus provide evidence for specific vascular changes that may contribute to alterations in cerebral blood flow and IOP that are thought to underlie changes in visual acuity after long-duration spaceflight.

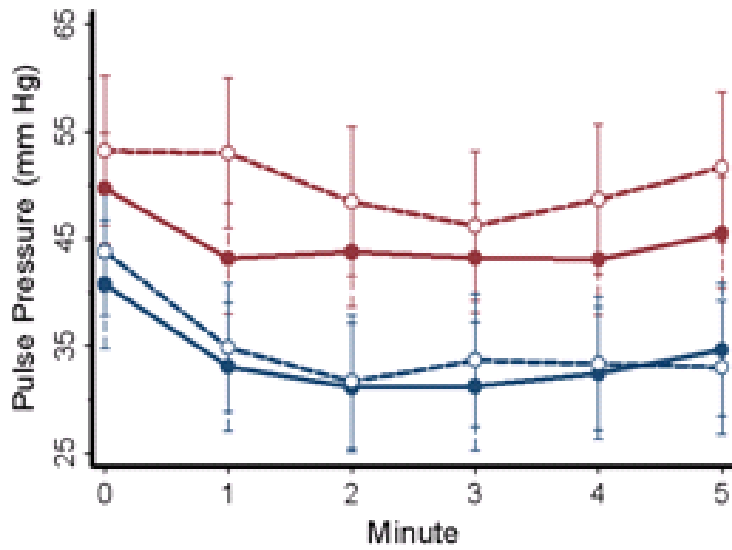


Figure 40: Arterial pulse pressure (mm Hg) during the first 5 minutes of a tilt test, before flight (closed circles) and after flight (open circles) in astronauts who flew both Shuttle (blue) and on the ISS (maroon). Pulse pressure was significantly higher ($P = 0.009$) before and after being on the ISS compared with before and after flying on Shuttle ($N = 20$).

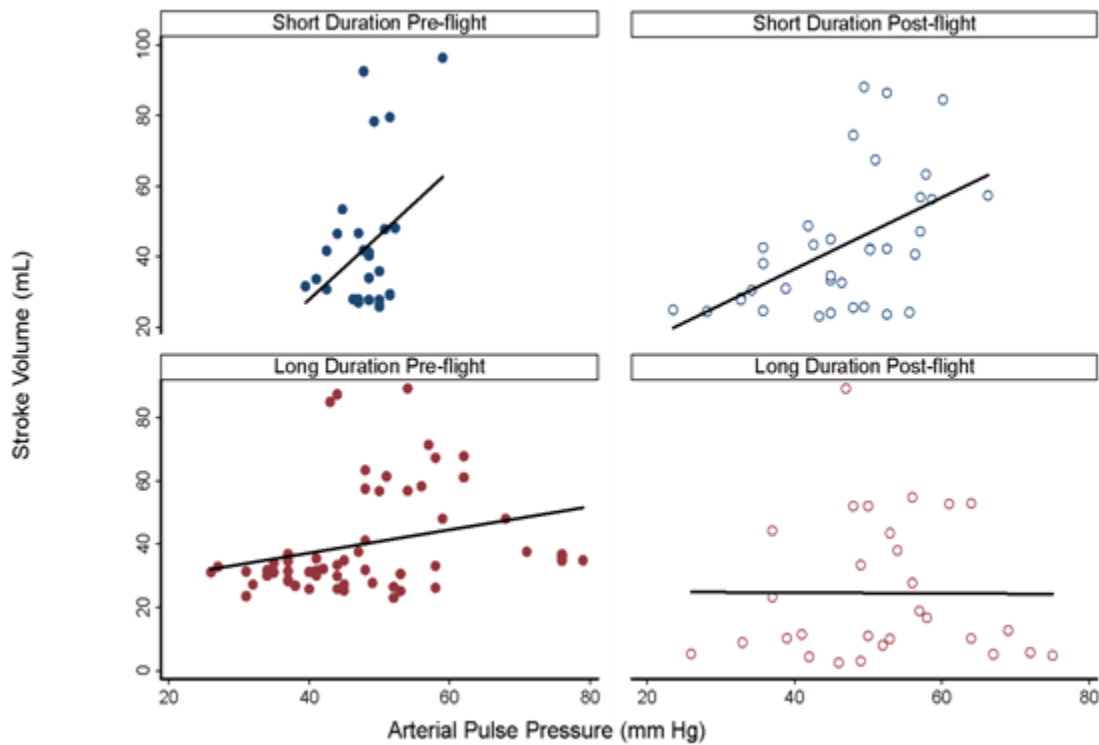


Figure 41: Relation between stroke volume and arterial pulse pressure during the first 5 minutes of a tilt test in astronauts who flew both on the Shuttle (blue) and on the ISS (maroon) before flight (closed circles) and after flight (open circles) ($N = 20$).

i) **Lymphatic Flow**

Perhaps the least well understood component of the vascular system in the human body is the lymphatics; this is especially true for lymphatic structure and function of the brain. In fact, the current understanding suggests that there are no organized lymphatic vessels draining the brain [165-167]. Fluid is believed to drain directly into the blood via arachnoid villi, [167, 168] flow down cranial nerves to collecting nodes [169] or follow blood vessels to collect in cervical lymph nodes (Figure 42) [166, 167]. It is not well documented which of these routes predominates in the human, as much of the work has been done in quadrupedal mammals, though it is likely that all three pathways play some role. What is striking about all three of these drainage pathways is the lack of an active pumping mechanism involved in bulk flow of lymph, unlike the lymphatic vasculature of other tissue beds. There are no lymphangions, no valves, and no pressure/flow sensitive pumping action. This makes the lymphatic drainage of the brain potentially more sensitive to the effects of gravity. Lymphatic drainage of the eye is also a matter of some disagreement, and the precise structures/routes taken by the lymph are not well characterized [170].

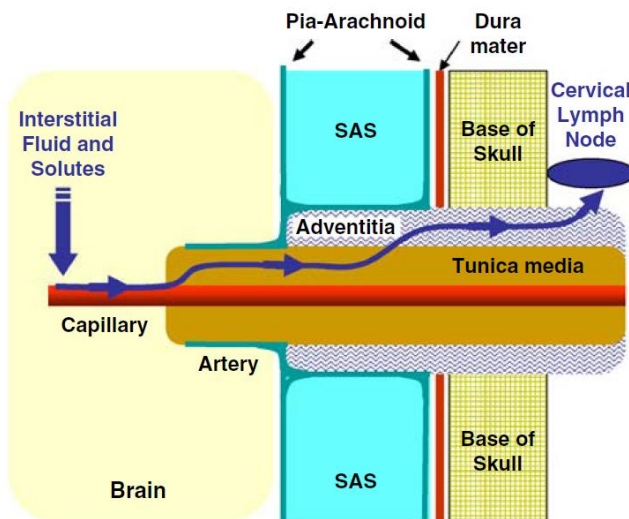


Figure 42: Proposed perivascular drainage route of brain lymph. Reproduced from Weller RO, and others [167] with permission of the World Federation of Neurology and Springer-Verlag, obtained via Copyright Clearance Center, Inc.

Perivascular Lymphatic Drainage of the Brain

To our knowledge, no research exists on the effects of spaceflight on lymphatic drainage of the brain or eye. Only one well controlled study has been conducted on the effects of simulated microgravity on lymphatic contractile function [171]. These investigators used a rat hind-limb unloading model, a very common animal model for simulating the effects of spaceflight on the musculoskeletal system. Lymphatic vessels were studied from four different areas of the body; cervical, thorax, mesenteric, and femoral to sample vessels of different sizes and with different hemotologic conditions during tilt. The selection of the cervical lymphatics in this study is critical for our purposes, as both the brain and eye ultimately drain into the cervical lymph. After 2 weeks of hind-limb unloading, inhibition of contraction frequency (cervical), ejection fraction (all) and fractional pump flow (Figure 43) were found in the lymphatics [88].

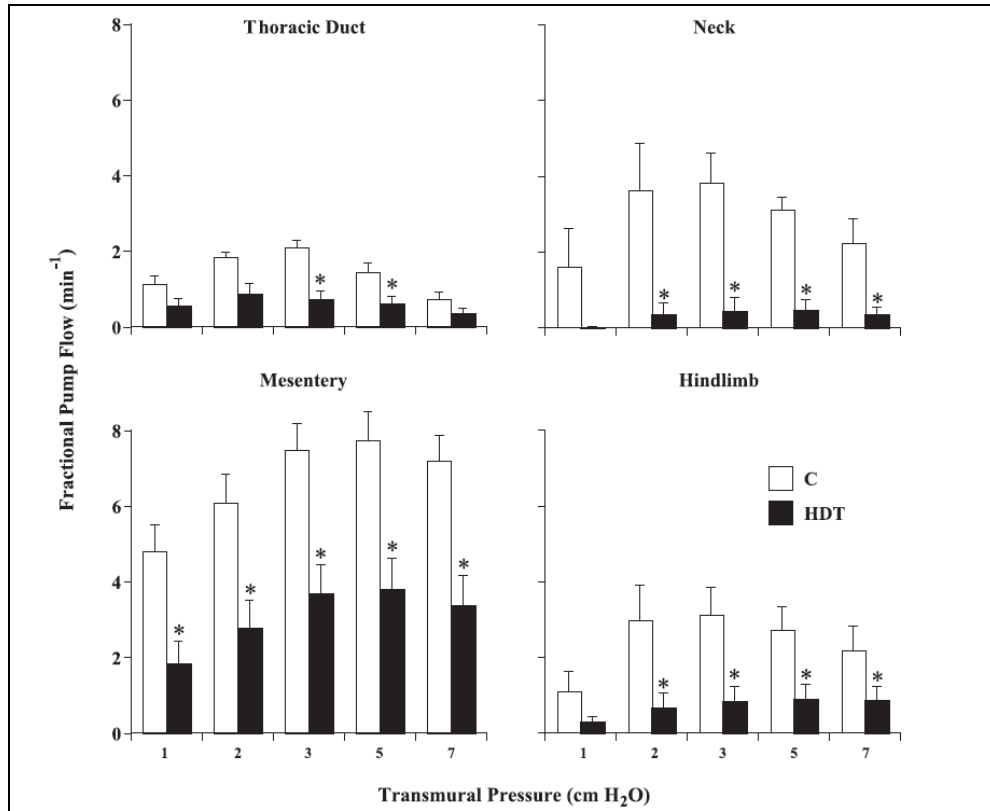


Figure 43: Effect of 14 days hind-limb unloading on the fractional pump flows of isolated lymphatic vessels from four different tissue beds. Reproduced from Gashev AA, et al. [171] with permission from The American Physiological Society via Copyright Clearance Center, Inc.

The degree of inhibition was dependent on the pressures and/or flows through the vessels. The authors concluded that simulated microgravity ‘profoundly’ inhibited the active pumping of lymph in all four tissues. They further propose that this inhibition may contribute to the fluid redistribution seen during spaceflight. It is somewhat surprising that vessels from all four areas were affected in the same way. Studies of arterial vessels in rats [172] and humans, during bed rest [173] have shown that the vessels of the lower body and upper body react differently.

3. Spaceflight-Induced Central Nervous System Adaptations

The ocular changes documented in the astronauts affected by the VIIP syndrome may be due to the cephalad-fluid shift caused by spaceflight exposure and presumed, prolonged increase in ICP. The symptoms (choroidal folds, globe flattening, hyperopic shift, and optic-disc edema) seen in affected astronauts after long-duration spaceflight are similar to those seen in the terrestrial IHH condition [174]. It should be noted that the astronauts do not display all of the classic IHH symptoms such as chronic headaches, diplopia, transient visual obscurations, or pulse-synchronous tinnitus. This section will give a brief overview of retrospective data analyzed as part of an occupational surveillance activity and hypothesized changes in the central nervous

system as a result of long-duration spaceflight. As further data is collected, this section will be expanded to include additional information.

a) *Intracranial Pressure*

The pressure inside the rigid cranium, referred to as ICP, is determined by the sum of the intracranial constituents: the brain parenchyma, interstitial fluid, arterial blood, venous blood and CSF. Normal ICP ranges from 5 to 15 mm Hg (or 6.8-20.4 cm H₂O) depending upon body position. The ICP is lower when standing due to the shift of fluids towards the feet and a decrease in intracranial mass as a result of a shift in venous blood and CSF out of the cranium. The ICP is higher when supine or lying down as venous blood and CSF shifts towards the head and inside the cranium leading to increased intracranial mass. Such changes underlie the relationship between pressure and density, where:

$$\text{ICP} = \frac{\text{sum density of intracranial contents (mass inside cranium/volume cranium)}}{\text{volume cranium}} \times \text{acceleration/area cranium}$$

As volume and area of the cranium, as well as acceleration are constants, the changing mass within the cranium dictates changes in ICP as venous and CSF volume enters and exits the semi closed space.

The pressure-volume relationship between ICP, volume of CSF, blood, and brain tissue, is known as the Monro-Kellie doctrine [175]. The cranium's constituents (blood, CSF, and brain tissue) maintain a homeostasis, such that any increase in volume of one of the cranial constituents must be compensated by a decrease in volume of another. However, there is a small buffering capacity for increases in intracranial volume (more appropriately referred to as intracranial mass) primarily by the volume of CSF and to a lesser extent, the volume of venous blood. These buffers respond to increases in volume of the remaining intracranial constituents. For example, in a head trauma patient with an expanding epidural hematoma the increased mass will be compensated by the displacement of CSF and venous blood out of the cranium [175]. For example, in a head trauma patient with an expanding epidural hematoma the increased mass will be compensated by the displacement of CSF and venous blood out of the cranium (Figure 44).

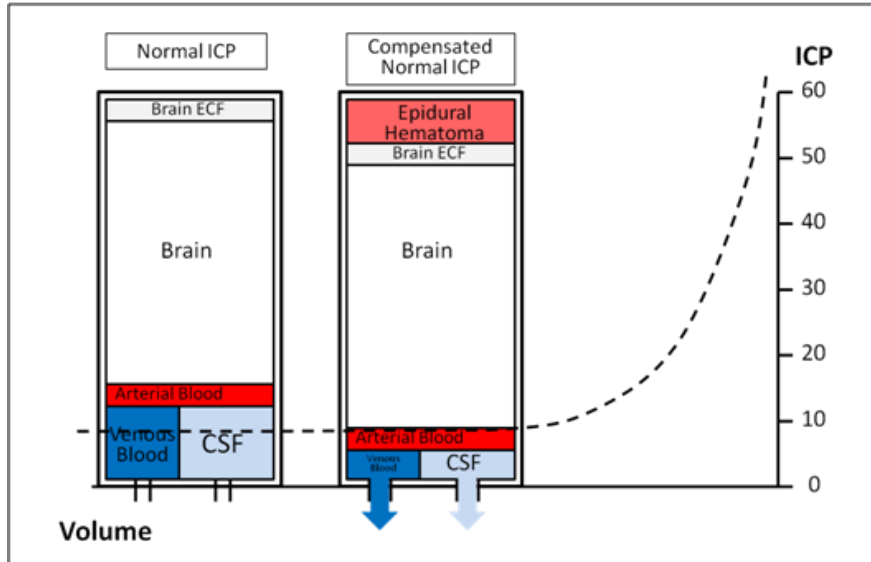


Figure 44: Diagram showing the small buffering capacity that allows for increases in intracranial volume.

Fundamental changes in both vascular and interstitial fluid distribution occur upon exposure to microgravity. In a 1-G environment, acceleration due to gravity creates a downward force that acts on the body's fluids. As a consequence, a hydrostatic pressure gradient exists across the body's axis resulting in a higher pressure in the most dependant regions and lower pressure at the head. This is most evident in the standing position. For example, according to Hargens and Richardson [176] the arterial pressure in a standing male of average height is 200 mm Hg at the foot, while only 70 mm Hg at the head (Figure 45). The venous blood is also subject to the hydrostatic gradient. In fact, gravity assists cerebral venous drainage from the cranium, preventing cerebral venous congestion and elevations in ICP. Upon exposure to microgravity and loss of the hydrostatic gradient, there is a cephalad-fluid shift from the lower body on the order of 1-2 liters. Consequently, arterial pressure across the body's axis equalizes so that pressure at the foot and the head is 100 mm Hg. Such fluid shifts occur on a daily basis on Earth upon assuming a supine position during sleep. Vascular and interstitial fluid moves from the dependant regions to the abdomen, thorax, and head. Interestingly, Rowell [177] reported that arterial pressure was approximately 98 mm Hg at the foot, and 99 mm Hg at the head when supine.

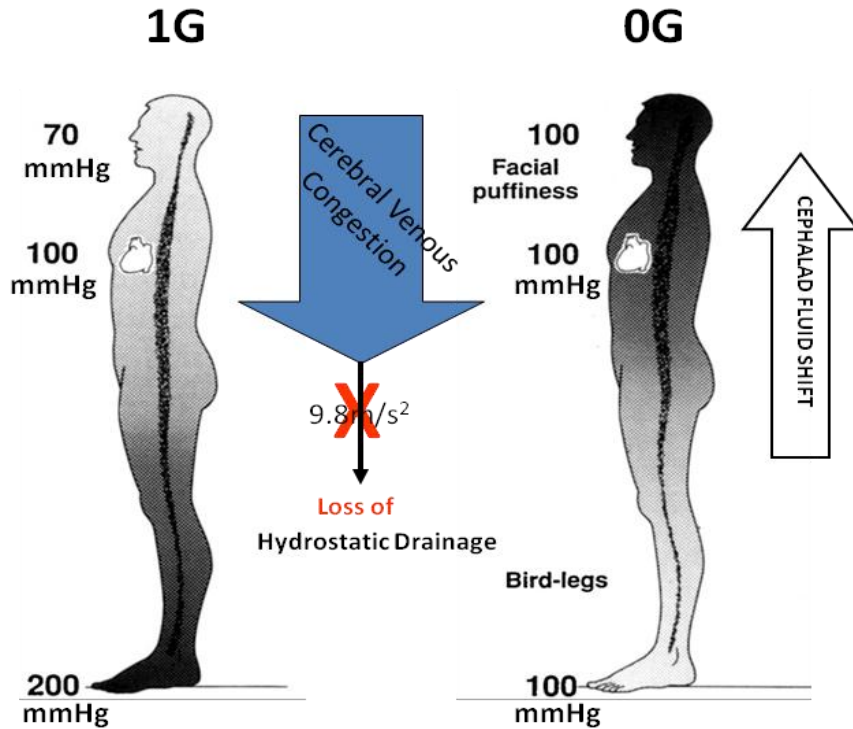


Figure 45. Loss of hydrostatic pressure gradient drainage and cerebral venous congestion. Adapted from Hargens AR, et al. [176], with permission of Elsevier BV, obtained via Copyright Clearance Center, Inc.

An indication of the changes that occur as a result of fluid shifts on central and cerebral hemodynamics in spaceflight may be illustrated by the terrestrial work of Chapman et al. [178] and Hirvonen et al. [179]. Chapman [178] instrumented a group of normal subjects with intraventricular catheters and measured ICP while tilting the subject's long axis at multiple tilt angles. Similarly, Hirvonen and Kauko [179] measured CVP in normal subjects at similar tilt angles. In the upright position (0 degree), ICP in a representative subject was found to be -2.3 mm Hg (-3.1 cm H₂O), while Hirvonen and Kauko found the CVP to be 0 mm Hg. In the supine position (90 degrees), ICP increased by 11.5 mm Hg (15.6 cm H₂O) from -2.3 mm Hg (-3.1 cm H₂O) to 9.2 mm Hg (12.5 cm H₂O), correspondingly, CVP in the same position increased from 0 to 5 mm Hg. When subjects were subjected to HDT (-30 degrees) ICP increased an additional 14.8 mm Hg (20.1 cm H₂O) from the supine position to 24.0 mm Hg (32.6 cm H₂O), while CVP in a similarly tilted subjects increased to 9 mm Hg. These invasive experiments document the effect that cephalad-fluid shift has on raising CVP and ICP. In the case of ICP, the acute effect of cerebral venous engorgement is an increase in blood volume within the rigid cranium. As the cranium is nonexpansile, pressure increases modestly, and within the normal limits of ICP (10 to 15mmHg or 13 to 20 cm H₂O). However, in these experiments, subjects were tilted for brief periods lasting no longer than 5 to 15 minutes. In the case of the ISS astronauts, the fluid shift exposure is constant for approximately 180 days.

Evidence suggests that changes in venous and interstitial fluid shifts may provide the largest contribution to potential increases in ICP during spaceflight. To gain a greater sense for the venous changes that occur, several terrestrial studies were reviewed. Gisolf et al. [180] noted that

venous pressure at the head in the standing position could be assumed to be -20 mm Hg. It is well known that the right atrium of the heart represents the hydrostatic indifferent point for venous pressures in the upright human. Thus, as in the arterial system, pressures below the right atrium increase due to hydrostatic pressure, but above the right atrium venous pressures become increasingly negative in the standing position. Upon entry into microgravity however, the loss of the hydrostatic gradient results in a redistribution of venous pressures across the body's axis causing an increase in venous pressures above the right atrium in comparison to standing in 1 G. As described earlier, Hirvonen and Kauko [179] showed an increase in CVP with fluid shift from standing to supine in terrestrial subjects, and Gisolf et al. [180] reported an increase in venous pressures from standing to supine of approximately 40 mm Hg from -20 mm Hg standing to 15 to 20 mm Hg supine. The shift in venous volume to the cranium is responsible for the acute change in ICP, as demonstrated by Chapman [178] and is illustrated by the equation for ICP:

$$\text{ICP} = \text{CSF}_{\text{out flow resistance}} \times \text{CSF}_{\text{formation}} + \text{Superior Saggital Sinus Pressure}$$

Although increases in CSF outflow resistance will increase ICP, the most immediate increase will be venous volume shift into the dural venous sinuses.

The data presented thus far is based upon ground studies examining positional fluid shifts. However, a series of rodent experiments by Gotoh [28, 181] using simulated microgravity is consistent with the proposed mechanisms for venous fluid shift and raised ICP in microgravity related VIIP. Gotoh et al. demonstrated that venous pressure at the jugular vein increased on average 1.3 mm Hg in seven rats during a 4.5 second drop test thereby demonstrating that by removing the force due to gravity, and the effect of hydrostatic cerebral venous drainage, the ensuing fluid shift causes venous pressure above the right atrium to increase. During the experiment, the rats were positioned in a 30-degree head up orientation. In an additional experiment, Gotoh et al. [182] measured ICP using a similar protocol, and found that ICP increased on average 2.5 mm Hg (3.4 cm H₂O) during the 4.5-second drop test. This represents a near doubling of the rise in venous pressure and may be accounted for by the rigid cranium and intracranial contents that limit dural expansion and contribute to elevated pressures, unlike the jugular vein that has more compliance due to the lack of a rigid container. Notable in this experiment, it is the rapidity of the changes with the onset of microgravity and its limited duration of 4.5 seconds that precludes additional contributions to raised pressure from exhaustion of volume compensation due to shift of CSF into the spinal space, interstitial fluid shift, and congested lymphatics, all factors that would raise ICP further.

Multiple effects are likely to occur as a result of acute cerebral venous congestion that may contribute to exacerbations in ICP elevation. CSF is produced at a constant rate and circulates throughout the ventricles of the CNS, the subarachnoid space, optic nerve sheath, and subarachnoid spinal space. CSF must be resorbed at a constant rate to prevent accumulation and increases in ICP. Invaginations into the dural venous sinuses from the subarachnoid space, called arachnoid granulations, allow CSF outflow by pressure-sensitive mechanisms related to hydrostatic gradients (directed from CSF to venous blood) and to active transport by arachnoidal cell pinocytotic (vesicular) mechanisms. The normal differential in the driving pressure is a ratio of 0.60 in favor of the CSF pressure. For example, in the supine position, CSF pressure may be

10 to 12 mm Hg (13.6 to 16.3 cm H₂O), while superior sagittal sinus pressure may be 5 to 7 mm Hg yielding a driving pressure of 3 to 5 mm Hg for CSF reabsorption. Thus, an increase in the venous pressure of just a few mm Hg would alter the diffusion gradient significantly and inhibit CSF reabsorption. As a result of venous congestion and the associated increase in venous pressure, CSF resorption could be decreased causing a back-up of CSF. Especially with downstream lymphatic congestion, interstitial fluid drainage along blood vessels may be reduced resulting in an increase in brain interstitial fluid volume. Alterations in CSF production in the choroid plexus may also contribute to potential changes in ICP, particularly during the postflight period.

According to the Starling-Landis equation, the fluid equilibrium between vessels and the interstitium is regulated by colloid osmotic pressures (in the plasma and the interstitial fluid), arterial blood pressure, interstitial fluid pressure, and capillary blood pressure [176]. There is a significant drop in the hydrostatic pressure from the capillaries to the venules, thus any increase in venous pressure due to venous congestion will increase transcapillary pressure and concomitant net permeation of fluid to the brain parenchyma (increased plasma from the vessels into the interstitium and decreased reabsorption into the capillary). The brain parenchyma swells, as occurs in high altitude brain edema [183], and in turn increases sinus venous pressure, both of which affect ICP. This phenomenon, according to the Starling-Landis concept, would take place under the assumption that the capillary bed of the blood-brain-barrier remains intact in microgravity. The integrity of the blood-brain barrier depends on the tightness of the endothelial cell-cell junctions in the walls of the intracranial capillary vessels (known as tight junctions). As Lakin et al. [125] explain, several components contribute to maintaining the tightness of these junctions on Earth. A major role is played by adhesion between the endothelial cells, and this component may or may not be affected by alterations in gravity. A study by Maseguin et al [77], examined (among other parameters) ultrastructural and functional measures of the tight junctions found between choroid plexus epithelial cells, in rats subjected to hindlimb suspension for 30 and 180 minutes. Study results demonstrated that tight junction structure and protein composition were unaltered (confirmed by freeze-fracture and conventional electron microscopy, and immunohistochemistry for typical tight junction proteins, respectively). Tight junction permeability was shown to be intact by injecting the rats with cytochrome C into the blood circulation, and then demonstrating that cytochrome C did not cross the blood-CSF barrier at the level of the choroid plexus. However, gravitational unloading of body tissues and fluids, one of the most pervasive changes caused by a microgravity environment, may have an ability to alter the integrity of the blood-brain barrier in other ways. In addition, as mentioned in a previous section of this evidence report, exposure to higher levels of radiation in space may also affect the biology of endothelial cells in a way that will reduce tightness.

Another route for CSF resorption is via the cranial and spinal lymphatics. CSF travels via the perineural sheath of the olfactory nerve crossing the cribiform plate and is absorbed by the lymphatics of the submucosa in the olfactory and respiratory epithelium. In a similar fashion, lymphatics associated with spinal nerves absorb some CSF from the spinal subarachnoid space. CSF absorption values vary among different reports of animal experiments, with 13% to 80% of CSF being absorbed via the lymphatic system [184]. In addition to the cephalad shift in vascular fluid, there is also a head-ward shift in interstitial fluids from the dependant regions of the body. The elevated venous pressures, particularly in the face may also inhibit resorption of interstitial

fluid as described previously thereby compounding facial edema a common complaint among astronauts in space.

Within the premise of the involvement of venous congestion in determining ICP changes, MRI venography evaluation may provide some information about stenosis and compressing structures. Some potential compressive zones have also been proposed as possibly relevant in contributing to the venous congestion in microgravity [185].

b) Intracranial Hypertension

IIH, also known as pseudotumor cerebri, is a condition characterized by increased ICP without clinical, laboratory, or radiologic evidence of an intracranial space-occupying lesion, meningeal inflammation or venous outflow obstruction. This increased ICP can lead to optic disc swelling (papilledema) caused by high CSF pressure in the distal optic nerve sheath, elevation of the pressure in the central retinal vein, and impaired perfusion of the neurons as their axons traverse the LC [186].

Several MRI findings [29] have been found to be a common occurrence among IIH patients and VIIP cases (Table 3). A majority of imaging assessment parameters listed by Maralani et al. [187] have been reported in at least some of the VIIP cases, while others like stenosis score, were not clinically indicated and remain to be evaluated.

Table 3: Comparison Table of MRI Findings in IIH Patients Compared to Those Identified in the VIIP Population

MRI Signs of Elevated ICP: IIH versus VIIP		
Imaging Assessment	Present in IIH (Specificity)	Seen in VIIP
Combined Stenosis Score	100%	Unknown
Flattening of Posterior Globes	100%	Yes
Tight Subarachnoid Space	100%	Unknown
Partially Empty Sella Turcica	95.3%	Yes
Optic Nerve Sheath Distension	88.4%	Yes
Optic Nerve Tortuosity	86%	Yes
Slit-like Ventricles	79.1%	Unknown

The debate about the etiology of IIH or pseudotumor cerebri focuses on the role of elevated intracranial venous pressure. Bilateral transverse sinus (TS) narrowing in patients with IIH can be found regularly on MR imaging and may cause venous outflow obstruction. Some patients benefit from stent treatment of these venous sinus obstructions; however, others do not. Restenosis of the TS after pressure reduction and repeated increase of ICP suggests that increased ICP may be the primary problem leading to compression of the venous sinus and not venous sinus stenosis leading to ICP. Consequently, venous sinus stenoses could be reduced or eliminated by CSF diversion procedures as shown in the case report [188] below (Figure 46).

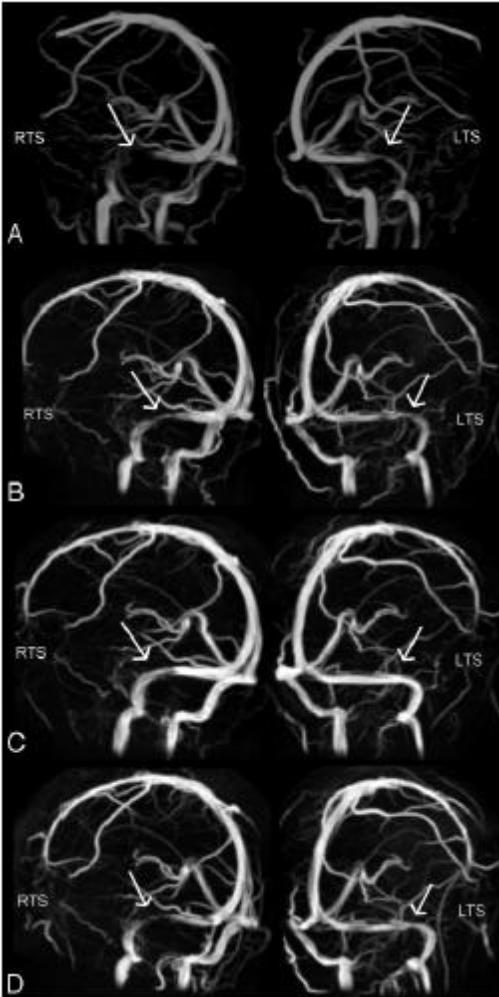


Figure 46: Reversibility of venous sinus obstruction with reduction of CSF pressure: case report. Adapted from Rohr A, et al. [188], with permission of the American Society of Neuroradiology, obtained via Copyright Clearance Center, Inc.

A – ICP of 50 cm H₂O, with bilateral stenosis of the transverse sinus

B – After lumbar puncture with removal of CSF and resultant reduction in ICP

C – After a second lumbar puncture

D – After placement of a ventriculoperitoneal shunt for continuous CSF drainage and further ICP reduction.

Stenoses in both the left and right transverse sinuses (LTS, RTS), as marked with arrows, are reduced in accordance with a lowered CSF pressure with complete resolution in C. Some residual narrowing is noted in the transverse sinuses in D, attributed to the relatively high opening pressure of the shunt valve. However, the vessels retained a greater degree of patency in comparison to the initial presentation

c) Increased CSF Production

The choroid plexus, comprised of a rich capillary bed, pia mater, and choroid epithelial cells, is the primary producer of CSF and does so at a rate of 0.3 to 0.6 mL/min, generating a total volume of 500 to 600 mL of CSF daily [189]. However, the total volume of CSF in humans is estimated to be 150 to 270 mL, which demonstrates the high turnover of this fluid, completely replacing the CSF approximately every 8 hours [190]. Flow of CSF is pulsatile and the fluid courses from its origin at the choroid plexus to exit at the foramina of the fourth ventricle out to the basal cisterns, then flows into the spinal and cortical subarachnoid spaces. Recently a paradigm shift has occurred in the presumed path of CSF clearance. Previously, absorption by arachnoid granulations was considered the primary mechanism of CSF clearance, whereas newer data is more consistent with reabsorption after bulk flow convection across the cribriform plate and along the olfactory, optic, facial and vestibulocochlear cranial nerves [189, 191-196]. From the nerve sheaths, the CSF passes into the cervical lymphatic system and then drains into the venous blood. The arachnoid granulations are now thought to have a role in regulating CSF drainage in times of increased pressure [189, 197, 198]. The normal CSF pressure in humans is about 10 cm H₂O, which is slightly higher than the venous pressure in the dural sinuses [189]. This pressure gradient drives the flow of CSF out of the brain toward reabsorption into the

systemic vasculature. Although there is a good understanding of the mechanisms of CSF production terrestrially, whether CSF production and/or outflow resistance increases and/or intracranial compliance decreases in microgravity is not known.

Terrestrially, arterial hypertension has been documented to increase CSF production in a rodent model [199] and further research is needed to determine the contributions of arterial hypertension to the spaceflight VIIP syndrome. Alperin et al. (Figure 47) described the influence of increased CO₂ levels (described in further detail later in the evidence report) on arterial hypertension and potentially ICP [200].

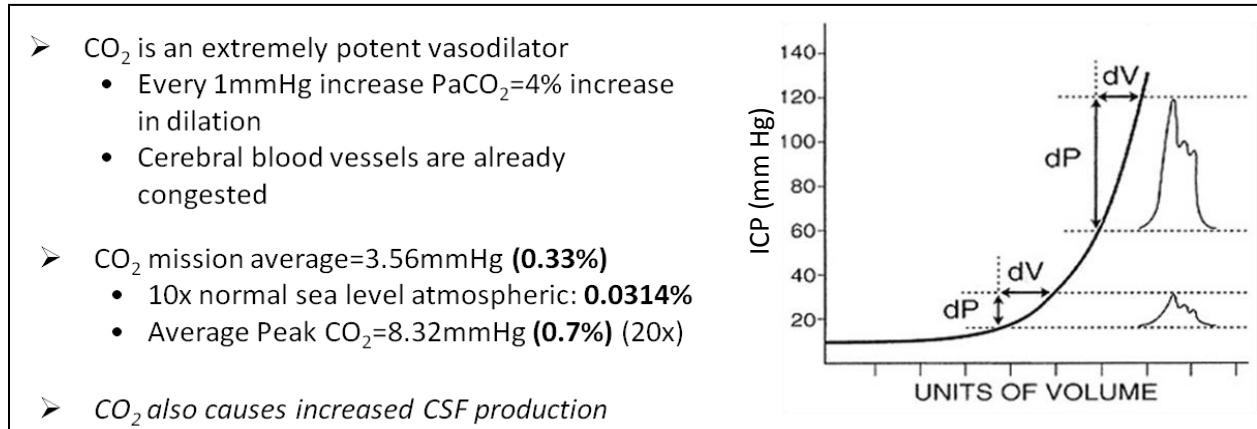


Figure 47: Normal ISS operating CO₂ levels are 10 times greater than the levels seen on Earth [201] that may cause vasodilation, increased CSF production, and increased ICP levels. Adapted from Alperin NJ, et al. [200], with permission of the Radiological Society of North America.

Animal studies, conducted by Tomassoni et al. (Figure 48), have shown that animals with arterial hypertension have an increased expression of Aquaporin 1 (AQP1) in the choroid plexus [202]. This increased AQP1 protein expression may lead to increase CSF production. Research conducted by Gabrion et al. used a rat model to evaluate choroidal cell responses to the spaceflight environment as compared to hind-limb unloading to simulate spaceflight-induced fluid shifts and ground controls [203]. The study data showed AQP1 membrane proteins were reduced 64% after 14 days of spaceflight and 44% and 68% in the hind-limb unloaded groups (14 and 28 days respectively). This decrease in AQP1 suggests an adaptation during spaceflight and hind-limb unloading that leads to a reduction in CSF secretory activity. Subsequently, upon readaptation, 2 days for spaceflight animals and 6 hours for hind-limb unloaded animals, AQP1 expression was increased over controls (48% in spaceflight and 57% in 14-day hind-limb suspended animals), suggesting increased CSF production.

Very limited astronaut data is available for evaluation, but the postflight MRI review of one long-duration astronaut measured the CSF production and flow through the aqueduct at 30 and 180 days postflight (Kramer, unpublished data). Interestingly, the CSF production and peak velocity approximately doubled during the postflight period (at 30 days CSF production rate = 305 μ L/min and peak velocity = 3.65 cm/s; 180 days CSF production rate = 682 μ L/min and peak velocity = 7.80 cm/s). Lumbar puncture was performed on this astronaut 57 days postflight with an opening pressure of 38.7 cm H₂O (28.5 mm Hg). This leads to the hypothesis that there may be a new set-point for ICP during

spaceflight that leads to increased CSF production via up-regulated AQP1 protein expression upon return to Earth. It should be noted that CSF production and flow were evaluated during the postflight period only on one astronaut and the animal experiments previously described were completed by 2 days post-readaptation, so additional data is required to further develop this hypothesis.

An overproduction of CSF may contribute to the VIIP syndrome seen in astronauts. This could be caused secondary to the increase in blood flow to the choroid plexus caused by the fluid shift associated with spaceflight, or the vascular dilation associated with the higher CO₂ levels that are tolerated on orbit. However, hypercapnia experiments producing an tripling of arterial pCO₂ and arterial dilation in the CNS, led to a reduction rather than elevation in CSF production [204].

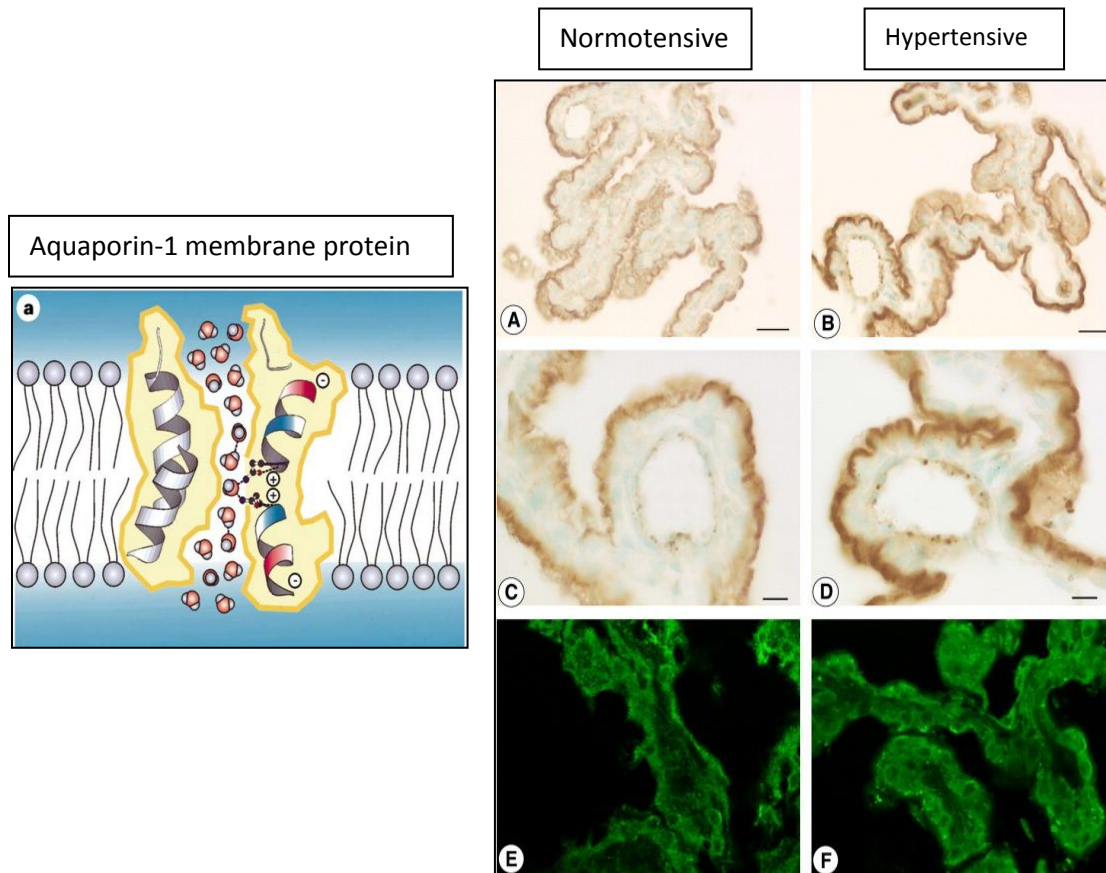


Figure 48: On the left – Aquaporin-1 membrane protein. Reproduced from Murata K, et al. [11], with permission of Nature Publishing Group, obtained via Copyright Clearance Center, Inc. On the right - Increased AQP1 expression in the choroid plexus of animals with arterial hypertension. A – F: Stronger AQP1 staining in the choroid plexus apical membrane of spontaneously hypertensive rats versus normotensive controls. Adapted from Tomassoni D, et al. [202] with permission of Elsevier BV, obtained via Copyright Clearance Center, Inc.

d) Decreased CSF Reabsorption

Edsbagge et al. [205] measured the magnitude of CSF reabsorption in healthy individuals as a function of activity, CSF production, ICP, and spinal CSF movement using lumbar puncture and

radionuclide cisternography. They found that as much as 76% of CSF reabsorption may take place via the spinal arachnoid villi/lymphatics when upright and decreased to 38% in the prone position. This implies that the hydrostatic gradients responsible for increased CSF spinal reabsorption may be significantly diminished in the spaceflight environment. Combining these phenomena with impaired cranial CSF absorption may lead to increased ICP in space in some astronauts. CSF is ultimately reabsorbed into venous blood and therefore spaceflight-induced alterations in lymphatic and venous drainage of the cranium and spine may influence CSF outflow resistance. Measuring preflight CSF outflow resistance with postural changes may identify a cohort of astronauts who have a poor CSF reabsorption reserve. Microgravity induced cranial lymphatic insufficiency may precipitate the changes we are seeing in symptomatic astronauts.

The following list contains CNS components that may be involved in the development of the VIIP syndrome. As additional data is collected these items will be reviewed for their potential contribution.

- **Inflammatory cytokines, signaling molecules**
- **Arachnoid villi –defects in absorption (such as subarachnoid hemorrhage - scarring)**
- **Elevated ICP and inflammatory damage to the arachnoid membrane**
- Venous and lymphatics – elongation and stretching of neural and vascular structures
- Impaired cranial lymphatic drainage with cephalad-fluid shift
- Interparenchymal interstitial fluid accumulation
- Risk of onset of normal pressure hydrocephalus, or spontaneous CSF leak: does prolonged elevated pressure within the CSF space precipitate a spontaneous rupture and CSF leak

e) Decreased Intracranial Compliance

Decreased intracranial compliance is another risk factor that is a potential contributor to development of the VIIP syndrome. Alperin et al. [200], measured volume and pressure changes in humans and baboons by using phase-contrast MRI studies of blood and CSF flow. They calculated intracranial volume changes from the net transcranial CSF and blood volumetric flow rates. The change in ICP was derived from the change in the CSF pressure gradient calculated from CSF velocity. An elastance index was then derived from the ratio of pressure to volume change. This study is significant in that CSF pressure gradient waveforms were derived from the CSF velocity phase-contrast images by using the Navier-Stokes relationship between pressure gradient and temporal and spatial derivatives of the fluid velocity for incompressible fluid in a rigid tube. The velocity information from cine phase contrast MRI allows for the noninvasive estimation of pressure gradients and fluid flow through various areas of interest such as the fourth ventricle or foramen magnum.

f) Using Ultrasound to Estimate ICP

Recent studies have implied a causal relationship between estimated ICP and ONSD measured by sonographic imaging [206] (Figure 49). Ultrasound imaging of the eye in the emergency room is more commonly used to rule out any visual defect secondary to retinal detachment,

vitreous detachment, or bleeding. Numerous techniques have been devised to estimate relative and absolute changes in ICP. Helmke et al. [207, 208] showed that a segment of the ONSD approximately 3 mm behind the papilla showed maximal diameter fluctuations induced by gelatinous injections in postmortem preparations. This ONSD landmark has been used in several clinical trials correlating elevated CSF pressure with ONSD derived ICP [209-212]. Hansen et al. [64] used B-mode ultrasound imaging of ONSD during intrathecal infusion of Ringer's lactate. They found a linear relationship between ONSD and CSF pressure ($R^2 = 0.752$). The ONSD dilation depends on the communication of the perineural CSF compartment around the optic nerve and the craniospinal subarachnoid space.

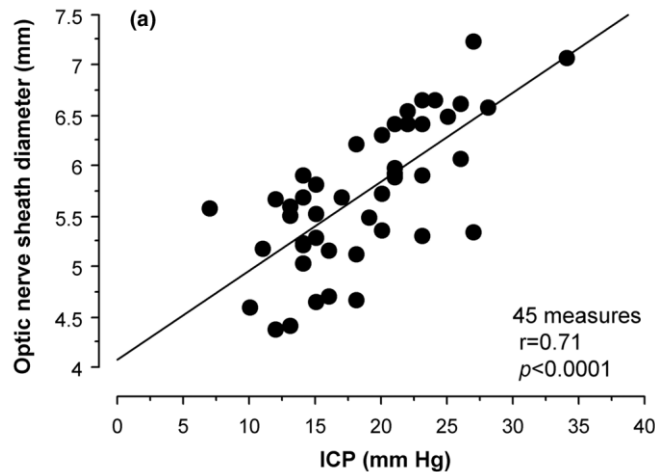


Figure 49: Terrestrial correlation of ONSD measurement and optic nerve diameter with ICP. ICP was measured by lumbar puncture. Reproduced from Geeraerts T, and others [206] which is an open access article, distributed under the terms of the Creative Commons Attribution License (<http://creativecommons.org/licenses/by/2.0>), which permits unrestricted use, distribution, and reproduction in any medium, provided the original work is properly cited. © 2008 Geeraerts and others.; licensee BioMed Central Ltd.

g) Central Nervous System Conclusions

In summary, the microgravity induced fluid shift could lead to an increase in ICP by several proposed mechanisms. The spaceflight-induced jugular vein distension could cause potential cerebral venous congestion and decreased CSF outflow leading to increased ICP. Other mechanisms include increased CSF production and decreased CSF absorption. The theory that ICP is increased as a result of spaceflight is supported by some of the symptoms, optic-disc edema, posterior globe flattening, choroidal folds, and hyperopic shifts, although other notable symptoms have not been shown in the VIIP syndrome. The putative ICP increase may be also related to other functional, sensory and cognitive changes seen in spaceflight. These effects could be more pronounced in astronauts with genetic, anatomical, or lifestyle factors which increase the likelihood of manifesting the symptoms. Increased ICP may only be one of several factors causing the constellation of symptoms seen in the VIIP syndrome.

V. CONTRIBUTING FACTORS

Several factors contribute to this unique environment including microgravity, potential alterations in localized CO₂ levels and a high sodium level in a closed food system. The factors are likely to be important contributors to the visual changes seen during flight.

A. Potential In-flight Factors

1. Alterations in Carbon Dioxide (CO₂) Metabolism

An additional risk factor for the development of the VIIP syndrome and the elevated ICP measures may be localized elevations in CO₂ levels encountered by astronauts on the ISS. The ISS is a closed system and a rise in CO₂ levels as a product of respiration would be expected. CO₂ is normally removed by external venting or chemical ‘scrubbing’. On Earth, the ambient CO₂ concentration is about 0.03% by volume (0.23 mm Hg) [213]. Nominal CO₂ levels on the ISS are between 2.3 to 5.3 mm Hg. The CO₂ levels that the VIIP affected astronauts were exposed to during their ISS missions did not exceed 5 mm Hg. Although this is more than 20 times higher than the 0.23 mm Hg on the Earth’s surface, this CO₂ level terrestrially is generally not thought to cause long-term detrimental physiologic effects [214, 215]. Perhaps long-term exposure to these levels in conjunction with the effects of microgravity fluid shifts may have an impact on ICP.

Carbon dioxide is a natural product of metabolism. Each person exhales about 200 mL of CO₂ per minute at rest and may produce over 4.0 L/min at maximal exercise [216]. Left unchecked, CO₂ can accumulate quickly inside a closed environment. Other sources of CO₂ include combustion, decay of organic matter, and fire suppression systems.

Several important physiologic processes in the human body are modulated by CO₂. When blood CO₂ levels rise, ventilation and heart rate increase to enhance the body’s elimination of CO₂. Hypercapnia also stimulates vasodilation of cerebral blood vessels, increased cerebral blood flow, and elevated ICP, presumably leading to headache, visual disturbance, impaired mental function, and other central nervous system (CNS) symptoms. Carbon dioxide is known to be a potent vasodilator and an increase in cerebral perfusion pressure will increase the CSF fluid production by about 4% [217].

Physiologic tolerance time for various CO₂ concentrations and acute health effects of exposure to high concentrations of CO₂ are summarized in Table 4.

Table 4: Physiologic Tolerance Time for Various CO₂ Concentrations and Acute Health Effects of High Concentrations of CO₂

Physiologic Tolerance			Acute Health Effects	
ppCO ₂ mm Hg	%	Maximum Exposure Limit (Minutes)	Duration of Exposure	Effects
3.8	0.5%	Indefinite		
7.5	1.0%	Indefinite		
11	1.5%	480		
15	2.0%	60	Several hours	Headache, dyspnea upon mild exertion
23	3.0%	20	1 hour	Headache, sweating, dyspnea at rest
30	4.0%	10	(4% to 5%)	Headache, dizziness, increased blood pressure, uncomfortable dyspnea
38	5.0%	7	Within few minutes	
45	6.0%	5	1 to 2 minutes ≤16 minutes Several hours	Hearing, visual disturbances Headache, dyspnea, tremors
53	7.0%	<3	(7% to 10%)	Unconsciousness, near-unconsciousness
68	9.0%	N/A	Few minutes 1.5 minutes to 2 hours 9% for 5 minutes	Headache, increased heart rate, shortness of breath, dizziness, sweating, rapid breathing <i>Lowest published lethal concentration</i>
75	10%	N/A	(>10% to 15%)	Dizziness, drowsiness, severe muscle twitching, unconsciousness
113	15%	N/A	1 minute to several minutes	
128	17%	N/A	(17% to 30%) Within 1 minute	Loss of controlled and purposeful activity, unconsciousness, convulsions, coma, death

Adapted from EPA 2000 [218].

a) Local Fluctuations in CO₂ Levels

Because air convection is significantly reduced in microgravity, local pockets of CO₂ may form around sources of CO₂ such as the nose and mouth. A computational fluid dynamics analysis revealed that without adequate ventilation, ppCO₂ could rise above 9 mm Hg within 10 minutes around a sleeping astronaut’s mouth and chin [219].

Few investigations to date have measured true CO₂ exposures. The ISS and Shuttle sensors (Major Constituent Analyzer or MCA) have fixed locations that do not necessarily reflect local CO₂ levels around astronauts as they move inside the crew compartments. Even the portable CO₂ monitors (CDMs) may not measure truly local ppCO₂, unless the monitors are worn by the astronauts close to their breathing zone. Generally, the CDMs are placed on cabin walls and not directly next to the crew. In other words, CDM data may not be representative of what the crew truly experiences. What little data are available already show fluctuations in the CDM ppCO₂ readings that are not detected by the MCA, especially during exercise. Local effects have yet to

be characterized during known rapid changes in ppCO₂ that the MCA can measure, for example when a CO₂ scrubber is being changed out or when one vehicle docks with another that has a different level of CO₂ [213].

All in all, more data are needed to further the understanding of individual and environmental factors that contribute to CO₂-related symptoms in microgravity. It may be that certain individuals or genders are more susceptible to CO₂ retention and increased ICP, but until true exposure data are available to correlate symptoms and ppCO₂, no conclusion can be drawn at this time about CO₂ susceptibility in spaceflight.

b) Crew Reports of Symptoms

One of the first reports of possible CO₂ toxicity on the ISS came from the ISS-2A crew. Headache was reported on two occasions: one while crewmembers were working inside a confined space where there was reduced air flow and the other when all of the crewmembers were gathered in a single location. Both times, crewmembers described their symptoms as similar to those they experienced when they were intentionally exposed to excess CO₂ during ground training [213]. Similarly, the crew of STS-123 reported ill effects and feeling of confinement that were attributed to CO₂ overexposure when the entire crew tried to gather together for a meal [220].

Other informal reports of ‘CO₂-like symptoms’ on board the ISS were recorded on STS-112/ISS-9A, STS-113/ISS-11A, and Expedition 6 [221]. An analysis of the LSAH examined the symptoms of headache and blurred/altered vision. All instances of complaints voiced during private medical conferences (PMCs) and open communication were recorded. Peak levels of CO₂ were evaluated with associated symptoms over 24-hour (Figure 50) and 7-day (Figure 51) periods.

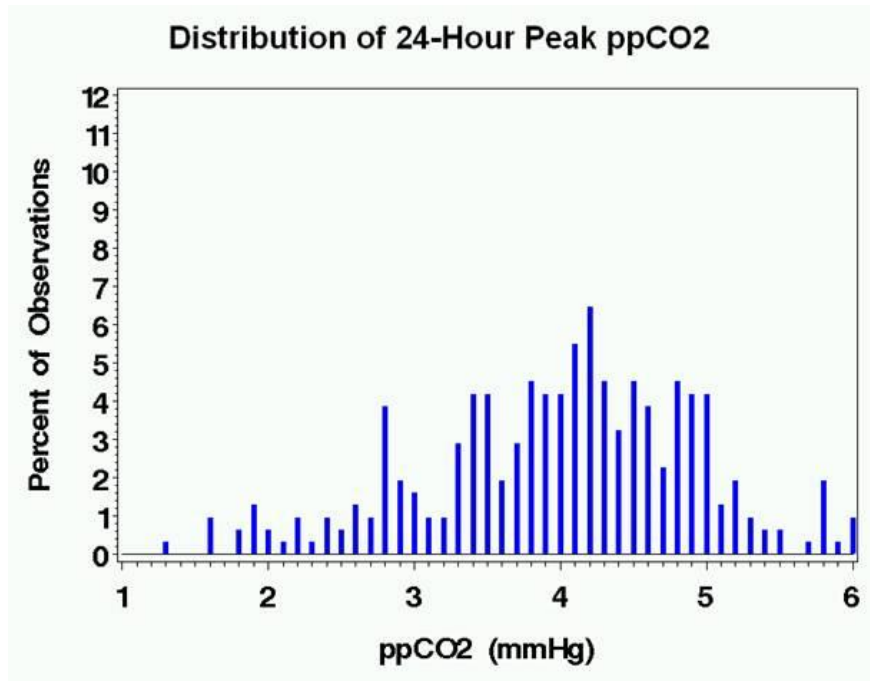


Figure 50: Reported observations and corresponding peak ppCO₂ levels during a 24-hour period.

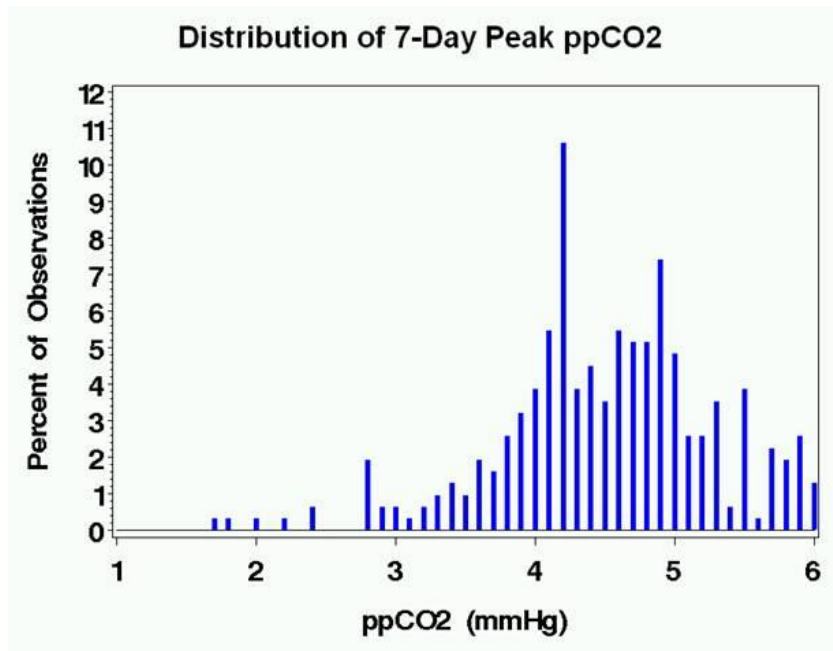


Figure 51: Reported observations and corresponding peak ppCO₂ levels during a 7-day period.

These symptoms were completely resolved with the lowering of the ppCO₂. It was also noticed that the symptoms were alleviated temporarily with nonsteroidal anti-inflammatory drugs (NSAIDs), but not completely resolved or exacerbated with the NSAID levels waning and CO₂ not returning to routine levels.

Data from several studies show that ambient CO₂ readings are normal. However, those ambient readings do not reflect the reduced airflow in the station, nor do they reflect the pockets of CO₂ that can accumulate around the crewmembers' noses and mouths.

c) CO₂ Susceptibility

Both individual and environmental factors may contribute to crewmembers' susceptibility to CO₂ effects in microgravity. Some individuals appear to be more prone to CO₂ retention and therefore develop symptoms at lower CO₂ levels. Differences in physiologic adaptation to microgravity may also be a factor in individual susceptibilities. Nonetheless, high enough levels of CO₂ will cause toxicity in all crewmembers. While ambient spacecraft CO₂ levels have generally remained below flight limits, local elevations not measured by fixed sensors may be responsible for the development of CO₂-related symptoms.

d) Environmental Factor: CO₂ Conclusion

The effects of ambient CO₂ and exposure limits have been well studied on Earth. However, informal crew reports on the ISS have suggested that astronauts are developing CO₂-related symptoms such as headache and lethargy at lower than expected CO₂ levels and that symptoms tend to resolve when CO₂ level is decreased. In-flight data to date support an association between elevated ppCO₂ and CO₂-related symptoms, but more research is needed to conclude causality. What appears to be increased CO₂ sensitivity in microgravity may be attributable to individual predisposition to CO₂ retention, adaptation to microgravity, and local fluctuations in CO₂ that are not measured by fixed sensors.

2. Alterations in Sodium

A link between increased ICP and altered sodium and water retention was suggested by a report in which 77% of IIIH patients had evidence of peripheral edema and 80% had orthostatic retention of sodium and water [222]. Impaired saline and water load excretions were noted in the upright posture in IIIH patients with orthostatic edema compared to lean and obese controls without IIIH. However, the precise mechanisms linking orthostatic changes and IIIH were not defined, and many IIIH patients do not have these sodium and water abnormalities. Astronauts are well known to have orthostatic intolerance upon return to gravity after long-duration spaceflight, and the dietary sodium on orbit is also known to be in excess of 5 grams per day in some cases. The majority of the NASA cases did have high dietary sodium during their increment. The ISS program is working to decrease in-flight dietary sodium intake to less than 3 grams per day. Sodium has been described in detail in other evidence reports [222].

3. Exercise

Exercise is an important countermeasure used to maintain muscle, bone, and cardiac health during spaceflight. However, the effects of exercise on ICP and IOP during spaceflight or simulated spaceflight have yet to be examined. Historically, Russian scientists have used a variety of exercise hardware and in-flight exercise protocols during long-duration spaceflight (up to and beyond 1 year) on board the Mir space station. On the ISS, a combination of resistive and aerobic exercise is used. For missions to the moon, establishment of a lunar base, and interplanetary travel to Mars or to an asteroid, the functional requirements for physical human performance during each specific phase of these missions have not been sufficiently defined to determine whether currently developed exercise countermeasures are adequate. Long-duration missions and exploration missions with several transitions between gravitational environments present the greatest challenges to risk mitigation and to development of countermeasures of proven efficacy.

a) Effects of Resistive Exercise on ICP and IOP

Despite its benefits on skeletal morphology and function, the effects of resistive exercise on the development of elevated ICP remain controversial. In an early investigation, Hamilton et al. reported that the increase in intrathoracic pressure during a brief (phase I) Valsalva maneuver was transmitted directly to the intracranial compartment, resulting in a concomitant rise in ICP [223]. Two recent investigations used transcranial Doppler ultrasound techniques to examine cerebral hemodynamics (cerebral blood flow [CBF]) during resistance exercise [224, 225]. Unfortunately, this noninvasive technique can only measure blood velocity through a cerebral artery, and does not allow a true understanding of cerebral hemodynamic changes associated with resistive exercise. To address this issue, Haykowsky et al. invasively examined ICP in fully cooperative, alert, and clinically stable patients who received a ventricular drain as part of their surgical procedure and postoperative care. They reported that resistive exercise without a Valsalva maneuver resulted in no change in peak systolic pressure or ICP [226].

The effects of resistive exercise on IOP are less controversial. An early study reported that resistive exercise training induced an increase in IOP [227]. A significant increase in IOP was also reported immediately after a static squat done until voluntary termination [228], and during bench press [229]. A dramatic increase in IOP (115%) was observed in experienced strength trained subjects during a maximal static muscle contraction combined with Valsalva maneuver

[230]. However, IOP was decreased after static muscular actions, such as handgrip exercise in subjects with normal IOP values [231]. Post-exercise, IOP then declined to 14% less than the pre-exercise values [228]. The only study that incorporated dynamic muscular contractions reported that IOP was reduced 40% after a series of isokinetic muscular actions in subjects with normal IOP [232]. More recently, Chromiak et al. demonstrated that IOP declines after one or more sets of chest press and leg press performed at moderate intensity [233]. Consequently, it appears as though resistance exercise performed without a Valsalva maneuver will not elevate ICP or IOP during exercise, and may even decrease ocular and cranial pressures post-exercise.

b) Effects of Aerobic Exercise on ICP and IOP

In contrast to numerous investigations examining the effects of resistive exercise on cranial pressures, there is a dearth of information regarding the consequences of aerobic exercise on ICP. To our knowledge the only study to examine ICP during aerobic exercise invasively measured ICP in patients with normal and increased ICP [234]. The researchers found that exercise tended to decrease ICP both in patients with intracranial hypertension and those with normal ICP. They suggested that because aerobic exercise is generally conducted without Valsalva maneuvers, it is unlikely that ICP will increase during exercise. However, other studies have demonstrated that in both animals and humans global brain blood flow increases 20% to 30% during the transition from rest to moderate exercise [235, 236]. Interestingly, more recent work has shown that an increase in exercise intensity up to ~60% VO_2 max results in an increase in CBF, after which CBF decreases towards baseline values (sometimes decreasing below baseline values) with increasing exercise intensity [237-240]. These findings suggest that high intensity exercise may be a key countermeasure to decrease CBF and thus potentially ICP.

It is well established that IOP decreases transiently with aerobic exercise in proportion to intensity and duration (Figure 52) [241]. For example, IOP was reduced 28% immediately after cycling at a low intensity for 1 hour in sedentary subjects [242]. In individuals with elevated IOP (18 mmHg or greater), IOP was reduced after a single bout of aerobic exercise [243]. Another investigation demonstrated that IOP was decreased by 30% after an incremental cycle test to exhaustion in subjects with IOP values of 22 mmHg or greater [244]. These exercise-induced decreases in IOP have important implications for spaceflight and simulated spaceflight, where significant increases in IOP have been documented [40].

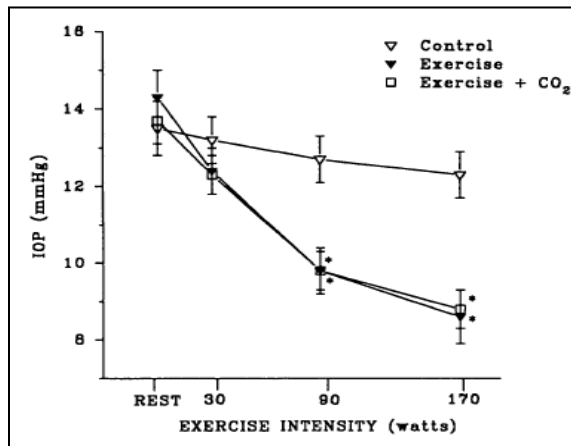


Figure 52: Impact of aerobic exercise on IOP. Reproduced from Harris A, and others [241], with permission of the Association for Research in Vision and Ophthalmology, obtained via Copyright Clearance Center, Inc.

B. Genetic Factors/Markers

1. One-Carbon Metabolism (Homocysteine)

About 20% of astronauts on long-duration ISS missions have developed measurable ophthalmic changes after flight[1]. The current in-flight nutrition study (Nutrition SMO 016E) has provided biochemical evidence that the folate-dependent one-carbon metabolic pathway may be altered in those individuals. Serum concentrations of homocysteine, cystathionine, 2-methylcitric acid, and methylmalonic acid were significantly ($P < 0.001$) higher (25% to 45%) in astronauts with ophthalmic changes than in those without such changes [245, 246]. These differences existed before, during, and after flight. Serum folate tended to be lower ($P = 0.06$) in individuals with ophthalmic changes. Preflight serum concentrations of cystathionine and 2-methylcitric acid, and mean in-flight serum folate, were significantly ($P < .05$) correlated with changes in refraction (postflight relative to preflight). At first, investigators thought the ophthalmic changes were caused by fluid shifts and increased ICP brought on by microgravity, but data from the Nutrition SMO 016E provided evidence for an alternative hypothesis: that individuals with this altered metabolic pathway may be predisposed to anatomic and/or physiologic changes that render them susceptible to ophthalmologic damage during spaceflight. These data have been submitted for peer review and publication, and a follow-on proposal has been submitted to HRP to follow up and clarify this finding.

2. Biomarkers

There are several potential biomarkers that may be used for early detection of the VIIP syndrome or to identify astronauts with increased risk for developing the syndrome. The Panel members of the 2010 Visual Impairment Summit suggested several biomarkers as potential candidates including S-100, platelet count, albumin, CRP/inflammation markers, insulin-like growth factor, somatostatin, tet-transactivator (TTA), myelin basic protein, immunoglobulin G index, oligoclonal bands, atrial natriuretic peptide, vasopressin, and aquaporin. In addition, gene expression profiling, epigenetic modifications of gene expression, proteomics, metabolomics, CO₂ retaining variants, single nucleotide polymorphisms, and copy number variants should be expanded in order to better characterize the individual susceptibility to develop the VIIP syndrome. As the etiology of the symptoms is more clearly defined the appropriate biomarkers will be evaluated.

VI. CASE DEFINITION/CLINICAL PRACTICE GUIDELINES

In response to the identification of the symptoms, the Space Medicine Division developed clinical practice guidelines for the treatment of affected astronauts. According to the guidelines, all long-duration astronauts that have demonstrated postflight refractive changes should be considered a suspected case; cases could be further differentiated by definitive imaging studies establishing the postflight presence of optic-disc edema, increased ONSD, and altered OCT findings. The results of the imaging studies are divided into five classes that determine the follow-up testing/monitoring that is required. The definition of the classes and Frisén scale used for optic-disc edema diagnosis are listed below.

Class 0

- $< .50$ diopter cycloplegic refractive change
- No evidence of optic-disc edema, nerve sheath distention, choroidal folds, globe flattening, scotoma, or cotton-wool spots compared to baseline

Class 1 (repeat OCT and visual acuity in 6 weeks)

- Refractive changes $\geq .50$ diopter cycloplegic refractive change and/or cotton-wool spot
- No evidence of optic-disc edema, nerve sheath distention, choroidal folds, globe flattening, scotoma, compared to baseline
- CSF opening pressure (if measured) ≤ 25 cm H₂O

Class 2 (repeat OCT, cycloplegic refraction, fundus examination and threshold visual field every 4 to 6 weeks \times 6 months, repeat MRI in 6 months)

- $\geq .50$ diopter cycloplegic refractive changes or cotton-wool spot
- Choroidal folds and/or ONS distension and/or globe flattening and/or scotoma
- No evidence of optic-disc edema
- CSF opening pressure ≤ 25 cm H₂O (if measured)

Class 3 (repeat OCT, cycloplegic refraction, fundus examination and threshold visual field every 4 to 6 weeks \times 6 months, repeat MRI in 6 months)

- $\geq .50$ diopter cycloplegic refractive changes and/or cotton-wool spot
- Optic nerve sheath distension, and/or globe flattening and/or choroidal folds and/or scotoma
- Optic-disc edema of Grade 0-2
- CSF opening pressure ≤ 25 cm H₂O

Class 4 (institute treatment protocol as per Clinical Practice Guideline)

- $\geq .50$ diopter cycloplegic refractive changes and/or cotton-wool spot
- Optic nerve sheath distension, and/or globe flattening and/or choroidal folds and/or scotoma
- Optic-disc edema Grade 2 or above
- Presenting symptoms of new headache, pulsatile tinnitus and/or transient visual obscurations
- CSF opening pressure > 25 cm H₂O

Optic-disc edema will be graded based on the Frisén Scale [247] as below:

Stage 0 – Normal Optic Disc

Blurring of nasal, superior and inferior poles in inverse proportion to disc diameter. Radial nerve fiber layer (NFL) without NFL tortuosity. Rare obscuration of a major blood vessel, usually on the upper pole.

Stage 1 – Very Early Optic-disc edema

Obscuration of the nasal border of the disc. No elevation of the disc borders. Disruption of the normal radial NFL arrangement with grayish opacity accentuating nerve fiber layer bundles. Normal temporal disc margin. Subtle grayish halo with temporal gap (best seen with indirect ophthalmoscopy). Concentric or radial retrochoroidal folds.

Stage 2 – Early Optic-disc edema

Obscuration of all borders. Elevation of the nasal border. Complete peripapillary halo.

Stage 3 – Moderate Optic-disc edema

Obscuration of all borders. Increased diameter of ONH. Obscuration of one or more segments of major blood vessels leaving the disc. Peripapillary halo-irregular outer fringe with finger-like extensions.

Stage 4 – Marked Optic-disc edema

Elevation of the entire nerve head. Obscuration of all borders. Peripapillary halo. Total obscuration on the disc of a segment of a major blood vessel.

Stage 5 – Severe Optic-disc edema

Dome-shaped protrusions representing anterior expansion of the ONH. Peripapillary halo is narrow and smoothly demarcated. Total obscuration of a segment of a major blood vessel may or may not be present. Obliteration of the optic cup.

VII. GAPS

The risk of microgravity-induced VIIP has recently been identified. Currently, there is little pre-, in-, and postflight data to characterize this risk. Below is a list of related unanswered issues that will help to define the VIIP syndrome and characterize the risk for exploration class missions.

Current knowledge gaps:

- VIIP1: What is the etiology of visual acuity and ocular structural and functional changes seen in-flight and postflight?
- VIIP3: Identify in-flight diagnostic tools to measure changes in ocular structure and function and/or ICP related to the VIIP syndrome. (hardware/techwatch)
- VIIP12: What are the suitable ground-based analogs to study the VIIP spaceflight-associated phenomenon? (analog)
- VIIP13: What are the safe and effective countermeasures (CMs) to mitigate changes in ocular structure and function and intracranial hypertension for spaceflight? (countermeasures)

VIII. CONCLUSIONS

In summary, fifteen long-duration male astronauts ranging in age from 45 to 55 years have experienced confirmed in-flight and postflight visual and anatomical changes including optic-disc edema, globe flattening, choroidal folds, and hyperopic shifts. Four of these astronauts experienced above normal CSF pressure measured during lumbar puncture postflight. This requires careful interpretation though, as it should be noted that preflight measures were not collected. Although many astronauts experience only visual acuity changes, other astronauts experience more concerning changes such as optic-disc edema and choroidal folds, and the duration and severity of these changes are not consistent across those affected. While the underlying etiology of these changes is unknown at this time, the spaceflight community at NASA, as well as an external expert panel, suspects that the microgravity-induced cephalad-fluid shift and commensurate changes in physiology play a significant role. Astronauts exposed to microgravity experience a cephalad-fluid shift, and both symptomatic and asymptomatic (with respect to changes in visual acuity) astronauts have exhibited ONS enlargement on MRI. The etiology of these intraocular and orbital findings is unknown, but we hypothesize that they may result from obstructed vascular (venous) outflow, a rise in ICP or as a result of a constellation of localized events, occurring within the intraorbital optic nerve without a rise in CSF pressure [40, 248]. This fluid shift may lead to increases in stroke volume [90, 91], cardiac output [92], ICP [249], and likely elevates IOP [40]. It is likely that there is significant variation across subjects in the type and volume of the fluid shift experienced in spaceflight [89]. Contributing factors may include pockets of increased CO₂ and high sodium diet, but it seems unlikely that resistive or aerobic exercise is involved. In fact, they may be potential countermeasures to reduce IOP and ICP in-flight.

The current knowledge gaps have been identified and a research plan is being developed to address these questions in a prioritized manner. As studies are completed and the knowledge of the condition is increased, the evidence report and research plan will be updated and reviewed.

IX. REFERENCES

1. Mader TH, Gibson CR, Pass AF, Kramer LA, Lee AG, Fogarty J, Tarver WJ, Dervay JP, Hamilton DR, Sargsyan A, Phillips JL, Tran D, Lipsky W, Choi J, Stern C, Kuyumjian R, Polk JD. Optic disc edema, globe flattening, choroidal folds, and hyperopic shifts observed in Astronauts after long-duration space flight. *Ophthalmology*, 2011; 118(10): 2058-69.
2. Fogarty J, Otto C, Kerstman E, Oubre C, Wu J. The visual impairment intracranial pressure summit report. National Aeronautics and Space Administration. 2011(Technical Publication): TP-2011-216160.
3. National Aeronautics and Space Administration. Papilledema summit: summary report. 2010(Technical Publication): TM-2010-216114.
4. Alemayehu W. Pseudotumor cerebri (toxic effect of the "magic bullet"). *Ethiop Med J*, 1995; 33(4): 265-70.
5. Allen JB, Jeng PS, Levitt H. Evaluation of human middle ear function via an acoustic power assessment. *J Rehabil Res Dev*, 2005; 42(4 Suppl 2): 63-78.
6. Alperin N. MR-intracranial compliance and pressure: a method for noninvasive measurement of important neurophysiologic parameters. *Methods Enzymol*, 2004; 386: 323-49.
7. Alperin N, Hushek SG, Lee SH, Sivaramakrishnan A, Lichtor T. MRI study of cerebral blood flow and CSF flow dynamics in an upright posture: the effect of posture on the intracranial compliance and pressure. *Acta Neurochir Suppl*, 2005; 95: 177-81.
8. Alperin N, Kulkarni K, Loth F, Roitberg B, Foroohar M, Mafee MF, Lichtor T. Analysis of magnetic resonance imaging-based blood and cerebrospinal fluid flow measurements in patients with Chiari I malformation: a system approach. *Neurosurg Focus*, 2001; 11(1): E6.
9. Alperin N, Lee SH, Mazda M, Hushek SG, Roitberg B, Goddwin J, Lichtor T. Evidence for the importance of extracranial venous flow in patients with idiopathic intracranial hypertension (IIH). *Acta Neurochir Suppl*, 2005; 95: 129-32.
10. Alperin N, Lee SH, Sivaramakrishnan A, Hushek SG. Quantifying the effect of posture on intracranial physiology in humans by MRI flow studies. *J Magn Reson Imaging*, 2005; 22(5): 591-6.
11. Mayasnikov VI, Stepanova SI, Features of cerebral hemodynamics in cosmonauts before and after flight on the MIR Orbital Station, in *Orbital Station MIR Vol 2*; 2008; Institute of Biomedical Problems: State Scientific Center of Russian Federation. 300-305.
12. Liu JH, Kripke DF, Hoffman RE, Twa MD, Loving RT, Rex KM, Gupta N, Weinreb RN. Nocturnal elevation of intraocular pressure in young adults. *Invest Ophthalmol Vis Sci*, 1998; 39(13): 2707-12.
13. Liu JH, Bouligny RP, Kripke DF, Weinreb RN. Nocturnal elevation of intraocular pressure is detectable in the sitting position. *Invest Ophthalmol Vis Sci*, 2003; 44(10): 4439-42.
14. Mosaed S, Liu JH, Weinreb RN. Correlation between office and peak nocturnal intraocular pressures in healthy subjects and glaucoma patients. *Am J Ophthalmol*, 2005; 139(2): 320-4.
15. Liu JH, Zhang X, Kripke DF, Weinreb RN. Twenty-four-hour intraocular pressure pattern associated with early glaucomatous changes. *Invest Ophthalmol Vis Sci*, 2003; 44(4): 1586-90.

16. Craven ER, Raised episcleral venous pressure, in *Ophthalmology*, Y.a. Duker, Editor 2008; Mosby.
17. Mansouri K, Weinreb RN, Liu JH. Effects of aging on 24-hour intraocular pressure measurements in sitting and supine body positions. *Invest Ophthalmol Vis Sci*, 2012; 53(1): 112-6.
18. Phelps CD, Armaly MF. Measurement of episcleral venous pressure. *Am J Ophthalmol*, 1978; 85(1): 35-42.
19. Gordon MO, Beiser JA, Brandt JD, Heuer DK, Higginbotham EJ, Johnson CA, Keltner JL, Miller JP, Parrish RK, 2nd, Wilson MR, Kass MA. The ocular hypertension treatment study: baseline factors that predict the onset of primary open-angle glaucoma. *Arch Ophthalmol*, 2002; 120(6): 714-20; discussion 829-30.
20. Xu X, Li L, Cao R, Tao Y, Guo Q, Geng J, Li Y, Zhang Z. Intraocular pressure and ocular perfusion pressure in myopes during 21 min head-down rest. *Aviat Space Environ Med*, 2010; 81(4): 418-22.
21. Jinkins JR. "Papilledema": neuroradiologic evaluation of optic disk protrusion with dynamic orbital CT. *AJR Am J Roentgenol*, 1987; 149(4): 793-802.
22. Morgan WH, Chauhan BC, Yu DY, Cringle SJ, Alder VA, House PH. Optic disc movement with variations in intraocular and cerebrospinal fluid pressure. *Invest Ophthalmol Vis Sci*, 2002; 43(10): 3236-42.
23. Morgan WH, Yu DY, Alder VA, Cringle SJ, Cooper RL, House PH, Constable IJ. The correlation between cerebrospinal fluid pressure and retrolaminar tissue pressure. *Invest Ophthalmol Vis Sci*, 1998; 39(8): 1419-28.
24. Quigley HA, Addicks EM, Green WR. Optic nerve damage in human glaucoma. III. Quantitative correlation of nerve fiber loss and visual field defect in glaucoma, ischemic neuropathy, papilledema, and toxic neuropathy. *Arch Ophthalmol*, 1982; 100(1): 135-46.
25. Lashutka MK, Chandra A, Murray HN, Phillips GS, Hiestand BC. The relationship of intraocular pressure to intracranial pressure. *Ann Emerg Med*, 2004; 43(5): 585-91.
26. Sajjadi SA, Harirchian MH, Sheikhabahaei N, Mohebbi MR, Malekmadani MH, Saberi H. The relation between intracranial and intraocular pressures: study of 50 patients. *Ann Neurol*, 2006; 59(5): 867-70.
27. Spentzas T, Henricksen J, Patters AB, Chaum E. Correlation of intraocular pressure with intracranial pressure in children with severe head injuries. *Pediatr Crit Care Med*, 2010; 11(5): 593-8.
28. Gotoh TM, Fujiki N, Tanaka K, Matsuda T, Gao S, Morita H. Acute hemodynamic responses in the head during microgravity induced by free drop in anesthetized rats. *Am J Physiol Regul Integr Comp Physiol*, 2004; 286(6): R1063-8.
29. Kramer LA, Sargsyan AE, Hasan KM, Polk JD, Hamilton DR. Orbital and intracranial effects of microgravity: findings at 3-T MR imaging. *Radiology*, 2012; 263(3): 819-27.
30. Khanna RK, Pham CJ, Malik GM, Spickler EM, Mehta B, Rosenblum ML. Bilateral superior ophthalmic vein enlargement associated with diffuse cerebral swelling. Report of 11 cases. *J Neurosurg*, 1997; 86(5): 893-7.
31. Lirng JF, Fuh JL, Wu ZA, Lu SR, Wang SJ. Diameter of the superior ophthalmic vein in relation to intracranial pressure. *AJNR Am J Neuroradiol*, 2003; 24(4): 700-3.
32. Chen WT, Fuh JL, Lirng JF, Lu SR, Wu ZA, Wang SJ. Collapsed superior ophthalmic veins in patients with spontaneous intracranial hypotension. *Neurology*, 2003; 61(9): 1265-7.

33. Smith TJ, Lewis J. Effect of inverted body position intraocular pressure. *Am J Ophthalmol*, 1985; 99(5): 617-8.
34. Hayreh SS. Orbital vascular anatomy. *Eye (Lond)*, 2006; 20(10): 1130-44.
35. Czarnik T, Gawda R, Latka D, Kolodziej W, Sznajd-Weron K, Weron R. Noninvasive measurement of intracranial pressure: is it possible? *J Trauma*, 2007; 62(1): 207-11.
36. Czarnik T, Gawda R, Kolodziej W, Latka D, Sznajd-Weron K, Weron R. Associations between intracranial pressure, intraocular pressure and mean arterial pressure in patients with traumatic and non-traumatic brain injuries. *Injury*, 2009; 40(1): 33-9.
37. Muchnok T, Deitch K, Giraldo P. Can intraocular pressure measurements be used to screen for elevated intracranial pressure in emergency department patients? *J Emerg Med*, 2010.
38. Mader TH, Gibson CR, Caputo M, Hunter N, Taylor G, Charles J, Meehan RT. Intraocular pressure and retinal vascular changes during transient exposure to microgravity. *Am J Ophthalmol*, 1993; 115(3): 347-50.
39. Draeger J, Hanke K. Postural variations of intraocular pressure--preflight experiments for the D1-mission. *Ophthalmic Res*, 1986; 18(1): 55-60.
40. Draeger J, Schwartz R, Groenhoff S, Stern C. Self-tonometry under microgravity conditions. *Aviat Space Environ Med*, 1995; 66(6): 568-70.
41. Draeger J, Schwartz R, Groenhoff S, Stern C. [Self tonometry during the German 1993 Spacelab D2 mission]. *Ophthalmologie*, 1994; 91(5): 697-9.
42. Mader TH, Taylor GR, Hunter N, Caputo M, Meehan RT. Intraocular pressure, retinal vascular, and visual acuity changes during 48 hours of 10 degrees head-down tilt. *Aviat Space Environ Med*, 1990; 61(9): 810-3.
43. Taibbi G CR, Zanello S, Yarbough P, Vizzeri G, Evaluation of ocular outcomes in two 14-day bed rest studies, in *Association for Research in Vision and Ophthalmology (ARVO)2012*: Ft Lauderdale, FL.
44. Chiquet C, Custaud MA, Le Traon AP, Millet C, Gharib C, Denis P. Changes in intraocular pressure during prolonged (7-day) head-down tilt bedrest. *J Glaucoma*, 2003; 12(3): 204-8.
45. Wilson MR, Baker RS, Mohammadi P, Wheeler NC, Lee DA, Scott C. Reproducibility of postural changes in intraocular pressure with the Tono-Pen and Pulsair tonometers. *Am J Ophthalmol*, 1993; 116(4): 479-83.
46. Liu JH, Kripke DF, Twa MD, Gokhale PA, Jones EI, Park EH, Meehan JE, Weinreb RN. Twenty-four-hour pattern of intraocular pressure in young adults with moderate to severe myopia. *Invest Ophthalmol Vis Sci*, 2002; 43(7): 2351-5.
47. Friberg TR, Weinreb RN. Ocular manifestations of gravity inversion. *JAMA*, 1985; 253(12): 1755-7.
48. Weinreb RN, Cook J, Friberg TR. Effect of inverted body position on intraocular pressure. *Am J Ophthalmol*, 1984; 98(6): 784-7.
49. Shinojima A, Iwasaki K, Aoki K, Ogawa Y, Yanagida R, Yuzawa M. Subfoveal choroidal thickness and foveal retinal thickness during head-down tilt. *Aviat Space Environ Med*, 2012; 83(4): 388-93.
50. Kuzmin M. Reactions of eye retinal vessels and intraocular pressure during man's 120 day restriction to a horizontal position. *Kosmicheskaya Biologiya I Meditsina*, 1973; 7(2).

51. Delaey C, Van De Voorde J. Regulatory mechanisms in the retinal and choroidal circulation. *Ophthalmic Res*, 2000; 32(6): 249-56.
52. Jonas JB, Berenshtein E, Holbach L. Lamina cribrosa thickness and spatial relationships between intraocular space and cerebrospinal fluid space in highly myopic eyes. *Invest Ophthalmol Vis Sci*, 2004; 45(8): 2660-5.
53. Linder BJ, Trick GL, Wolf ML. Altering body position affects intraocular pressure and visual function. *Invest Ophthalmol Vis Sci*, 1988; 29(10): 1492-7.
54. Frey MA, Mader TH, Bagian JP, Charles JB, Meehan RT. Cerebral blood velocity and other cardiovascular responses to 2 days of head-down tilt. *J Appl Physiol*, 1993; 74(1): 319-25.
55. Drozdova NT, Grishin EP. [State of the visual analyzer during hypokinesia]. *Kosm Biol Med*, 1972; 6(4): 46-9.
56. Mekjavic PJ, Eiken O, Mekjavic IB. Visual function after prolonged bed rest. *J Gravit Physiol*, 2002; 9(1): P31-2.
57. Tso MO, Hayreh SS. Optic disc edema in raised intracranial pressure. IV. Axoplasmic transport in experimental papilledema. *Arch Ophthalmol*, 1977; 95(8): 1458-62.
58. Berdahl JP, Allingham RR. Intracranial pressure and glaucoma. *Curr Opin Ophthalmol*, 2010; 21(2): 106-11.
59. Burgoyne CF, Downs JC, Bellezza AJ, Suh JK, Hart RT. The optic nerve head as a biomechanical structure: a new paradigm for understanding the role of IOP-related stress and strain in the pathophysiology of glaucomatous optic nerve head damage. *Prog Retin Eye Res*, 2005; 24(1): 39-73.
60. Sigal IA, Flanagan JG, Ethier CR. Factors influencing optic nerve head biomechanics. *Invest Ophthalmol Vis Sci*, 2005; 46(11): 4189-99.
61. Schirmer CM, Hedges TR, 3rd. Mechanisms of visual loss in papilledema. *Neurosurg Focus*, 2007; 23(5): E5.
62. Killer HE, Laeng HR, Flammer J, Groscurth P. Architecture of arachnoid trabeculae, pillars, and septa in the subarachnoid space of the human optic nerve: anatomy and clinical considerations. *Br J Ophthalmol*, 2003; 87(6): 777-81.
63. Liu D, Kahn M. Measurement and relationship of subarachnoid pressure of the optic nerve to intracranial pressures in fresh cadavers. *Am J Ophthalmol*, 1993; 116(5): 548-56.
64. Hansen HC, Helmke K. Validation of the optic nerve sheath response to changing cerebrospinal fluid pressure: ultrasound findings during intrathecal infusion tests. *J Neurosurg*, 1997; 87(1): 34-40.
65. Hansen HC, Lagreze W, Krueger O, Helmke K. Dependence of the optic nerve sheath diameter on acutely applied subarachnoid pressure - an experimental ultrasound study. *Acta Ophthalmol*, 2011; 89(6): e528-32.
66. Ansari R, Manuel FK, Geiser M, Moret F, Messer RK, King JF, Suh KI, Measurement of choroidal blood flow in zero gravity, in *Ophthalmic technologies XII : 19-20 January 2002, San Jose, USA*, F. Manns, P.G. Söderberg, and A. Ho, Editors. 2002; SPIE: Bellingham, Wash. 4951:177-184.
67. Lavinsky J, Lavinsky D, Lavinsky F, Frutuoso A. Acquired choroidal folds: a sign of idiopathic intracranial hypertension. *Graefes Arch Clin Exp Ophthalmol*, 2007; 245(6): 883-8.

68. Anand-Apte B, Hollyfield JG, Developmental anatomy of the retinal and choroidal vasculature, in *Encyclopedia of the eye*, E. D. A. Dartt, Editor. 2010 Elsevier and ScienceDirect. pp. 9-15.
69. Downs JC, Roberts MD, and Burgoyne CF. Biomechanics of the Optic Nerve Head. 2010: 183-201.
70. Bellezza AJ, Hart RT, Burgoyne CF. The optic nerve head as a biomechanical structure: initial finite element modeling. *Invest Ophthalmol Vis Sci*, 2000; 41(10): 2991-3000.
71. Norman RE, Flanagan JG, Sigal IA, Rausch SM, Tertinegg I, Ethier CR. Finite element modeling of the human sclera: influence on optic nerve head biomechanics and connections with glaucoma. *Exp Eye Res*, 2011; 93(1): 4-12.
72. Sigal IA, Flanagan JG, Tertinegg I, Ethier CR. Finite element modeling of optic nerve head biomechanics. *Invest Ophthalmol Vis Sci*, 2004; 45(12): 4378-87.
73. Margulies SS, Thibault LE. A proposed tolerance criterion for diffuse axonal injury in man. *J Biomech*, 1992; 25(8): 917-23.
74. Albon J, Karwatowski WS, Avery N, Easty DL, Duance VC. Changes in the collagenous matrix of the aging human lamina cribrosa. *Br J Ophthalmol*, 1995; 79(4): 368-75.
75. Karwatowski WS, Jeffries TE, Duance VC, Albon J, Bailey AJ, Easty DL. Preparation of Bruch's membrane and analysis of the age-related changes in the structural collagens. *Br J Ophthalmol*, 1995; 79(10): 944-52.
76. Albon J, Karwatowski WS, Easty DL, Sims TJ, Duance VC. Age related changes in the non-collagenous components of the extracellular matrix of the human lamina cribrosa. *Br J Ophthalmol*, 2000; 84(3): 311-7.
77. Maseguin C, Mani-Ponset L, Herbute S, Tixier-Vidal A, Gabrion J. Persistence of tight junctions and changes in apical structures and protein expression in choroid plexus epithelium of rats after short-term head-down tilt. *J Neurocytol*, 2001; 30(5): 365-77.
78. Fechtner RD, Weinreb RN. Mechanisms of optic nerve damage in primary open angle glaucoma. *Surv Ophthalmol*, 1994; 39(1): 23-42.
79. Yablonski ME, Asamoto A. Hypothesis concerning the pathophysiology of optic nerve damage in open angle glaucoma. *J Glaucoma*, 1993; 2(2): 119-27.
80. Yan DB, Coloma FM, Metheetrairut A, Trope GE, Heathcote JG, Ethier CR. Deformation of the lamina cribrosa by elevated intraocular pressure. *Br J Ophthalmol*, 1994; 78(8): 643-8.
81. Ren R, Jonas JB, Tian G, Zhen Y, Ma K, Li S, Wang H, Li B, Zhang X, Wang N. Cerebrospinal fluid pressure in glaucoma: a prospective study. *Ophthalmology*, 2010; 117(2): 259-66.
82. Morgan WH, Yu DY, Cooper RL, Alder VA, Cringle SJ, Constable IJ. The influence of cerebrospinal fluid pressure on the lamina cribrosa tissue pressure gradient. *Invest Ophthalmol Vis Sci*, 1995; 36(6): 1163-72.
83. Kupersmith MJ, Sibony P, Mandel G, Durbin M, Kardon RH. Optical coherence tomography of the swollen optic nerve head: deformation of the peripapillary retinal pigment epithelium layer in papilledema. *Invest Ophthalmol Vis Sci*, 2011; 52(9): 6558-64.
84. Arbeille P, Shoemaker K, Kerbeci P, Schneider S, Hargens A, Hughson R. Aortic, cerebral and lower limb arterial and venous response to orthostatic stress after a 60-day bedrest. *Eur J Appl Physiol*, 2011.

85. Herauld S, Fomina G, Alferova I, Kotovskaya A, Poliakov V, Arbeille P. Cardiac, arterial and venous adaptation to weightlessness during 6-month MIR spaceflights with and without thigh cuffs (bracelets). *Eur J Appl Physiol*, 2000; 81(5): 384-90.
86. Thornton WE, Hoffler GW, Rummel JA, Anthropometric changes and fluid shifts, in *Biomedical Results from Skylab1977*; NASA: Washington D.C.
87. Moore TP, Thornton WE. Space shuttle inflight and postflight fluid shifts measured by leg volume changes. *Aviat Space Environ Med*, 1987; 58(9 Pt 2): A91-6.
88. Arborelius M, Jr., Balldin UI, Lila B, Lundgren CE. Regional lung function in man during immersion with the head above water. *Aerosp Med*, 1972; 43(7): 701-7.
89. Montgomery LD. Body volume changes during simulated weightlessness: an overview. *Aviat Space Environ Med*, 1987; 58(9 Pt 2): A80-5.
90. Lathers CM, Charles JB, Elton KF, Holt TA, Mukai C, Bennett BS, Bungo MW. Acute hemodynamic responses to weightlessness in humans. *J Clin Pharmacol*, 1989; 29(7): 615-27.
91. Liu J, Verheyden B, Beckers F, Aubert AE. Haemodynamic adaptation during sudden gravity transitions. *Eur J Appl Physiol*, 2011.
92. Norsk P, Damgaard M, Petersen L, Gybel M, Pump B, Gabrielsen A, Christensen NJ. Vasorelaxation in space. *Hypertension*, 2006; 47(1): 69-73.
93. Leach CS, Alfrey CP, Suki WN, Leonard JI, Rambaut PC, Inners LD, Smith SM, Lane HW, Krauhs JM. Regulation of body fluid compartments during short-term spaceflight. *J Appl Physiol*, 1996; 81(1): 105-16.
94. Rowell LB, Human cardiovascular control.1993: Oxford University Press.
95. Kas'ian, II, Talavrinov VA, Luk'ianchikov VI, Kobzev EA. [Effect of antiorthostatic hypokinesia and space flight factors on changes in crural volume]. *Kosm Biol Aviakosm Med*, 1980; 14(4): 51-5.
96. Kirsch KA, Baartz FJ, Gunga HC, Rocker L. Fluid shifts into and out of superficial tissues under microgravity and terrestrial conditions. *Clin Investig*, 1993; 71(9): 687-9.
97. Thornton WE, Linder BJ, Moore TP, Pool SL. Gastrointestinal motility in space motion sickness. *Aviat Space Environ Med*, 1987; 58(9 Pt 2): A16-21.
98. Leach H, Lewis M, Luscombe DK, Nicholls PJ. Studies of plasma levels and the excretion of beclamide in normal human subjects [proceedings]. *Br J Clin Pharmacol*, 1975; 2(4): 377P-378P.
99. Hoffler GW JR, Apollo flight crew cardiovascular evaluations, in *Biomedical results of Apollo*, 1975; Scientific and Technical Information Office, National Aeronautics and Space Administration.
100. Hoffler GW BS, Nicgossian AE, In-flight lower limb volume measurements, in *The Apollo-Soyuz Test Project: Medical Report*, 1977; Scientific and Technical Information Office, National Aeronautics and Space Administration. 63-9.
101. Buckley JC, Jr., Lane LD, Levine BD, Watenpaugh DE, Wright SJ, Moore WE, Gaffney FA, Blomqvist CG. Orthostatic intolerance after spaceflight. *J Appl Physiol*, 1996; 81(1): 7-18.
102. Waters WW, Ziegler MG, Meck JV. Postspaceflight orthostatic hypotension occurs mostly in women and is predicted by low vascular resistance. *J Appl Physiol*, 2002; 92(2): 586-94.

103. Johnson P DT, LeBlanc A., Blood volume changes, in *Biomedical results from Skylab*, 1977; Scientific and Technical Information Office, National Aeronautics and Space Administration.
104. Alfrey CP, Udden MM, Leach-Huntoon C, Driscoll T, Pickett MH. Control of red blood cell mass in spaceflight. *J Appl Physiol*, 1996; 81(1): 98-104.
105. Udden MM, Driscoll TB, Pickett MH, Leach-Huntoon CS, Alfrey CP. Decreased production of red blood cells in human subjects exposed to microgravity. *J Lab Clin Med*, 1995; 125(4): 442-9.
106. Leach CS, Inners LD, Charles JB. Changes in total body water during spaceflight. *J Clin Pharmacol*, 1991; 31(10): 1001-6.
107. Drummer C, Heer M, Dressendorfer RA, Strasburger CJ, Gerzer R. Reduced natriuresis during weightlessness. *Clin Investig*, 1993; 71(9): 678-86.
108. Norsk P. Cardiovascular and fluid volume control in humans in space. *Curr Pharm Biotechnol*, 2005; 6(4): 325-30.
109. Norsk P. Renal adjustments to microgravity. *Pflugers Arch*, 2000; 441(2-3 Suppl): R62-5.
110. Norsk P, Foldager N, Bonde-Petersen F, Elmann-Larsen B, Johansen TS. Central venous pressure in humans during short periods of weightlessness. *J Appl Physiol*, 1987; 63(6): 2433-7.
111. Foldager N, Andersen TA, Jessen FB, Ellegaard P, Stadeager C, Videbaek R, Norsk P. Central venous pressure in humans during microgravity. *J Appl Physiol*, 1996; 81(1): 408-12.
112. Kirsch KA, Rocker L, Gauer OH, Krause R, Leach C, Wicke HJ, Landry R. Venous pressure in man during weightlessness. *Science*, 1984; 225(4658): 218-9.
113. Buckey JC, Gaffney FA, Lane LD, Levine BD, Watenpaugh DE, Blomqvist CG. Central venous pressure in space. *N Engl J Med*, 1993; 328(25): 1853-4.
114. Buckey JC, Jr., Gaffney FA, Lane LD, Levine BD, Watenpaugh DE, Wright SJ, Yancy CW, Jr., Meyer DM, Blomqvist CG. Central venous pressure in space. *J Appl Physiol*, 1996; 81(1): 19-25.
115. Arbeille P, Fomina G, Roumy J, Alferova I, Tobal N, Herault S. Adaptation of the left heart, cerebral and femoral arteries, and jugular and femoral veins during short- and long-term head-down tilt and spaceflights. *Eur J Appl Physiol*, 2001; 86(2): 157-68.
116. Videbaek R, Norsk P. Atrial distension in humans during microgravity induced by parabolic flights. *J Appl Physiol*, 1997; 83(6): 1862-6.
117. White RJ, Blomqvist CG. Central venous pressure and cardiac function during spaceflight. *J Appl Physiol*, 1998; 85(2): 738-46.
118. Prisk GK, Guy HJ, Elliott AR, Deutschman RA, 3rd, West JB. Pulmonary diffusing capacity, capillary blood volume, and cardiac output during sustained microgravity. *J Appl Physiol*, 1993; 75(1): 15-26.
119. Diridollou S, Pavy-Le Traon A, Maillet A, Bellossi F, Black D, Patat F, Lagarde JM, Berson M, Gall Y. Characterisation of gravity-induced facial skin edema using biophysical measurement techniques. *Skin Res Technol*, 2000; 6(3): 118-27.
120. Linnarsson D, Tedner B, Eiken O. Effects of gravity on the fluid balance and distribution in man. *Physiologist*, 1985; 28(6 Suppl): S28-9.

121. Hsieh ST, Ballard RE, Murthy G, Hargens AR, Convertino VA. Plasma colloid osmotic pressure increases in humans during simulated microgravity. *Aviat Space Environ Med*, 1998; 69(1): 23-6.
122. Parazynski SE, Hargens AR, Tucker B, Aratow M, Styf J, Crenshaw A. Transcapillary fluid shifts in tissues of the head and neck during and after simulated microgravity. *J Appl Physiol*, 1991; 71(6): 2469-75.
123. Hargens AR. Fluid shifts in vascular and extravascular spaces during and after simulated weightlessness. *Med Sci Sports Exerc*, 1983; 15(5): 421-7.
124. Hargens AR, Watenpaugh DE. Cardiovascular adaptation to spaceflight. *Med Sci Sports Exerc*, 1996; 28(8): 977-82.
125. Lakin WD, Stevens SA, Penar PL. Modeling intracranial pressures in microgravity: the influence of the blood-brain barrier. *Aviat Space Environ Med*, 2007; 78(10): 932-6.
126. Christ F, Gamble J, Baranov V, Kotov A, Chouker A, Thiel M, Gartside IB, Moser CM, Abicht J, Messmer K. Changes in microvascular fluid filtration capacity during 120 days of 6 degrees head-down tilt. *J Appl Physiol*, 2001; 91(6): 2517-22.
127. Diedrich A, Paranjape SY, Robertson D. Plasma and blood volume in space. *Am J Med Sci*, 2007; 334(1): 80-5.
128. Berry CA. The medical legacy of Gemini. *Life Sci Space Res*, 1968; 6: 1-19.
129. Baisch F, Beck L, Blomqvist G, Wolfram G, Drescher J, Rome JL, Drummer C. Cardiovascular response to lower body negative pressure stimulation before, during, and after space flight. *Eur J Clin Invest*, 2000; 30(12): 1055-65.
130. Blomqvist CG, Buckey JC, Gaffney FA, Lane LD, Levine BD, Watenpaugh DE. Mechanisms of post-flight orthostatic intolerance. *J Gravit Physiol*, 1994; 1(1): P122-4.
131. Fritsch-Yelle JM, Whitson PA, Bondar RL, Brown TE. Subnormal norepinephrine release relates to presyncope in astronauts after spaceflight. *J Appl Physiol*, 1996; 81(5): 2134-41.
132. Watenpaugh DE, Buckey JC, Lane LD, Gaffney FA, Levine BD, Moore WE, Wright SJ, Blomqvist CG. Effects of spaceflight on human calf hemodynamics. *J Appl Physiol*, 2001; 90(4): 1552-8.
133. Bleeker MW, De Groot PC, Pawelczyk JA, Hopman MT, Levine BD. Effects of 18 days of bed rest on leg and arm venous properties. *J Appl Physiol*, 2004; 96(3): 840-7.
134. Buckey JC, Lane LD, Plath G, Gaffney FA, Baisch F, Blomqvist CG. Effects of head down tilt for 10 days on the compliance of the lower limb. *Physiologist*, 1990; 33(1 Suppl): S167-8.
135. Buckey JC, Lane LD, Plath G, Gaffney FA, Baisch F, Blomqvist CG. Effects of head-down tilt for 10 days on the compliance of the leg. *Acta Physiol Scand Suppl*, 1992; 604: 53-9.
136. Convertino VA, Doerr DF, Stein SL. Changes in size and compliance of the calf after 30 days of simulated microgravity. *J Appl Physiol*, 1989; 66(3): 1509-12.
137. Tuday EC, Meck JV, Nyhan D, Shoukas AA, Berkowitz DE. Microgravity-induced changes in aortic stiffness and their role in orthostatic intolerance. *J Appl Physiol*, 2007; 102(3): 853-8.
138. Waters WW, Platts SH, Mitchell BM, Whitson PA, Meck JV. Plasma volume restoration with salt tablets and water after bed rest prevents orthostatic hypotension and changes in supine hemodynamic and endocrine variables. *Am J Physiol Heart Circ Physiol*, 2005; 288(2): H839-47.

139. Convertino VA. G-factor as a tool in basic research: mechanisms of orthostatic tolerance. *J Gravit Physiol*, 1999; 6(1): P73-6.
140. Fu Q, Witkowski S, Levine BD. Vasoconstrictor reserve and sympathetic neural control of orthostasis. *Circulation*, 2004; 110(18): 2931-7.
141. Bonnin P, Ben Driss A, Benessiano J, Mailliet A, Pavy le Traon A, Levy BI. Enhanced flow-dependent vasodilatation after bed rest, a possible mechanism for orthostatic intolerance in humans. *Eur J Appl Physiol*, 2001; 85(5): 420-6.
142. Lee SM, Moore AD, Jr., Fritsch-Yelle JM, Greenisen MC, Schneider SM. Inflight exercise affects stand test responses after space flight. *Med Sci Sports Exerc*, 1999; 31(12): 1755-62.
143. Preston DL, Shimizu Y, Pierce DA, Suyama A, Mabuchi K. Studies of mortality of atomic bomb survivors. Report 13: Solid cancer and noncancer disease mortality: 1950-1997. *Radiat Res*, 2003; 160(4): 381-407.
144. Ivanov VK, Gorski AI, Maksoutov MA, Tsyb AF, Souchkevitch GN. Mortality among the Chernobyl emergency workers: estimation of radiation risks (preliminary analysis). *Health Phys*, 2001; 81(5): 514-21.
145. Kolesnick R, Fuks Z. Radiation and ceramide-induced apoptosis. *Oncogene*, 2003; 22(37): 5897-906.
146. Menendez JC, Casanova D, Amado JA, Salas E, Garcia-Unzueta MT, Fernandez F, de la Lastra LP, Berrazueta JR. Effects of radiation on endothelial function. *Int J Radiat Oncol Biol Phys*, 1998; 41(4): 905-13.
147. Tishkin SM, Rekalov VV, Ivanova IV, MoreLand RS, Soloviev AI. Ionizing non-fatal whole-body irradiation inhibits Ca²⁺-dependent K⁺ channels in endothelial cells of rat coronary artery: possible contribution to depression of endothelium-dependent vascular relaxation. *Int J Radiat Biol*, 2007; 83(3): 161-9.
148. Bourlier V, Diserbo M, Joyeux M, Ribuot C, Multon E, Gourmelon P, Verdetti J. Early effects of acute gamma-radiation on vascular arterial tone. *Br J Pharmacol*, 1998; 123(6): 1168-72.
149. Simone NL, Soule BP, Ly D, Saleh AD, Savage JE, Degraff W, Cook J, Harris CC, Gius D, Mitchell JB. Ionizing radiation-induced oxidative stress alters miRNA expression. *PLoS One*, 2009; 4(7): e6377.
150. Soloviev AI, Tishkin SM, Parshikov AV, Ivanova IV, Goncharov EV, Gurney AM. Mechanisms of endothelial dysfunction after ionized radiation: selective impairment of the nitric oxide component of endothelium-dependent vasodilation. *Br J Pharmacol*, 2003; 138(5): 837-44.
151. Soucy KG, Lim HK, Benjo A, Santhanam L, Ryoo S, Shoukas AA, Vazquez ME, Berkowitz DE. Single exposure gamma-irradiation amplifies xanthine oxidase activity and induces endothelial dysfunction in rat aorta. *Radiat Environ Biophys*, 2007; 46(2): 179-86.
152. Suvorava T, Luksha L, Bulanova KY, Lobanok LM. Dose-rate dependent effects of ionizing radiation on vascular reactivity. *Radiat Prot Dosimetry*, 2006; 122(1-4): 543-5.
153. Soucy KG KJ, Bugaj L, Ryoo S, Vandegaer KM, Nyhan D, et al., Xanthine oxidase inhibition attenuates vascular endothelial dysfunction in irradiated rats., in *NASA Human Research Program Investigator Workshop 2009*: League City, Texas.
154. Hodes PJ, Perryman CR, Chamberlain RH. Cerebral angiography. *Am J Roentgenol Radium Ther*, 1947; 58(5): 543-83.

155. Wellens DL, Wouters LJ, De Reese RJ, Beirnaert P, Reneman RS. The cerebral blood distribution in dogs and cats. An anatomical and functional study. *Brain Res*, 1975; 86(3): 429-38.
156. Kawai Y, Murthy G, Watenpaugh DE, Breit GA, Deroshia CW, Hargens AR. Cerebral blood flow velocity in humans exposed to 24 h of head-down tilt. *J Appl Physiol*, 1993; 74(6): 3046-51.
157. Bassett DR, Jr., Howley ET, Lightfoot TJ. Hemodynamic responses to exercise in blacks and whites. *J Appl Physiol*, 1993; 75(4): 1920-2.
158. Iwasaki K, Levine BD, Zhang R, Zuckerman JH, Pawelczyk JA, Diedrich A, Ertl AC, Cox JF, Cooke WH, Giller CA, Ray CA, Lane LD, Buckey JC, Jr., Baisch FJ, Eckberg DL, Robertson D, Biaggioni I, Blomqvist CG. Human cerebral autoregulation before, during and after spaceflight. *J Physiol*, 2007; 579(Pt 3): 799-810.
159. Greaves DK, Arbeille P, Hughson RL. WISE 2005: altered cerebrovascular autoregulation after 60 day head-down bed rest. *J Gravit Physiol*, 2007; 14(1): P61-2.
160. Jeong SM, Shibata S, Levine BD, Zhang R. Exercise plus volume loading prevents orthostatic intolerance but not reduction in cerebral blood flow velocity after bed rest. *Am J Physiol Heart Circ Physiol*, 2012; 302(2): H489-97.
161. Geary GG, Krause DN, Purdy RE, Duckles SP. Simulated microgravity increases myogenic tone in rat cerebral arteries. *J Appl Physiol*, 1998; 85(5): 1615-21.
162. Wilkerson MK, Colleran PN, Delp MD. Acute and chronic head-down tail suspension diminishes cerebral perfusion in rats. *Am J Physiol Heart Circ Physiol*, 2002; 282(1): H328-34.
163. Wilkerson MK, Lesniewski LA, Golding EM, Bryan RM, Jr., Amin A, Wilson E, Delp MD. Simulated microgravity enhances cerebral artery vasoconstriction and vascular resistance through endothelial nitric oxide mechanism. *Am J Physiol Heart Circ Physiol*, 2005; 288(4): H1652-61.
164. Stevens SA, Lakin WD, Penar PL. Modeling steady-state intracranial pressures in supine, head-down tilt and microgravity conditions. *Aviat Space Environ Med*, 2005; 76(4): 329-38.
165. Califano JC, Uribe A, Chang JL, Becker CL, Napier JJ, Kishore V, Zhou D, Love G, Gernhardt K, Tolle JC. Concept and synthetic approach for a kilogram scale synthesis of octa-D-arginine amide nonahydrochloride salt. *Adv Exp Med Biol*, 2009; 611: 205-6.
166. Clapham R, O'Sullivan E, Weller RO, Carare RO. Cervical lymph nodes are found in direct relationship with the internal carotid artery: significance for the lymphatic drainage of the brain. *Clin Anat*, 2010; 23(1): 43-7.
167. Weller RO, Djuanda E, Yow HY, Carare RO. Lymphatic drainage of the brain and the pathophysiology of neurological disease. *Acta Neuropathol*, 2009; 117(1): 1-14.
168. Cserr HF, Harling-Berg CJ, Knopf PM. Drainage of brain extracellular fluid into blood and deep cervical lymph and its immunological significance. *Brain Pathol*, 1992; 2(4): 269-76.
169. Knopf PM, Cserr HF, Nolan SC, Wu TY, Harling-Berg CJ. Physiology and immunology of lymphatic drainage of interstitial and cerebrospinal fluid from the brain. *Neuropathol Appl Neurobiol*, 1995; 21(3): 175-80.
170. Kim M, Johnston MG, Gupta N, Moore S, Yucel YH. A model to measure lymphatic drainage from the eye. *Exp Eye Res*, 2011.

171. Gashev AA, Delp MD, Zawieja DC. Inhibition of active lymph pump by simulated microgravity in rats. *Am J Physiol Heart Circ Physiol*, 2006; 290(6): H2295-308.
172. Zhang LF. Vascular adaptation to microgravity: what have we learned? *J Appl Physiol*, 2001; 91(6): 2415-30.
173. Platts SH, Martin DS, Stenger MB, Perez SA, Ribeiro LC, Summers R, Meck JV. Cardiovascular adaptations to long-duration head-down bed rest. *Aviat Space Environ Med*, 2009; 80(5 Suppl): A29-36.
174. Friedman DI. Idiopathic intracranial hypertension. *Curr Pain Headache Rep*, 2007; 11(1): 62-8.
175. Mokri B. The Monro-Kellie hypothesis: applications in CSF volume depletion. *Neurology*, 2001; 56(12): 1746-8.
176. Hargens AR, Richardson S. Cardiovascular adaptations, fluid shifts, and countermeasures related to space flight. *Respir Physiol Neurobiol*, 2009; 169 Suppl 1: S30-3.
177. Rowell LB, Blackmon JR. Venomotor responses during central and local hypoxia. *Am J Physiol*, 1988; 255(4 Pt 2): H760-4.
178. Chapman PH, Cosman ER, Arnold MA. The relationship between ventricular fluid pressure and body position in normal subjects and subjects with shunts: a telemetric study. *Neurosurgery*, 1990; 26(2): 181-9.
179. Hirvonen EA, Nuutinen LS, Kauko M. Hemodynamic changes due to Trendelenburg positioning and pneumoperitoneum during laparoscopic hysterectomy. *Acta Anaesthesiol Scand*, 1995; 39(7): 949-55.
180. Gisolf J, van Lieshout JJ, van Heusden K, Pott F, Stok WJ, Karemaker JM. Human cerebral venous outflow pathway depends on posture and central venous pressure. *J Physiol*, 2004; 560(Pt 1): 317-27.
181. Gotoh TM, Fujiki N, Matsuda T, Gao S, Morita H. Roles of baroreflex and vestibulosympathetic reflex in controlling arterial blood pressure during gravitational stress in conscious rats. *Am J Physiol Regul Integr Comp Physiol*, 2004; 286(1): R25-30.
182. Gotoh TM, Tanaka K, Fujiki N, Matsuda T, Gao S, Morita H. Cerebral hemodynamics during microgravity. *Biol Sci Space*, 2003; 17(3): 204-5.
183. Wilson MH, Newman S, Imray CH. The cerebral effects of ascent to high altitudes. *Lancet Neurol*, 2009; 8(2): 175-91.
184. Koh L, Zakharov A, Johnston M. Integration of the subarachnoid space and lymphatics: is it time to embrace a new concept of cerebrospinal fluid absorption? *Cerebrospinal Fluid Res*, 2005; 2.
185. Wiener TC. Space obstructive syndrome: intracranial hypertension, intraocular pressure, and papilledema in space. *Aviat Space Environ Med*, 2012; 83(1): 64-6.
186. Brazis PW, Lee AG. Elevated intracranial pressure and pseudotumor cerebri. *Curr Opin Ophthalmol*, 1998; 9(6): 27-32.
187. Maralani PJ, Hassanlou M, Torres C, Chakraborty S, Kingstone M, Patel V, Zackon D, Bussiere M. Accuracy of brain imaging in the diagnosis of idiopathic intracranial hypertension. *Clin Radiol*, 2012.
188. Rohr A, Dorner L, Stingele R, Buhl R, Alfke K, Jansen O. Reversibility of venous sinus obstruction in idiopathic intracranial hypertension. *AJNR Am J Neuroradiol*, 2007; 28(4): 656-9.

189. Johanson CE, Duncan JA, 3rd, Klinge PM, Brinker T, Stopa EG, Silverberg GD. Multiplicity of cerebrospinal fluid functions: New challenges in health and disease. *Cerebrospinal Fluid Res*, 2008; 5: 10.
190. Redzic ZB, Segal MB. The structure of the choroid plexus and the physiology of the choroid plexus epithelium. *Adv Drug Deliv Rev*, 2004; 56(12): 1695-716.
191. Brown PD, Davies SL, Speake T, Millar ID. Molecular mechanisms of cerebrospinal fluid production. *Neuroscience*, 2004; 129(4): 957-70.
192. Jaggi GP, Harlev M, Ziegler U, Dotan S, Miller NR, Killer HE. Cerebrospinal fluid segregation optic neuropathy: an experimental model and a hypothesis. *Br J Ophthalmol*, 2010; 94(8): 1088-93.
193. Johnston M. The importance of lymphatics in cerebrospinal fluid transport. *Lymphat Res Biol*, 2003; 1(1): 41-4; discussion 45.
194. Killer HE, Jaggi GP, Flammer J, Miller NR, Huber AR, Mironov A. Cerebrospinal fluid dynamics between the intracranial and the subarachnoid space of the optic nerve. Is it always bidirectional? *Brain*, 2007; 130(Pt 2): 514-20.
195. Killer HE, Laeng HR, Groscurth P. Lymphatic capillaries in the meninges of the human optic nerve. *J Neuroophthalmol*, 1999; 19(4): 222-8.
196. Silver I, Kim C, Mollanji R, Johnston M. Cerebrospinal fluid outflow resistance in sheep: impact of blocking cerebrospinal fluid transport through the cribriform plate. *Neuropathol Appl Neurobiol*, 2002; 28(1): 67-74.
197. Andersson N, Malm J, Eklund A. Dependency of cerebrospinal fluid outflow resistance on intracranial pressure. *J Neurosurg*, 2008; 109(5): 918-22.
198. Eklund A, Smielewski P, Chambers I, Alperin N, Malm J, Czosnyka M, Marmarou A. Assessment of cerebrospinal fluid outflow resistance. *Med Biol Eng Comput*, 2007; 45(8): 719-35.
199. Ruchoux MM, Rosati C, Gelot A, Lhuintre Y, Garay R. Ultrastructural study of the choroid plexus of spontaneously hypertensive rats. *Am J Hypertens*, 1992; 5(11): 851-6.
200. Alperin NJ, Lee SH, Loth F, Raksin PB, Lichtor T. MR-Intracranial pressure (ICP): a method to measure intracranial elastance and pressure noninvasively by means of MR imaging: baboon and human study. *Radiology*, 2000; 217(3): 877-85.
201. James JT, Meyers VE, Sipes W, Scully RR, Matty CM, Crew Health and Performance Improvements with Reduced Carbon Dioxide Levels and the Resources Impact to Accomplish Those Reductions, in *41st International Conference on Environmental Systems*, 2011; AIAA: Portland, Oregon.
202. Tomassoni D, Bramanti V, Amenta F. Expression of aquaporins 1 and 4 in the brain of spontaneously hypertensive rats. *Brain Res*, 2010; 1325: 155-63.
203. Gabrion J, Herbute S, Oliver J, Maurel D, Davet J, Clavel B, Gharib C, Fareh J, Fagette S, Nguyen B. Choroidal responses in microgravity. (SLS-1, SLS-2 and hindlimb-suspension experiments). *Acta Astronaut*, 1995; 36(8-12): 439-48.
204. Martins AN, Doyle TF, Newby N. PCO₂ and rate of formation of cerebrospinal fluid in the monkey. *Am J Physiol*, 1976; 231(1): 127-31.
205. Edsbacke M, Tisell M, Jacobsson L, Wikkelso C. Spinal CSF absorption in healthy individuals. *Am J Physiol Regul Integr Comp Physiol*, 2004; 287(6): R1450-5.
206. Geeraerts T, Newcombe VF, Coles JP, Abate MG, Perkes IE, Hutchinson PJ, Outtrim JG, Chatfield DA, Menon DK. Use of T2-weighted magnetic resonance imaging of the optic nerve sheath to detect raised intracranial pressure. *Crit Care*, 2008; 12(5): R114.

207. Helmke K, Hansen HC. Fundamentals of transorbital sonographic evaluation of optic nerve sheath expansion under intracranial hypertension II. Patient study. *Pediatr Radiol*, 1996; 26(10): 706-10.
208. Helmke K, Hansen HC. Fundamentals of transorbital sonographic evaluation of optic nerve sheath expansion under intracranial hypertension. I. Experimental study. *Pediatr Radiol*, 1996; 26(10): 701-5.
209. Blaivas M. Bedside emergency department ultrasonography in the evaluation of ocular pathology. *Acad Emerg Med*, 2000; 7(8): 947-50.
210. Blaivas M, Theodoro D, Sierzenski PR. A study of bedside ocular ultrasonography in the emergency department. *Acad Emerg Med*, 2002; 9(8): 791-9.
211. Tsung JW, Blaivas M, Cooper A, Levick NR. A rapid noninvasive method of detecting elevated intracranial pressure using bedside ocular ultrasound: application to 3 cases of head trauma in the pediatric emergency department. *Pediatr Emerg Care*, 2005; 21(2): 94-8.
212. Galetta S, Byrne SF, Smith JL. Echographic correlation of optic nerve sheath size and cerebrospinal fluid pressure. *J Clin Neuroophthalmol*, 1989; 9(2): 79-82.
213. James JT, The headache of carbon dioxide exposures, 2007; Society of Automotive Engineers. 07ICES-42.
214. Bacal K, Beck G, Barratt MR, Hypoxia, hypercarbia, and atmospheric control, in *Principles of clinical medicine for space flight*, M.R. Barratt and S.L. Pool, Editors. 2008; Springer Sciences+business Media: New York. 459.
215. Wong KL, Carbon dioxide, in *Spacecraft maximum allowable concentrations for selected airborne contaminants*, N.R. Council, Editor 1996; National Academy Press: Washington, DC. 105-188.
216. Williams WJ, Physiological responses to oxygen and carbon dioxide in the breathing environment, 2009; National Institute for Occupational Safety and Health Public Meeting slides: Pittsburgh, PA.
217. Ainslie PN, Duffin J. Integration of cerebrovascular CO₂ reactivity and chemoreflex control of breathing: mechanisms of regulation, measurement, and interpretation. *Am J Physiol Regul Integr Comp Physiol*, 2009; 296(5): 1473-95.
218. Carbon dioxide as a fire suppressant: examining the risks. 2000; Environmental Protection Agency.
219. Son CH, Zapata JL, Lin CH, Investigation of airflow and accumulation of carbon dioxide in the Service Module crew quarters. 2002; Society of Automotive Engineers. 2002-01-2341.
220. International Space Station Program Mission Integration and Operations Control Board (MIOCB). Interim report meeting minutes, 9 July 2009, Houston, TX. 2009: http://iss-www.jsc.nasa.gov/nwo/ppco/cbp_miocb/bbt_docs/bbtcal/Minutes.6.09-Jul-2009.htm.
221. Felker P, Assessment of crew reports on ISS carbon dioxide symptoms, in *Internal Report*, 2003.
222. Smith SMZ, S. R.; Kloeris, V; Heer M., Nutritional biochemistry of spaceflight. 2009; New York: Nova Science Publishers.
223. Junqueira LF, Jr. Teaching cardiac autonomic function dynamics employing the Valsalva (Valsalva-Weber) maneuver. *Adv Physiol Educ*, 2008; 32(1): 100-6.
224. Edwards MR, Martin DH, Hughson RL. Cerebral hemodynamics and resistance exercise. *Med Sci Sports Exerc*, 2002; 34(7): 1207-11.

225. Dickerman RD, McConathy WJ, Smith GH, East JW, Rudder L. Middle cerebral artery blood flow velocity in elite power athletes during maximal weight-lifting. *Neurol Res*, 2000; 22(4): 337-40.
226. Haykowsky MJ, Eves ND, DE RW, Findlay MJ. Resistance exercise, the Valsalva maneuver, and cerebrovascular transmural pressure. *Med Sci Sports Exerc*, 2003; 35(1): 65-8.
227. Lempert P, Cooper KH, Culver JF, Tredici TJ. The effect of exercise on intraocular pressure. *Am J Ophthalmol*, 1967; 63(6): 1673-6.
228. Movaffaghy A, Chamot SR, Petrig BL, Riva CE. Blood flow in the human optic nerve head during isometric exercise. *Exp Eye Res*, 1998; 67(5): 561-8.
229. Vieira GM, Oliveira HB, de Andrade DT, Bottaro M, Ritch R. Intraocular pressure variation during weight lifting. *Arch Ophthalmol*, 2006; 124(9): 1251-4.
230. Dickerman RD, Smith GH, Langham-Roof L, McConathy WJ, East JW, Smith AB. Intraocular pressure changes during maximal isometric contraction: does this reflect intracranial pressure or retinal venous pressure? *Neurol Res*, 1999; 21(3): 243-6.
231. Marcus DF, Edelhauser HF, Maksud MG, Wiley RL. Effects of a sustained muscular contraction on human intraocular pressure. *Clin Sci Mol Med*, 1974; 47(3): 249-57.
232. Avunduk AM, Yilmaz B, Sahin N, Kapicioglu Z, Dayanir V. The comparison of intraocular pressure reductions after isometric and isokinetic exercises in normal individuals. *Ophthalmologica*, 1999; 213(5): 290-4.
233. Chromiak JA, Abadie BR, Braswell RA, Koh YS, Chilek DR. Resistance training exercises acutely reduce intraocular pressure in physically active men and women. *J Strength Cond Res*, 2003; 17(4): 715-20.
234. Brimiouille S, Moraine JJ, Norrenberg D, Kahn RJ. Effects of positioning and exercise on intracranial pressure in a neurosurgical intensive care unit. *Phys Ther*, 1997; 77(12): 1682-9.
235. Kashimada A, Machida K, Honda N, Mamiya T, Takahashi T, Kamano T, Osada H. Measurement of cerebral blood flow with two-dimensional cine phase-contrast mR imaging: evaluation of normal subjects and patients with vertigo. *Radiat Med*, 1995; 13(2): 95-102.
236. Delp MD, Armstrong RB, Godfrey DA, Laughlin MH, Ross CD, Wilkerson MK. Exercise increases blood flow to locomotor, vestibular, cardiorespiratory and visual regions of the brain in miniature swine. *J Physiol*, 2001; 533(Pt 3): 849-59.
237. Jorgensen LG, Perko G, Secher NH. Regional cerebral artery mean flow velocity and blood flow during dynamic exercise in humans. *J Appl Physiol*, 1992; 73(5): 1825-30.
238. Jorgensen LG, Perko M, Hanel B, Schroeder TV, Secher NH. Middle cerebral artery flow velocity and blood flow during exercise and muscle ischemia in humans. *J Appl Physiol*, 1992; 72(3): 1123-32.
239. Hellstrom G, Fischer-Colbrie W, Wahlgren NG, Jogestrand T. Carotid artery blood flow and middle cerebral artery blood flow velocity during physical exercise. *J Appl Physiol*, 1996; 81(1): 413-8.
240. Moraine JJ, Lamotte M, Berre J, Niset G, Leduc A, Naeije R. Relationship of middle cerebral artery blood flow velocity to intensity during dynamic exercise in normal subjects. *Eur J Appl Physiol Occup Physiol*, 1993; 67(1): 35-8.
241. Harris A, Malinovsky V, Martin B. Correlates of acute exercise-induced ocular hypotension. *Invest Ophthalmol Vis Sci*, 1994; 35(11): 3852-7.

242. Qureshi IA, Xi XR, Huang YB, Wu XD. Magnitude of decrease in intraocular pressure depends upon intensity of exercise. *Korean J Ophthalmol*, 1996; 10(2): 109-15.
243. Qureshi IA. The effects of mild, moderate, and severe exercise on intraocular pressure in glaucoma patients. *Jpn J Physiol*, 1995; 45(4): 561-9.
244. Passo MS, Goldberg L, Elliot DL, Van Buskirk EM. Exercise training reduces intraocular pressure among subjects suspected of having glaucoma. *Arch Ophthalmol*, 1991; 109(8): 1096-8.
245. Smith SM, Heer M, Wang Z, Huntoon CL, Zwart SR. Long-duration space flight and bed rest effects on testosterone and other steroids. *J Clin Endocrinol Metab*, 2012; 97(1): 270-8.
246. Zwart SR, Gibson CR, Mader TH, Ericson K, Ploutz-Snyder R, Heer M, Smith SM. Vision changes after spaceflight are related to alterations in folate- and vitamin B-12-dependent one-carbon metabolism. *J Nutr*, 2012; 142(3): 427-31.
247. Frisen L. Swelling of the optic nerve head: a staging scheme. *J Neurol Neurosurg Psychiatry*, 1982; 45(1): 13-8.
248. Nixon JV, Murray RG, Bryant C, Johnson RL, Jr., Mitchell JH, Holland OB, Gomez-Sanchez C, Vergne-Marini P, Blomqvist CG. Early cardiovascular adaptation to simulated zero gravity. *J Appl Physiol*, 1979; 46(3): 541-8.
249. Keil LC, McKeever KH, Skidmore MG, Hines J, Severs WB. The effect of head-down tilt and water immersion on intracranial pressure in nonhuman primates. *Aviat Space Environ Med*, 1992; 63(3): 181-5.

X. APPENDICES

Appendix A: Previous and Expanded In-flight Medical Requirements Testing for Crewmembers (MEDB 1.10)

Pre- and Postflight

Imaging:

- 2D Ultrasound
 - L-12/9 months and L-6/3 months
 - R+1/3 days
- MRI
 - L-21/18 months
 - R+1/3 days
 - 3Tesla or better

Ocular Exam:

- Vision exam
- Fundoscopy
- Tonometry
- OCT

In-flight L+30 Days & R-30 Days

- Vision Examination(includes L+100 days)
- Fundoscopy
- Tonometry
- 2D Ultrasound

Appendix B: Additional Central Nervous System Work/Topic Areas that will be Incorporated into the Evidence Base

- Intracranial Pressure
 - Cerebrospinal fluid (CSF) formation, outflow resistance and superior sagittal sinus pressure
 - Cerebrovascular resistance changes in microgravity
 - Changes in cerebral perfusion pressure in microgravity
 - Normotensive versus hypertensive mean arterial pressure (MAP) and the impact on ICP
 - Loss of hydrostatic drainage in zero gravity (venous congestion)
 - Cerebral venous drainage in zero gravity (internal jugular drainage)
 - Hypertension and increased CSF formation:
 - Increased choroidal plexus blood flow
 - Elevated CSF secretion
 - Elevated CSF pressure
 - Increased expression of Aquaporin 1 (AQP1) in hypertensive animals
 - Effects of CO₂ on cerebrovascular dilation and ICP
- CSF Production
 - Aquaporin 1 and 4 production
 - Down regulation of AQP1 in rats exposed to 0G
 - AQP1 knockout mice have 25% reduction in CSF production
 - Hydrocephalic rats demonstrate a significant down regulation of AQP1 expression in the choroid plexus
 - Up regulation of AQP1 in rats upon exposure to 1 G after 0-G exposure
 - Changes upon return to 1-G a mechanism for continued elevated ICP
 - Role of increased ANP in-flight and decreased CSF production
 - Elevated ICP and CSF production postflight in an ISS astronaut
- CSF Absorption:
 - Inflammatory cytokines, signaling molecules
 - Arachnoid villi – defects in absorption (for example, subarachnoid hemorrhage – scarring)
 - Elevated ICP and inflammatory damage to the arachnoid membrane
 - Venous lymphatics – elongation stretching neural and vascular structures
 - Impaired cranial lymphatic drainage with cephalad-fluid shift
 - Interparenchymal interstitial fluid accumulation
 - Risk of onset normal pressure hydrocephalus, or spontaneous CSF leak: does prolonged elevated pressure within the CSF space precipitate a spontaneous rupture and CSF leak
- CSF Biomarkers:
 - Myelin basic protein
 - oligo-clonal bands
 - Q albumin
 - IGF –a neurotrophic factor
 - IGG index
 - Somatostatin-an inhibitory neuroendocrine hormone
 - Markers of inflammation (cytokines and inflammatory markers)
 - Markers of CSF production (ANP or BNP, vasopressin, aquaporin)

Appendix C: Acronyms

ANP	Atrial natriuretic peptide
AQP1	Aquaporin 1
BM	Basement membrane
BNP	Brain natriuretic peptide
CBF	Cerebral blood flow
CDM	Carbon dioxide monitor
cm H ₂ O	Centimeters of water
CM	Countermeasure
CNS	Central nervous system
CO ₂	Carbon dioxide
CO	Carbon monoxide
CPG	Clinical Practice Guideline
CRP	C-reactive protein
CRV	Central retinal vein
CSF	Cerebrospinal fluid
CSFp	Cerebrospinal fluid pressure
CT	Computer tomography
CVP	Central venous pressure
CVST	Cerebral venous sinus thrombosis
D	Diopters
EP	Esophageal pressure
EVA	Extravehicular activity
ExMC	Exploration Medical Capability Group
G	Gravity
H ₂ O	Water
HDT	Head-down tilt
HRP	Human Research Program
ICP	Intracranial pressure
IGF	Insulin-like growth factor
IIH	Idiopathic intracranial hypertension
IOP	Intraocular pressure
IRCO ₂	Infrared carbon dioxide sensor
ISS	International Space Station
L	Liter
LC	Lamina cribosa
LSAH	Lifetime Surveillance of Astronaut Health
MAP	Mean arterial pressure
μL	Microliter
MCA	Middle cerebral artery

Risk of Microgravity-Induced Visual Impairment/Intracranial Pressure (ICP)

mm	Millimeters
mm Hg	Millimeters of mercury
MR	Medical Requirement
MRA	Magnetic resonance angiography
MRI	Magnetic resonance imaging
MRIDs	Medical Requirements Integration Documents
MRV	Magnetic resonance venogram
NASA	National Aeronautics and Space Administration
NSAID	Non-steroidal anti-inflammatory drug
NFL	Nerve fiber layer
NIRS	Near-infrared spectroscopy
O ₂	Oxygen
OCT	Optical coherence tomography
OD	Right eye
ONH	Optic nerve head
ONSD	Optic nerve sheath diameter
OS	Left eye
OU	Both eyes
PMC	Private medical conference
POAG	Primary open angle glaucoma
ppCO ₂	Partial pressure of carbon dioxide
PRA	Probabilistic risk assessment
RCAP	Research Clinical Advisory Panel
RNFL	Retinal nerve fiber layer
RPE	Retinal pigment epithelium
SAS	Subarachnoid space
SDTO	Supplemental detailed test objective
SLS	Spacelab Life Sciences
SLSD	Space Life Sciences Directorate
SMO	Supplimental Medical Objective
SOV	Superior ophthalmic vein
SRP	Standing Review Panel
STS	Shuttle Transportation System
TCD	Transcranial Doppler
TLP	Translaminar pressure
TSNIT	Temporal, superior, nasal, inferior, to temporal
TeTTA	Tet-transactivator
VIIP	Visual Impairment/Intracranial Pressure